THE ROLE OF AP-2β IN INTRAOCULAR PRESSURE HOMEOSTASIS

THE ROLE OF TRANSCRIPTION FACTOR AP-2β IN THE DEVELOPMENT OF

OCULAR ANTERIOR SEGMENT STRUCTURES INVOLVED IN INTRAOCULAR

PRESSURE HOMEOSTASIS

BY MONICA AKULA, B.SC.

A Thesis Submitted to the School of Graduate Studies in Partial Fulfillment of the

Requirement for the Degree Doctor of Philosophy

DOCTOR OF PHILOSOPHY (Neuroscience, 2021), McMaster University, Hamilton, ON

TITLE: The Role of Transcription Factor AP-2β in the Development of Ocular Anterior Segment

Structures Involved in Intraocular Pressure Homeostasis

AUTHOR: Monica Akula (B.Sc.)

SUPERVISOR: Professor Judith West-Mays

PAGES: xv, 129

Lay abstract

Glaucoma is the leading cause of irreversible blindness worldwide. Primary angle closure glaucoma is one type of glaucoma resulting from abnormalities in structures that allow aqueous humour found in the front of the eye from exiting the eye through two major routes, including the conventional and unconventional pathways. Defects in these structures lead to increased intraocular pressure (IOP) that damages specialized cells important for vision. This project examines the role of transcription factor activating protein 2-beta (AP-2β) in development of structures responsible for IOP balance. Data from the current study showed that AP-2β is required for formation of the structures of the conventional pathway, but does not directly affect development of unconventional pathway structures. The two AP-2β deletion mutants used here can model human primary angle closure glaucoma to test the effect of various drugs and cell protection strategies aimed at treating glaucoma.

Abstract

Previously, we showed that transcription factor activating protein 2-beta (AP-2β) deletion from the periocular mesenchyme (POM)-derived neural crest cells (NCCs) using Wnt1Cre (AP-2β NCC knockouts/AP-2β NCC KOs) resulted in anterior segment abnormalities and increased intraocular pressure (IOP). The present study investigated the role of AP-2β in development of structures of the conventional pathway including the trabecular meshwork and Schlemm's canal, and the unconventional pathway including the ciliary muscle. Studies using NCC KOs revealed that the embryonic POM migrated appropriately, but a significant reduction in postnatal POM cell proliferation in the angle was observed, accompanied by reduced expression of trabecular meshwork and Schlemm's canal markers when compared to controls, which likely contributed to the elevated IOP in NCC KOs. However, since Wnt1Cre was expressed in multiple NCC derivatives, AP-2β was deleted specifically from the developing trabecular meshwork region (TMR) using *Mgp*-Cre knock-in (*Mgp*-Cre.KI) mice. Although migration of the POM giving rise to the trabecular meshwork was not affected, peripheral anterior synechia (PAS), a decrease in expression of trabecular meshwork and Schlemm's canal markers, and significantly increased IOP was observed in TMR KOs compared to controls, paired with loss of retinal ganglion cells (RGCs), and reduced retinal thickness and function. However, treatment with latanoprost, a prostaglandin analog that increases outflow through the unconventional pathway, significantly reduced elevated IOP in TMR KOs. Overall, the results suggest that AP-2β plays a cell-autonomous role in trabecular meshwork development and a non-cell-autonomous role in Schlemm's canal development, while also playing an indirect role in unconventional pathway function, and thus, is important for IOP homeostasis. Moreover, the AP-2β NCC KO and AP-2β TMR KO may serve as models of primary angle closure glaucoma that can be used to test IOP-lowering drugs, molecular targets and neuroprotective strategies to develop treatments for human glaucoma.

Table of Contents

List of Figures

List of Abbreviations

αSMA	α smooth muscle actin
AP-2	Transcription factor Activating Protein 2
AQP	Aquaporin
ASD	Anterior segment dysgenesis
BOFS	Branchio-oculo-facial syndrome
Brn3a	POU domain class 4, transcription factor 1
CITED2	CBP/p300-interacting transactivator 2
CITED4	CBP/p300-interacting transactivator 4
Cyp1b1	Cytochrome P450 1B1
DAPI	4′,6-diamidino-2-phenylindole
E	Embryonic day
Foxc1	Forkhead box C1
Foxc2	Forkhead box C2
GLA	vitamin K-dependent carboxylation/gamma-carboxyglutamic acid domain
H&E	Hematoxylin & eosin
IOP	Intraocular pressure
KO	Knockout
Lmx1b	LIM homeobox transcription factor 1-beta
Mgp	Matrix GLA protein
***Mgp*-Cre.KI**	*Mgp*-Cre knock-in
MMP	Matrix metalloproteinase
NCCs	Neural crest cells
NPS	Nail Patella Syndrome

OCT	Optical coherence tomography
P	Postnatal day
PAS	Peripheral anterior synechia
PFA	Paraformaldehyde
PH3	Phosphorylated histone H3
Pax6	Paired box gene 6
PBST	0.3% Triton-X in 1x phosphate buffered saline
Pitx2	Paired-like homeodomain transcription factor 2
POM	Periocular mesenchyme
RALDH	Retinaldehyde dehydrogenase
RAR	Retinoic acid receptor
RGCs	Retinal ganglion cells
TEM	Transmission electron microscopy
TFAP2	Transcription factor Activating Protein 2
TMR	Trabecular meshwork region
TUNEL	Terminal deoxynucleotidyl transferase dUTP nick end labelling

Academic Record

Akula, M., Taiyab, A., Deschamps, P., Yee, S., Ball, A. K., Williams, T., & West-Mays, J. A. (2020). AP-2β is required for formation of the murine trabecular meshwork and Schlemm's canal. *Experimental Eye Research*, 195. doi: 10.1016/j.exer.2020.108042.

Akula, M.*, Taiyab, A.*, Dham, J., Deschamps, P., Sheardown, H., Williams, T., Borras, T., & West-Mays, J. Deletion of transcription factor AP-2β from the developing trabecular meshwork region leads to progressive glaucomatous changes. Manuscript in preparation.

Taiyab, A.*, Saraco, A.*, Akula, M., Ball, A. K., Williams, T., & West-Mays, J. (2019). Progression of retinal ganglion cell loss observed as a result of anterior segment dysgenesis following conditional deletion of activating protein-2β in cranial neural crest cells. *Current Eye Research,* 30:1-7. doi: 10.1080/02713683.2021.1901939.

Martino, V. B., Sabljic, T., Deschamps, P., Green, R. M., Akula, M., Peacock, E., Ball, A. K., Williams, T., West-Mays, J. A. (2016). Conditional deletion of AP-2β in the cranial neural crest results in anterior segment dysgenesis and early-onset glaucoma. *Disease Models and Mechanisms,* 9, 849-861.

Akula, M., Park, J. W., & West-Mays, J. A. (2018). Relationship between neural crest cell specification and rare ocular diseases. *Journal of Neuroscience Research.* Doi 10.1002/jnr.24245.

Walker H, Akula M, & West-Mays JA. (2020). Corneal development: Role of the periocular mesenchyme and bi-directional signaling. *Exp Eye Res.*, 201. doi: 10.1016/j.exer.2020.108231.

*First co-authors

1. Chapter 1: General Introduction

Parts of Chapter 1 were extracted from the following published review article, for which I was involved in carrying out the literature review, writing the article and designing and preparing the schematic figures.

Akula, M.[1], Park, J. W.[1], & West-Mays, J. A[1]. (2018). Relationship between neural crest cell specification and rare ocular diseases. *Journal of Neuroscience Research*. DOI 10.1002/jnr.24245.

1. McMaster University, Health Sciences Centre

1.1. Glaucoma

Glaucoma is the leading cause of irreversible blindness worldwide, with about 76 million patients predicted to have been affected in 2020, and 111.8 million people projected to be affected by 2040, making it important to study the mechanisms of this disease (Allison et al., 2020). Up to 25% of all new cases of blindness in developing countries result from glaucoma (Abu-Hassan et al., 2014). Demographic risk factors for developing glaucoma include race, sex and age, while pathological risk factors include optic nerve head abnormalities, corneal thinning and increased intraocular pressure (IOP), with the last one being a modifiable risk factor (Abu-Hassan et al., 2014; Gould & John, 2002). High IOP can put mechanical pressure on the retina at the back of the eye, leading to damage of retinal ganglion cells (RGCs) and the optic nerve head (Gould & John, 2002). Due to optic nerve head cupping, axons closer to the centre of the optic nerve head responsible for peripheral vision are lost first, leading to a pattern of vision loss from the peripheral to the central regions of the visual field (Abu-Hassan et al., 2014; Gould & John, 2002).

Glaucoma can be subdivided into two major types, which are primary open angle glaucoma and primary angle closure glaucoma. The former occurs when the outflow pathway structures appear morphologically normal, yet there is an increase in IOP, and is the most common form of glaucoma, affecting 85% of individuals afflicted with glaucoma (Abu-Hassan et al., 2014). Although primary angle closure glaucoma is less common, it is the most common form of glaucoma affecting African and Asian populations (Allison et al., 2020; Wright et al., 2016). Angle closure glaucoma occurs when the angle formed by the iris and cornea is blocked due to apposition of the iris to the cornea, and aqueous humour is unable to exit the eye, leading to increased IOP (Wright et al., 2016). In addition to demographic risk factors, specific risk factors include having shallow anterior chambers and being farsighted (Wright et al., 2016). Peripheral anterior synechia (PAS) is an adhesion of the peripheral anterior iris to the cornea, which can result in blockade of aqueous outflow structures located at the iridocorneal angle region near the outer periphery of the iris, potentially leading to increased IOP (Lee et al., 2006).

1.2. Ocular Structures Relevant for Congenital Glaucoma and Anterior Segment Dysgenesis (ASD)

Congenital glaucoma arises from mutations in genes important for development of structures involved in IOP maintenance (Gould et al., 2004; Gould & John, 2002). Such mutations lead to anterior segment dysgenesis (ASD), in which the anterior portion of the eye, including the lens, iris, cornea, ciliary body, trabecular meshwork and Schlemm's canal develop abnormally, and is often associated with closed angle glaucoma (Gould & John, 2002). The eye can be divided into the anterior and posterior segments, with the anterior segment consisting of structures important for IOP maintenance, while the posterior segment contains the choroid, retinal pigment epithelium

and the retina including RGCs that are lost in glaucoma. The anterior segment can be further divided into the anterior chamber, the compartment between the cornea and the iris, as well as the posterior chamber, the portion between the iris and the lens (Fig. 1.1). The anterior chamber contains the trabecular meshwork and Schlemm's canal, while the posterior chamber contains the ciliary body. Aqueous humour released by the ciliary body found posterior to the iris flows through the pupil, and exits the eye via drainage structures located at the iridocorneal angle (Civan & Macknight, 2004). Disruption of outflow can lead to increased IOP that can then damage the RGCs of the retina, the sensory structure of the eye. Within the retina, photoreceptor axons propagate visual signals, and synapse onto bipolar and horizontal cell dendrites within the outer plexiform layer. Bipolar and amacrine cell nuclei found within the inner nuclear layer form synapses in the inner plexiform layer with RGCs, the cells that are progressively lost in glaucoma, and the axons for which form the optic nerve that relays visual signals to the brain (Gupta et al., 2016).

1.3. The Anterior Segment

The ciliary body within the posterior chamber produces aqueous humour, which is composed of water and ions that are secreted into the posterior chamber (Goel et al., 2010). The ciliary body consists of multiple layers, including the outer ciliary epithelium, which faces the ciliary stroma containing blood vessels and extracellular matrix, while the inner ciliary epithelium faces the inside of the posterior chamber and secretes aqueous humour, whereas the ciliary muscle can be found anterior to the ciliary stroma (Peces-Pena et al., 2013). Once secreted, aqueous humour passes the lens, a crystalline structure consisting of a single monolayer of epithelial cells on the anterior side and fibre cells that line the equatorial region (Gould et al., 2004). Aqueous humour then flows past the iris containing the posterior pigment epithelium layer and the iris stroma on the

anterior side that is continuous with the ciliary body stroma (Gould et al., 2004). After flowing

through the pupil, aqueous fluid passes between the iris stroma and the cornea, the latter being an

avascular dome-shaped structure composed of three main layers: the corneal endothelium facing

the anterior chamber, the corneal stroma comprising corneal keratocytes and collagenous

extracellular matrix, and the corneal epithelium (Swamynathan, 2013; Walker et al., 2020).

1.4. The Trabecular Meshwork

Aqueous humour exits the eye through the trabecular meshwork, a tissue consisting of flat

beams made of extracellular matrix components surrounded by endothelial-like trabecular

meshwork cells (Cvekl & Tamm, 2004). The major function of the trabecular meshwork is to help

regulate IOP by controlling aqueous humour outflow through this region (Stamer & Clark, 2017).

The trabecular meshwork contains three principal layers that, from the posterior to the anterior

aspects, include the uveal meshwork, the corneoscleral meshwork and the juxtacanalicular

meshwork (Abu-Hassan et al., 2014). The uveal and corneoscleral regions are mesh-like sub-

structures of the trabecular meshwork containing large spaces between the trabecular beams, which

are covered by trabecular meshwork cells (Stamer & Clark, 2017). Intertrabecular spaces decrease

in size from the uveal meshwork to the corneoscleral meshwork region (Abu-Hassan et al., 2014).

Both the uveal and corneoscleral regions are responsible for filtering cell debris and reactive

oxygen species from the aqueous humour through phagocytosis before aqueous fluid enters the

juxtacanalicular region and Schlemm's canal (Abu-Hassan et al., 2014; Stamer & Clark, 2017).

The anterior-most juxtacanalicular region found adjacent to the Schlemm's canal mostly contains

loosely arranged extracellular matrix embedded with trabecular meshwork cells (Stamer & Clark,

2017). Owing to the reduced number of open spaces between the extracellular matrix, this region provides the greatest resistance to aqueous humour outflow from the eye (Stamer & Clark, 2017).

Some validated markers of trabecular meshwork cells include aquaporin 1 (AQP1), collagen IV, myocilin and α-smooth muscle actin (αSMA) that are all expressed by trabecular meshwork cells to a greater extent compared to surrounding cell types, such as ciliary muscle cells, Schlemm's canal endothelial cells and corneal endothelial cells (Ko & Tan, 2013; Overby et al., 2014; Stamer & Clark, 2017). In particular, myocilin is heavily expressed in the trabecular meshwork tissues (Stamer & Clark, 2017). Other proteins that are also specifically expressed by trabecular meshwork cells include matrix GLA protein (Mgp) and chitinase-3 like-1 (CHI3L1) (Stamer & Clark, 2017; van Zyl et al., 2020). Mgp containing GLA, a vitamin K-dependent carboxylation/gamma-carboxyglutamic acid (GLA) domain, was originally believed to only play an anti-calcification role in arteries, but has now been shown to be expressed in the trabecular meshwork and appears to play a similar anti-calcification role in this tissue type, likely to reduce stiffness (Acott & Kelley, 2008).

Several different types of proteins make up the extracellular matrix of the trabecular meshwork, including collagen, laminin, elastin, myocilin, fibronectin, glycosaminoglycans and proteoglycans (Abu-Hassan et al., 2014). Specifically, trabecular beams are mainly composed of collagen fibrils and elastin, while the trabecular meshwork cells rest on a basement membrane consisting of collagen type IV, laminin and proteoglycans (Abu-Hassan et al., 2014). Glycosaminoglycans are localized primarily to the juxtacanalicular trabecular meshwork, with small amounts also found in the corneoscleral and uveal regions (Acott & Kelley, 2008). An important protein that forms a network linking together the numerous structures regulating IOP is elastin that forms microfibrils connecting the ciliary muscle with cells of the juxtacanalicular

trabecular meshwork and the endothelial cells of the Schlemm's canal, while myocilin is associated with the sheath material surrounding elastin fibres (Acott & Kelley, 2008; Ueda et al., 2002; Ueda & Yue, 2003).

1.5. Schlemm's canal

After exiting the trabecular meshwork, aqueous humour flows through the Schlemm's canal, an outflow structure lined by endothelial cells that lie on a discontinuous basement membrane located anterior to the juxtacanalicular region (Abu-Hassan et al., 2014). The Schlemm's canal displays characteristics of blood vessels and lymphatic vessels, expressing markers of both during development (Carreon et al., 2017; Kizhatil et al., 2014). The Schlemm's canal is able to offer outflow resistance by restricting fluid through only some of the pores that are present in the basement membrane of this structure (Abu-Hassan et al., 2014). When aqueous humour pushes against the basal side of endothelial cells, the fluid enters the cells through pores, and giant vacuoles form within these cells in response to aqueous humour pressure against the endothelial cell layer (Abu-Hassan et al., 2014).

1.6. IOP Homeostasis

IOP stems from the balance between aqueous humour production by the ciliary body and aqueous humour outflow through the two major pathways, which are the conventional pathway through the trabecular meshwork and Schlemm's canal, as well as the unconventional pathway through the ciliary muscle fibres, the sclera and choroid (Fig. 1.1) (Johnson et al., 2017; Lindsey & Weinreb, 2002; Tamm, 2009). The rates of aqueous humour production and outflow are approximately 2.5% of the anterior chamber volume in both humans and mice (Abu-Hassan et al.,

2014; Aihara et al., 2003). Factors that cause variations in IOP include time of the day, heart rate, breathing, blinking and consumption of fluids (Abu-Hassan et al., 2014). To maintain IOP homeostasis in response to temporary and lasting fluctuations, the eye regulates aqueous humour inflow and outflow, with the outflow pathways being the most amenable to modulation (Abu-Hassan et al., 2014).

1.7. Conventional Outflow of Aqueous Humour

Conventional outflow occurs through the trabecular meshwork and the Schlemm's canal into the collector channels, the aqueous veins, the episcleral veins and into the blood circulation (Fig. 1.1) (Carreon et al., 2017; Tamm, 2009). Aqueous humour initially enters the uveal meshwork after which aqueous humour travels into the corneoscleral meshwork, both of which contain beams and large intertrabecular spaces (Carreon et al., 2017). The aqueous humour next enters the juxtacanalicular trabecular meshwork, forming the majority of aqueous outflow resistance. The aqueous then flows through pores found within Schlemm's canal endothelial cells into giant vacuoles after which aqueous humour enters the Schlemm's canal lumen (Stamer & Clark, 2017). Upon exiting the Schlemm's canal, aqueous humour enters the intrascleral vascular plexus and subsequently enters collector channels found within the sclera, after which the fluid flows into episcleral veins and aqueous veins (Carreon et al., 2017).

In order to respond to IOP fluctuations, one mechanism through which trabecular meshwork cells control outflow is by sensing stretching and distortion of extracellular matrix via integrins found on trabecular meshwork and Schlemm's canal cell surface receptors (Abu-Hassan et al., 2014). These cell receptors activate downstream signalling events that recruit proteins like the matrix metalloproteinases (MMPs), which can cleave extracellular matrix components (Abu-

Hassan et al., 2014; Acott & Kelley, 2008). Furthermore, trabecular meshwork cells can remodel the extracellular matrix by modifying the types of extracellular matrix components. Trabecular meshwork cells can also change expression levels of water channels that allow the cells to regulate the amount of fluid within this tissue (Stamer & Clark, 2017). Additionally, in response to mechanical stretching, contractility of trabecular meshwork cells also plays a key role in regulating aqueous humour outflow, with the trabecular meshwork expressing the contractile marker, αSMA (Tian et al., 2009). Increased trabecular meshwork cell contractility increases obstruction of aqueous humour, since trabecular meshwork cell contraction reduces the size of spaces between trabecular meshwork cells, whereas reduced contractility increases aqueous outflow (Tamm, 2009). In addition, the ciliary muscle contracts or relaxes to modulate trabecular meshwork cell contractility through the elastin network that connects the ciliary muscle to the trabecular meshwork and Schlemm's canal (Stamer & Clark, 2017). For instance, contraction of the ciliary muscle pulls on the trabecular meshwork and increases the amount of space between trabecular meshwork cells, thereby increasing outflow through the conventional pathway (Stamer & Clark, 2017).

1.8. Unconventional Outflow of Aqueous Humour

Unconventional outflow involves aqueous humour passing through the ciliary muscle, and exiting the eye through the sclera and the choroid (Johnson et al., 2017). Although in humans, only a minor portion of aqueous outflow occurs through the unconventional pathway, in mice, up to 80% of outflow can occur through this pathway (Johnson et al., 2017). Aqueous humour first enters the spaces between the ciliary muscle fibres and seeps into the suprachoroidal space, into the choroid and the sclera (Johnson et al., 2017). When eyes are treated with pilocarpine, which

reduces spaces between ciliary muscle fibres, this leads to reduced outflow through the unconventional pathway (Crawford & Kaufman, 1987). On the other hand, treatment with prostaglandins, a class of molecules that increase outflow through the unconventional route by reducing the amount of extracellular matrix found between the ciliary muscle fibres, leads to an increase in unconventional outflow (Lutjen-Drecoll & Tamm, 1988).

In mice, 10 minutes after injection of 70 kDa dextran tracer into the anterior chamber, dextran first appeared in the iris root, ciliary muscle and supraciliary regions, especially in the anterior eye globe (Bernd et al., 2004; Lindsey & Weinreb, 2002). 20 minutes after injection, dextran was present in the ciliary body processes, the ciliary muscle, as well as the choroid in the anterior to central region of the eye globe, whereas 60 minutes post-injection, dextran was found in the choroid and sclera throughout the eye globe (Bernd et al., 2004; Lindsey & Weinreb, 2002). This suggests that fluid in the unconventional pathway of the mouse passes through the ciliary muscle fibres, and exits the eye primarily through the choroid and sclera (Lindsey & Weinreb, 2002). The unconventional pathway in the mouse has also been associated with specific markers, with the biggest cluster consisting of markers of smooth muscle cells, as well as markers of intramuscular capillaries found within the ciliary muscle (van Zyl et al., 2020). Understanding the development of both outflow pathways is an important step toward determining the etiology of congenital glaucoma.

1.9. Early Eye Development

During early embryonic development, the neural plate invaginates to form the neural tube, after which the neural tube closes and detaches from the surface ectoderm. Vertebrate eye development begins with the bilateral evagination of the diencephalon located at the anterior

region of the neural tube, forming the optic vesicles (Chow & Lang, 2001). The optic vesicle then moves laterally and come into contact with the non-neural surface ectoderm that thickens to form the lens placode, and through inductive signalling interactions, the optic vesicle and lens placode both invaginate to form the optic cup and lens vesicle, respectively (Chow & Lang, 2001). The lens vesicle subsequently pinches off the surface ectoderm to form the prospective lens structure. Within the optic cup, the inner layer gives rise to the future retina, whereas the outer layer gives rise to the retinal pigmented epithelium, and a fissure forms along the ventral region running from the prospective retina to the optic stalk known as the optic fissure (Chow & Lang, 2001). The pigmented portion of the anterior rim of the optic cup forms the outer ciliary epithelium and pigmented iris epithelium that are both continuous with each other, and with the retinal pigmented epithelium (Chow & Lang, 2001).

NCCs are multipotent stem cells with migratory ability that arise from the dorsal neural tube during early embryonic development (Beebe & Coats, 2000; Williams & Bohnsack, 2015). When the neuroectoderm invaginates to form the neural tube and detaches from the surface ectoderm, NCCs migrate out laterally from the junction between the neural tube and surface ectoderm (Beebe & Coats, 2000). NCCs can be divided into the cranial neural crest, the heart neural crest and the trunk neural crest, wherein cranial NCCs provide the major contribution to eye development (Beebe & Coats, 2000). The main cranial neural crest contribution to ocular development includes the periocular mesenchyme (POM), which are migratory mesenchymal cells composed of NCCs and paraxial mesoderm cells (Gage et al., 2005). The POM is derived from both the neural ectoderm and mesoderm, and in humans, undergoes three migratory waves that give rise to various ocular structures (Williams & Bohnsack, 2015). The first wave migrates into the region between the surface ectoderm and the newly invaginated optic vesicle, eventually

condensing to form the corneal endothelium (Cvekl & Tamm, 2004; Williams & Bohnsack, 2015). The second wave migrates between the corneal epithelium and corneal endothelium, giving rise to the corneal stroma (Cvekl & Tamm, 2004; Williams & Bohnsack, 2015). Finally, the third wave migrates into the space adjacent to the anterior rim of the developing optic cup, contributing to the stroma of the ciliary body and iris, as well as the trabecular meshwork (Cvekl & Tamm, 2004; Williams & Bohnsack, 2015).

In mice, POM cells first migrate into the space between the developing lens and the corneal epithelium at embryonic day (E) 12.5 (Fig. 1.2). Between E14.5 and E15.5, the monolayer of cells in the posterior region closest to the lens condenses to become the corneal endothelium, and the remaining mesenchymal cells form the keratocytes of the corneal stroma (Cvekl & Tamm, 2004). At E15.5, POM cell migration occurs into the space between the anterior rim of the optic cup and the corneal endothelium, and gives rise to the stroma of the ciliary body and iris, as well as the ciliary muscle (Cvekl & Tamm, 2004; Napier & Kidson, 2005; Smith et al., 2001). The last POM-derived tissues to form during anterior segment development are the outflow structures, including the trabecular meshwork and Schlemm's canal. Just before postnatal day (P) 1, POM cells occupy the iridocorneal angle, and between P4 and P10, these cells elongate and flatten, and differentiate into the trabecular meshwork cells that will begin to secrete extracellular matrix fibres (Fig. 1.3) (Cvekl & Tamm, 2004; Smith et al., 2001). At the same time, blood vessels form in the scleral region adjacent to the developing cornea (Cvekl & Tamm, 2004). By P14, extracellular fibres secreted by the developing trabecular meshwork form beams that are covered by trabecular meshwork cells, and the blood vessels in the angle fuse to form the Schlemm's canal (Cvekl & Tamm, 2004; Kizhatil et al., 2014). After the trabecular meshwork is fully formed, it consists of

trabecular beams interspersed with intertrabecular spaces through which the aqueous humour flows (Fig. 1.4) (Cvekl & Tamm, 2004; Smith et al., 2001).

1.10. Genes Important in Development of the Trabecular Meshwork and other Anterior Segment Structures

A number of genes have been shown to play important roles in the development of the anterior segment structures. In humans, several genes are responsible for causing the ASD phenotype, including *PITX2*, *FOXC1* and *FOXC2*, *LMX1B*, *RALDH* and *CYP1B1*, many of which are expressed in the NCCs giving rise to the POM and are also implicated in development of aqueous humour outflow structures, including the trabecular meshwork (Gage et al., 2005; Gould & John, 2002; Liu & Johnson, 2010; Matt et al., 2005; Pressman et al., 2000; Smith et al., 2001). Heterozygous mutations of these genes result in developmental anomalies in the anterior portion of the eye in both humans and mice (Gould & John, 2002).

1.11. *Pitx2*

Axenfeld-Rieger Syndrome is an ASD in humans that is typified by defects in the iris, cornea and iridocorneal angle tissue (Tumer & Bach-Holm, 2009; Volkmann et al., 2011). Problems with the iris include hypoplasia, polycoria, corectopia and iris strands connecting to the trabecular meshwork, in addition to posterior embryotoxon, sclerocornea and corneal opacities (Tumer & Bach-Holm, 2009). Patients with Axenfeld-Rieger Syndrome also exhibit glaucomatous features such as elevated IOP, which usually begins in adulthood (Tumer & Bach-Holm, 2009). Paired Like Homeodomain 2 (PITX2) transcription factor has been well-established as playing an

important role in anterior segment development, and mutations in this gene in humans have been reported to result in Axenfeld-Rieger Syndrome (Tumer & Bach-Holm, 2009).

In mice, Pitx2 is expressed in the POM by E11.5 (Gage et al., 2005), and mice in which conditional deletion of Pitx2 in the cranial neural crest have been created exhibit ocular defects that are initiated as early as E12.5, including absence of a corneal endothelium and corneal stroma (Chen et al., 2016). Even heterozygous null Pitx2 mutants demonstrated clinical features of Axenfeld-Rieger Syndrome. For example, by 3 weeks of age, mutants had reduced central corneal thickness, iridocorneal adhesions, and about half of the mutants showed iridial defects such as hypoplasticity (Chen, 2016). Finally, a large portion of the adult mutants showed high IOP, while also demonstrating optic nerve cupping and a spectrum of RGC loss when compared to controls (Chen, 2016).

1.12. *Foxc1*

Humans with Forkhead Box C1 (FOXC1) mutations also show classic features of Axenfeld-Rieger syndrome, with associated iris hypoplasia and polycoria, similar to PITX2 mutations, as well as posterior embryotoxon, aniridia, corneal opacities and congenital glaucoma (Tumer & Bach-Holm, 2009). At early embryonic stages in mice, Foxc1 is expressed in the POM, in addition to some parts of the paraxial mesoderm, whereas Foxc2 is expressed only in the neural crest region without any expression observed in the mesoderm region (Gage et al., 2005). Mice that are heterozygous for the null *Foxc1* allele had defects of outflow pathway tissue, including absence or a reduction in size of the Schlemm's canal and a hypoplastic trabecular meshwork region (Smith et al., 2000). Furthermore, conditional Foxc2 neural crest knockouts have been shown to demonstrate microphthalmia, misshapen irises, and vascularization and opacity in the cornea (Seo

et al., 2017). These Foxc2 conditional knockouts also showed thickening of the peripheral cornea and conjunctiva, while the corneal epithelium of these mutants contained mesenchymal cells rather than epithelial cells normally found in this structure (Seo et al., 2017). In addition, at E15.5, double neural crest conditional knockouts for Foxc1 and Foxc2 showed that the corneal epithelium adhered to the surface ectoderm, and by P0, these animals had misshapen irises and smaller pupils compared to controls (Seo et al., 2017). By E14.5, double mutants also had reduced expression of Pitx2 and Activating Protein 2 β (AP-2β), although expression was unchanged in single Foxc1 and Foxc2 knockouts, suggesting that both are required for maintaining Pitx2 expression during development (Seo et al., 2017).

1.13. *Lmx1b*

Nail Patella Syndrome (NPS) is another form of ASD in which patients display abnormalities of the eye, such as optic nerve damage, increased IOP in some cases, loss of outer retina tissue, as well as deteriorating vision (Romero et al., 2011a). Further molecular analysis of patients revealed the presence of missense mutations within the LIM Homeobox Transcription Factor 1 Beta (LMX1B) gene, suggesting that this gene plays a role in human eye development, with deficits leading to glaucomatous changes (Romero et al., 2011a). *LMX1B* is a gene thought to be involved in development of neural crest-derived structures, with a role in etiology of NPS (Liu & Johnson, 2010).

In mice, Lmx1b expression has been detected in the POM by E10.5 and then in the presumptive cornea beyond P21 (Liu & Johnson, 2010). Conditional knockout mice with Lmx1b deleted in NCCs show several anterior segment anomalies, including microphthalmia, iris hypoplasia and reduced anterior chamber size, as well as corneal vascularization and reduced

expression of the corneal endothelium marker, NCAM (Liu & Johnson, 2010). These mutant mice also had a thicker anterior lens epithelium layer, a slightly smaller lens, hypoplasia of the corneal endothelium, and reduced expression of myocilin, a marker of the trabecular meshwork (Liu & Johnson, 2010). When Lmx1b was deleted only in adult mice using a temporal knockout system, these mutants showed corneal opacities, vascularization in the cornea, a thinner corneal epithelium, and a reduction in corneal stroma keratocytes, along with disorganized collagen fibrils in the corneal stroma (Liu & Johnson, 2010).

1.14. Retinoic Acid Pathway Genes: *RALDH*, *RAR* and *Cyp1b1*

Previous work has pinpointed many genes implicated in ocular defects not characterized by a syndrome. One example of such a gene encodes retinaldehyde dehydrogenase (RALDH) enzyme that synthesizes retinoic acid, which is a derivative of retinol and is involved in neural crest signalling important for eye development (Luscher et al., 1989). Specifically, 2 isoforms exist for RALDH, which are RALDH1 and RALDH3, and both are both present in the retina and corneal epithelium (Matt et al., 2005). At E12.5, single mutants for RALDH3 deletion had a thicker POM between the retina and surface ectoderm compared to wild type animals (Matt et al., 2005). Mice with mutations in both forms of the enzyme had severe ocular defects in the eyelid, anterior segment, as well as in the lens, primary vitreous and retina (Matt et al., 2005). At E11.5 in the double mutants that had both RALDH1 and RALDH3 deletions, the POM was thicker than in controls, with this tissue type replacing the eyelid and cornea (Matt et al., 2005). By E18.5, double mutant animals also showed anterior segment defects, such as absence of the corneal and iris stroma, as well as absence of anterior chamber formation (Matt et al., 2005). The same defects were observed in mutants with retinoic acid receptor β (RARβ) and RARγ deleted specifically

from the neural crest, providing support for the idea that retinoic acid in the developing neural retina interacts with RAR found in the POM, influencing eye development by affecting the latter target tissue (Matt et al., 2005). In addition to RALDH, Cytochrome P450 1B1 (Cyp1b1) is an enzyme involved in various functions, one of which is conversion of retinol to retinal, which is one of the steps in the synthesis of retinoic acid (Chen et al., 2000). Although Cyp1b1 expression is mostly restricted to the inner ciliary epithelium, corneal epithelium, the inner nuclear layer and RGCs (Choudhary et al., 2008), mice with homozygous null mutations of the *Cy1b1* gene display abnormalities of the iridocorneal angle, including iridocorneal adhesions and a hypoplastic trabecular meshwork region (Libby et al., 2003).

1.15. The Activating Protein-2 (AP-2) Family of Transcription Factors

Previous work from our lab has focused on the AP-2 family of transcription factors in eye development, which are a group of retinoic acid-responsive proteins (Bassett et al., 2012; Bassett et al., 2007; Bassett et al., 2010; Kerr et al., 2014; Luscher et al., 1989; Pontoriero et al., 2008). This family includes AP-2α, AP-2β, AP-2γ, AP-2δ and AP-2ε, and the protein sequences contain a helix-span-helix domain at the carboxy terminal and a basic region in the centre of each protein, both of which have been found to be important in the formation of homodimers and heterodimers with other transcription factors in this gene family (Eckert et al., 2005). While the helix-span-helix motif was specifically found to be involved in formation of dimers, the basic region was shown to also be important for the ability of AP-2 proteins to bind to DNA (Williams & Tjian, 1991a). The basic region and the first of the two α helices of the AP-2α, AP-2β and AP-2γ proteins are encoded by parts of exons 4, 5 and 6, which are conserved across several species including *Drosophila*, *Xenopus*, the mouse and humans (Hilger-Eversheim et al., 2000).

The amino terminus contains a transactivation domain composed of proline and glutamine residues important for transcriptional activation of downstream genes (Williams & Tjian, 1991b). Since AP-2 proteins are transcription factors, they are localized primarily to the nucleus, where AP-2 typically binds to palindromic GC-rich sequences (Eckert et al., 2005; Williams & Tjian, 1991b). The binding affinity of AP-2δ to binding sites for AP-2 is typically lower than for other proteins of this family, which suggests that this particular protein may have somewhat different functions in gene regulation (Eckert et al., 2005). AP-2 family members are also able to interact with other proteins outside this family in order to affect function of proteins within the AP-2 family or the function of the protein to which they bind (Eckert et al., 2005).

1.16.   AP-2 in Human Disease

Branchio-Oculo-Facial Syndrome (BOFS) is a human syndrome characterized by craniofacial defects accompanied by ocular abnormalities, such as coloboma in the retina and choroid, as well as microphthalmia, iris coloboma and sclerocornea in humans (Gestri et al., 2009). *TFAP2A* is a human homolog of the mouse *Tfap2a* gene that has previously been linked to optic fissure closure defects, retinal abnormalities associated with coloboma and defects of craniofacial structures derived from NCCs in patients with BOFS (Gestri et al., 2009). In addition, Char syndrome is a neural crest disease where patients present with facial abnormalities, including increased width between the eyes and a heart condition called patent ductus arteriosus (Zhao et al., 2001). This condition is associated with mutations in the *TFAP2B* gene, a human analog of AP-2β in the mouse, although ocular defects have yet to be associated with this disorder in humans, and the rarity of this condition may help explain the lack of documented ocular defects (Zhao et al., 2001).

1.17. The Role of AP-2 During Development

In vertebrates, various proteins of the AP-2 family play important roles during embryonic development (Eckert et al., 2005). AP-2 proteins are expressed in multiple ectoderm-derived tissues, including the non-neuronal ectoderm and the neural crest, as well as the central and peripheral nervous systems, in addition to the kidney and urogenital tissue, with this family of proteins being important for development of these tissues (Eckert et al., 2005; Hilger-Eversheim et al., 2000; Moser et al., 1997b). Specifically, in zebrafish, both the genes encoding AP-2α and AP-2β, *Tfap2a* and *Tfap2b*, respectively, are expressed in the surface ectoderm and developing kidney tissue, but only *Tfap2a* is expressed in the neural crest (Eckert et al., 2005). Furthermore, in zebrafish, *Tfap2a* mutations result in aberrant development of neural crest-derived structures, including the craniofacial region, peripheral nervous system tissue and cells that produce pigment (Barrallo-Gimeno et al., 2004; Eckert et al., 2005; Knight et al., 2004).

On the other hand, in mice, AP-2α and AP-2β are expressed in the neural crest, mesenchymal cells of the limb, peripheral nervous system tissue and ectodermal tissue, with AP-2β also being expressed in developing renal tissues (Eckert et al., 2005). Consequently, AP-2α is important for development of craniofacial structures and the limb (Eckert et al., 2005), while AP-2β is crucial for kidney development (Moser et al., 1997a). On the other hand, AP-2γ is required for trophoectoderm cell formation after embryo implantation (Werling & Schorle, 2002), and AP-2δ expression is mainly restricted to the retina, central nervous system and heart tissue, playing a crucial role in midbrain development (Hesse et al., 2011). AP-2ε is expressed in olfactory bulb cells (Eckert et al., 2005) and plays an important role in development of this structure (Lin et al., 2018).

Recent studies using chick embryos have shown that members of the AP-2 family also interact with one another to affect development. For instance, Tfap2a and Tfap2c dimerize, and activate genes involved in induction of the neural plate border, and later during development, Tfap2a and Tfap2b dimerize to activate NCC specification (Rothstein & Simoes-Costa, 2020). In addition to the requirement for AP-2 proteins in embryonic development, AP-2 also serves as a co-activator for other genes that play a role in transcription of downstream genes. For example, the CBP/p300-interacting transactivator 2 (CITED2) co-activates AP-2 proteins and transactivates downstream genes important for neural tube, neural crest and heart development (Bamforth et al., 2001; Braganca et al., 2003). Mice with homozygous null mutations in the *CITED2* gene display heart abnormalities, absence of development of the adrenal gland, aberrant development of cranial nerve ganglia, derived in part from NCCs, and exencephaly (Bamforth et al., 2001). Furthermore, studies have also shown that CITED4, another member of the CITED family, also interacts with and co-activates AP-2 proteins (Braganca et al., 2002).

1.18. The Role of AP-2 in Eye Development

AP-2 proteins cooperate with retinoic acid-relevant genes to influence ocular development (Luscher et al., 1989). Treatment of pregnant mice with RAR antagonist led to a reduction in the percentage of AP-2-positive cells in the developing embryonic eye tissues, in addition to increased apoptosis (Zhou & Kochhar, 2004). In mice, since complete loss of AP-2 leads to a lethal prenatal phenotype, preventing analysis of defects at later stages of development, chimeric embryos composed of both wild type and AP-2 null cells were analyzed. These embryos showed ocular defects that overlapped with defects found in mice with retinoic acid overexpression, further

implicating the involvement of AP-2 in the retinoic acid pathway important for eye development (Nottoli et al., 1998).

AP-2α and AP-2β both play important roles in early retinal development. Although conditional deletion of AP-2α from the retina did not lead to retinal defects, null AP-2α mice display conversion of the retinal pigment epithelium to neural retina and absence of extension of the optic stalk, suggesting that AP-2α expression in cranial NCCs surrounding the developing optic vesicles is important for proper interaction between these tissues that is required for retinal development (Bassett et al., 2007; Bassett et al., 2010). AP-2α and AP-2β also appear to play redundant and overlapping roles in ocular development, as conditional deletion of AP-2α and AP-2β resulted in loss of amacrine and horizontal cell types, although deficits were not observed in single AP-2α or AP-2β conditional knockouts, suggesting that each protein can compensate for the loss of the other protein (Bassett et al., 2012; Hicks et al., 2018). On the other hand, expression of both AP-2γ and AP-2ε occurs at later stages, suggesting a role for these two members of the AP-2 family during later stages of retinal development (Jain et al., 2018). Additionally, expression of AP-2δ in a subset of RGCs during chick development appears to play an important role in growth of RGC axons (Li et al., 2014).

1.19. The Role of AP-2 in Anterior Segment Development

AP-2 proteins are expressed in embryonic tissues giving rise to anterior segment structures, including the cranial NCCs (Eckert et al., 2005), which give rise to the corneal stroma and endothelium, stroma of the ciliary body and iris, and the trabecular meshwork, as well as the surface ectoderm, which gives rise to the lens and corneal epithelium. By E8.75, AP-2α is expressed in the POM surrounding the optic vesicle of wild type mice, although expression ceases

in this region after E10.5 (Bassett et al., 2010). AP-2α null mice showed improper development of ciliary body and iris when compared to wild type animals (West-Mays et al., 1999). Moreover, the optic vesicle faced the POM to a greater extent as opposed to facing the surface ectoderm in AP-2α null mice when compared to controls (Bassett et al., 2010). AP-2α was also found to play a key role in normal development of the corneal stroma, with conditional mutations of AP-2α in the lens placode giving rise to the corneal epithelium leading to collagen disorganization in the corneal stroma (Dwivedi et al., 2005).

On the other hand, AP-2β is expressed in the lens placode, as well as the neural crest during development, and importantly, AP-2β is expressed in the POM during early eye development (Barzago et al., 2017; Bassett et al., 2007; West-Mays et al., 1999). During mouse embryogenesis, *Tfap2b* gene expression occurs in the neural plate border by E8.0, corresponding to the formation of the neural crest, and continues during the NCC migration phase (Van Otterloo et al., 2018). Subsequently, AP-2β is expressed in the derivatives of NCCs that migrate into the region between the surface ectoderm and lens vesicle, including the corneal endothelium and corneal stromal keratocytes (Martino et al., 2016). AP-2β is then strongly expressed in the POM that migrates into the space between corneal endothelium and anterior rim of the optic cup, with this POM cell population giving rise to the future trabecular meshwork (Bassett et al., 2007; Eckert et al., 2005; Martino et al., 2016; West-Mays et al., 1999). This hints at the importance of AP-2β expression for the development of ocular structures derived from the POM, such as the trabecular meshwork, ciliary body stroma and cornea (Cvekl & Tamm, 2004). For instance, in studies of mouse models with Pitx2 deletions, AP-2β has been shown to lie downstream of Pitx2 with respect to development of anterior segment tissue, and was shown to be required for specification of the

corneal endothelial cells, as well as angiogenic privilege in the cornea (Chen et al., 2016; Hara et al., 2019; Martino et al., 2016).

Furthermore, previous work from our lab using conditional deletion of AP-2β in cranial NCCs using the Wnt1Cre-LoxP system resulted in anterior segment defects (Martino et al., 2016). In 2–3 month-old mutant mice, defects of neural crest-derived structures were evident, including absence of a corneal endothelium, corneal vascularization and iridocorneal adhesions. Secondary defects were also observed, including corneolenticular adhesions, with the ciliary body containing fewer folds than control animals (Martino et al., 2016). Follow-up studies measuring IOP demonstrated a 3-fold increase in adult mutant animals compared to controls, possibly stemming from the aqueous blockade resulting from iridocorneal adhesions. This spike in IOP corresponded with RGC loss and a reduction in retinal ganglion axon myelination (Martino et al., 2016).

1.20. Rationale for the Study

Although previous work in our lab has focused on elucidating the role of AP-2β in anterior segment development and glaucoma pathophysiology (Martino et al., 2016), the specific role of AP-2β in development of anterior segment structures important for aqueous outflow, namely, the trabecular meshwork and Schlemm's canal, has not been examined previously. In addition, the cell-autonomous and non-cell-autonomous roles of AP-2β in development of POM-derived outflow structures has not been investigated in the past. Moreover, the role of AP-2β in function of the conventional and unconventional outflow pathways has not previously been studied.

1.21. Hypothesis and Aims

AP-2β plays an essential role in development of the trabecular meshwork and thus is important for maintaining IOP homeostasis.

Specific Aims

Aim 1:

The first aim is to characterize the defects in development of the trabecular meshwork in the AP-2β neural crest cell knockout (AP-2β NCC KO) mice and compare to control littermates.

Aim 2:

The second aim is to characterize defects in development of the trabecular meshwork in AP-2β trabecular meshwork region knockout (AP-2β TMR KO) mice and compare to control littermates.

Aim 3:

The third aim is to test whether unconventional outflow is present in AP-2β NCC KO mice and AP-2β TMR KO mice when compared to control littermates.
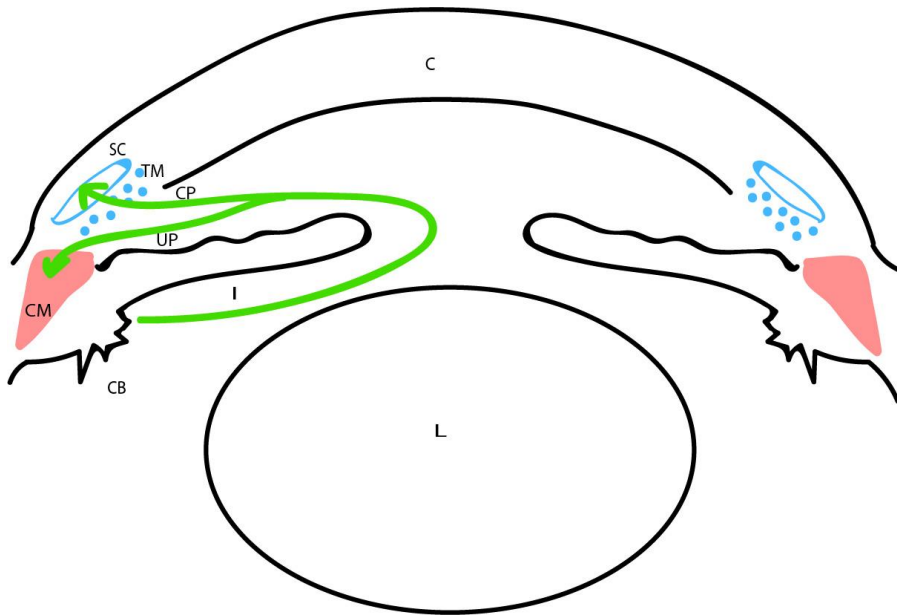
Fig. 1.1. Diagram of the eye depicting structures relevant for anterior segment dysgenesis (ASD) and the two major aqueous humour outflow pathways. This schematic illustrates the ocular structures affected in ASD, including the trabecular meshwork (TM) and Schlemm's canal (SC), both of which are implicated in congenital glaucoma, as well as the ciliary body (CB), ciliary muscle (CM), cornea (C), iris (I) and lens (L). The conventional pathway (CP) for aqueous humour outflow through the trabecular meshwork and Schlemm's canal, as well as the unconventional pathway (UP) through the ciliary muscle are shown using green arrows.
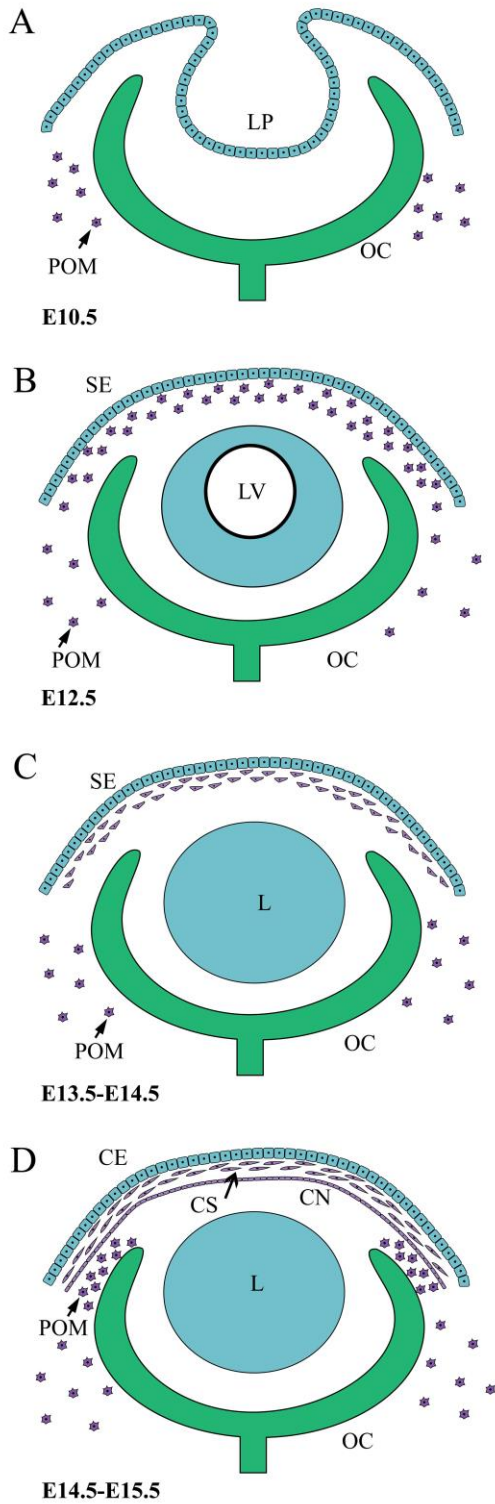
Fig. 1.2. Periocular mesenchyme (POM) cell migration and developmental progression of neural crest cell (NCC)-derived structures. A-B) Between embryonic day (E) 10.5 and E11.5,

the lens vesicle separates from the future corneal epithelium, and by E12.5, POM cells migrate into the space between the corneal epithelium and the lens. C) The newly migrated POM cells become flatter and more tightly packed between E13.5 and E14.5. D) At E15.5, POM cells between the corneal epithelium and the lens give rise to the corneal stroma and endothelium, while the POM cells that migrate into the region between the developing cornea and optic cup rim give rise to the future trabecular meshwork, Schlemm's canal, ciliary muscle, ciliary body stroma and iris stroma. POM, periocular mesenchyme; OC, optic cup; LV, lens vesicle; LP, lens placode; L, lens; CE, corneal epithelium; CS, corneal stroma; CN, corneal endothelium. Adapted from Walker et al. (2020).
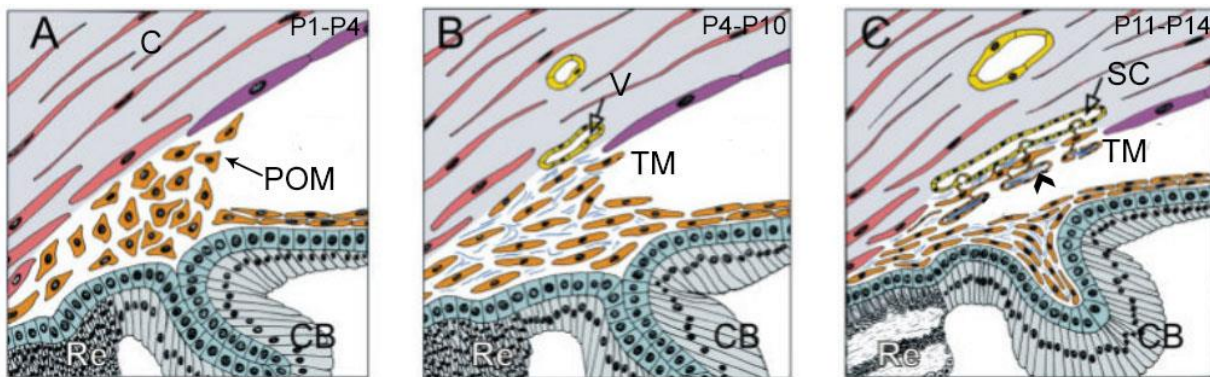
Fig. 1.3. Development of the trabecular meshwork. A) Between postnatal day (P) 1 and P4, POM cells (closed arrow) occupy the space at the iridocorneal angle. B) Between P4 and P10, extracellular matrix fibres fill the spaces between the POM cells, and blood vessels can be observed next to the POM cells in the sclera (V, open arrow). C) The extracellular matrix fibres form trabecular beams (open arrowhead) through reorganization, and the blood vessels in the sclera fuse to become the Schlemm's canal. P, postnatal day; POM, periocular mesenchyme; TM, trabecular meshwork; SC, Schlemm's canal; CB, ciliary body; V, blood vessel; C, cornea; Re, retina. Adapted from Cvekl and Tamm (2004).
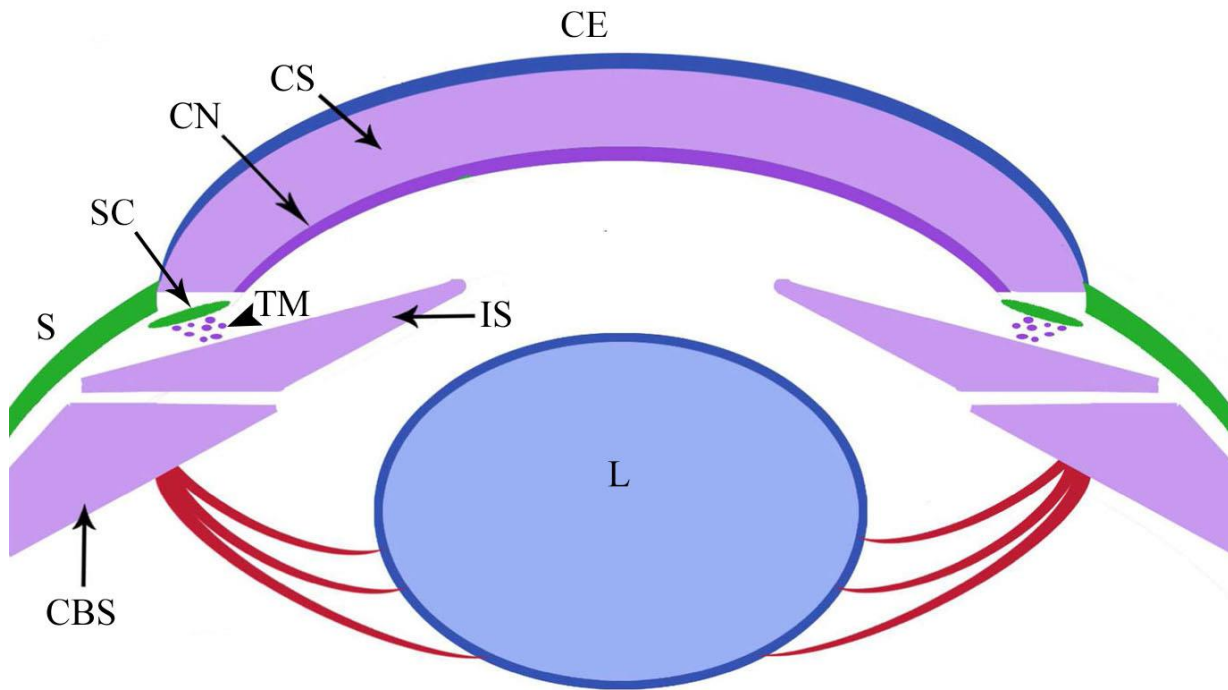
Fig. 1.4. Neural crest cell (NCC) specification. Structures derived from NCCs, such as the corneal stroma, corneal endothelium, ciliary body stroma and iris stroma, are shown in purple, whereas mesoderm-derived structures, like Schlemm's canal and the sclera, are represented in green, while the surface ectoderm-derived lens and corneal epithelium are depicted in blue. CE, corneal epithelium; CS, corneal stroma; CN, corneal endothelium; SC, Schlemm's canal; TM, trabecular meshwork; S, sclera; CBS, ciliary body stroma; IS, iris stroma; L, lens. Adapted from Akula et al. (2019).

2. Chapter 2: AP-2β is Required for Formation of the Murine Trabecular Meshwork and Schlemm's Canal

I was involved in experimental design, and I completed all the experiments presented, analyzed the data and wrote the manuscript. Dr. Aftab Taiyab was involved in experimental design, helping carry out experiments and helping with writing the manuscript. Paula Deschamps and Shannin Yee helped with performing the experiments. Dr. Judith West-Mays and Dr. Alexander Ball were involved in research design, providing reagents and writing the manuscript, while Dr. Trevor Williams was involved in research design, providing the materials, including the *Tfap2b^{lox/lox}* mice, and manuscript writing. Chapter 2 was extracted from the following published original manuscript.

Monica Akula[1], Aftab Taiyab[1], Paula Deschamps[1], Shannin Yee[1], Alexander K. Ball[1], Trevor Williams[2], & Judith A. West-Mays[1].

1. McMaster University, Health Sciences Centre
2. University of Colorado, Craniofacial Biology

Abstract

Previously, we have shown that Tfap2b, the gene encoding transcription factor AP-2β, is needed for normal mouse eye development. Specifically, targeted loss of Tfap2b in neural crest cells (NCCs) and their derivatives, particularly the POM, resulted in anterior segment defects

affecting the cornea and angle tissue. These defects were further associated with an increase in IOP. The present study investigates the underlying changes in embryonic and postnatal POM cell development and differentiation caused by loss of AP-2β in the NCCs, particularly in the structures that control aqueous outflow, using *Wnt1Cre$^{+/-}$; Tfap2b$^{-/lox}$; tdTomato$^{lox/+}$* mice (AP-2β NCC KO). Toluidine blue-stained sections and ultrathin sections stained with uranyl acetate and lead citrate were used to assess morphology and ultrastructure, respectively. Immunohistochemistry of KO and control eyes was performed at E15.5, E18.5, P1, P7 and P14 using phospho-histone H3 (PH3), αSMA, myocilin and endomucin antibodies, as well as a TUNEL assay. Conditional deletion of AP-2β in the NCC-derived POM resulted in defects that appeared during both embryogenesis and postnatal stages. Fate mapping of the knockout cells in the mutants revealed that the POM migrated appropriately into the eye during embryogenesis. However, during postnatal stages a significant reduction in POM proliferation in the angle region was observed in the mutants compared to controls. This was accompanied by a lack of expression of appropriate trabecular meshwork and Schlemm's canal markers. This is the first study to show that AP-2β is required for development and differentiation of the trabecular meshwork and Schlemm's canal. Together, these defects likely contributed to the elevated intraocular pressure previously reported in the AP-2β NCC KO mice.

2.1. Introduction

Anterior segment dysgenesis is a group of disorders in which structures in the anterior portion of the eye, including the iris, cornea, ciliary body, trabecular meshwork and Schlemm's canal, develop abnormally, typically due to genetic mutations (Gould & John, 2002). The mouse POM, which is composed mainly of NCCs and a smaller proportion of paraxial mesoderm cells, gives rise to the trabecular meshwork and the endothelial cells lining the Schlemm's canal, both

of which are responsible for aqueous humor outflow from the eye (Gage et al., 2005; Gould et al., 2004). The stroma and muscle of the ciliary body, the structure that secretes aqueous humor into the posterior chamber, are also derived from the POM. In mice, the first wave of POM cells migrates into the space between the developing lens and the corneal epithelium from E12.5 to E13.5. Between E14.5 and E15.5, the monolayer of cells in the posterior region closest to the lens condenses to become the corneal endothelium and the remaining mesenchymal cells form the keratocytes of the corneal stroma (Cvekl & Tamm, 2004). At E15.5, POM cell migration occurs into the space between the anterior rim of the optic cup and the corneal endothelium, and gives rise to the stroma of the ciliary body and iris (Cvekl & Tamm, 2004; Napier & Kidson, 2005; Smith et al., 2001). The last tissues to form during anterior segment development are the outflow structures, including the trabecular meshwork and Schlemm's canal. Just before P1, POM cells occupy the iridocorneal angle, and between P4 and P10, these cells elongate and flatten, and differentiate into the trabecular meshwork cells that will begin to secrete extracellular matrix fibres (Cvekl & Tamm, 2004; Smith et al., 2001). By P14, these extracellular fibres form trabecular beams that are covered by trabecular meshwork cells. After the trabecular meshwork is fully formed by P42, it consists of trabecular beams interspersed with intertrabecular spaces, and aqueous humor percolates through these spaces (Cvekl & Tamm, 2004; Smith et al., 2001).

A number of genes, some of which are also expressed in the POM, have been shown in humans to play important roles in the development of anterior segment structures, including the trabecular meshwork, ciliary body and cornea, and these include *PAX6, PITX2, PITX3, FOXC1, FOXE3,* and *LMX1B* (Chograni et al., 2014; Garcia-Montalvo et al., 2014; Romero et al., 2011b; Summers et al., 2008; Tümer & Bach-Holm, 2009). Many of the aforementioned genes have been further investigated in mice and mutations have been shown to produce anterior segment defects

(Gould & John, 2002). In mice, another important set of genes involved in ocular development are those encoding the AP-2 family of transcription factors, which are a group of retinoic acid-responsive proteins comprising AP-2α, AP-2β, AP-2γ, AP-2δ, and AP-2ε (Barzago et al., 2017; Bassett et al., 2012; Bassett et al., 2007; Bassett et al., 2010; Kerr et al., 2014; Martino et al., 2016; Pontoriero et al., 2008; West-Mays et al., 1999). During mouse embryogenesis, *Tfap2b* expression occurs in the neural plate border by E8.0, corresponding to the emergence of the neural crest, and continues during the NCC migration phase (Van Otterloo et al., 2018). Subsequently, AP-2β is expressed in the derivatives of NCC migration into the anterior segment giving rise to the corneal endothelium and corneal stromal cells (Martino et al., 2016). AP-2β is then strongly expressed in the POM at the anterior rim of the optic cup that gives rise to the future trabecular meshwork during early eye development (Bassett et al., 2007; Eckert et al., 2005; Martino et al., 2016; West-Mays et al., 1999). This hints at the importance of AP-2β expression for the development of ocular structures derived from the POM, such as the trabecular meshwork, ciliary body stroma and cornea (Cvekl & Tamm, 2004). Note that AP-2β is also expressed in tissue derived from other embryonic germ layers, such as the ectoderm-derived corneal epithelial cells (Martino et al., 2016).

Germ-line deletion of AP-2β in the mouse results in early postnatal lethality, before anterior segment development is complete (Moser, 1997). Therefore, in order to investigate the role of AP-2β in anterior segment development, we previously employed Wnt1Cre transgenic mice to conditionally delete AP-2β from the NCC population contributing to the POM. These crosses resulted in deletion of AP-2β at E8.5 in the NCCs contributing to the POM when Wnt1Cre is first expressed in this cell population (Lewis et al., 2013; Martino et al., 2016). The mice, termed the AP-2β NCC KO, displayed anterior segment defects, such as an absent corneal endothelium and iridocorneal adhesions resulting in a closed-angle phenotype. These defects were accompanied by

raised IOP and the loss of RGCs (Martino et al., 2016). Although this earlier study characterized the phenotype of these mice and the associated glaucomatous changes, details regarding the early developmental defects in the POM that contributed to the phenotype remain uncertain. Here, we investigate the effect(s) of AP-2β deletion on development and differentiation of POM derived tissues including the trabecular meshwork and Schlemm's canal. Our findings show that AP-2β deletion in the NCCs did not disrupt POM migration into the eye, but did lead to a significant reduction in POM proliferation in the angle region during early postnatal development. This was accompanied by a loss of markers indicative of trabecular meshwork and Schlemm's canal differentiation. Thus, lack of proper formation of these structures, which regulate aqueous outflow, likely contributed to the previously reported elevated IOP in the AP-2β NCC KO mice.

2.2. Methods

2.2.1. Animal Husbandry

All procedures were conducted in accordance with the Association for Research in Vision and Ophthalmology (ARVO) Statement for the Use of Animals in Ophthalmic and Vision Research. AP-2β NCC KO mice were used to examine development of the trabecular meshwork (Martino et al., 2016). In this model, the gene encoding AP-2β, *Tfap2b*, has loxP sites flanking exon 6, and this region was conditionally deleted from the NCC population through the use of the Cre transgene under control of the *Wnt1* promoter. Briefly, *Wnt1Cre$^{+/-}$* mice (*H2az2$^{Tg(Wnt1-cre)11Rth}$* Tg(Wnt1-GAL4)11Rth/J, Jackson Lab, Bar Harbor, ME) were bred with *Tfap2b$^{+/-}$* mice (Chen et al., 2016; Martino et al., 2016). Male *Wnt1Cre$^{+/-}$; Tfap2b$^{+/-}$* offspring were then bred with female *Tfap2b$^{lox/lox}$* mice to produce *Wnt1Cre$^{+/-}$; Tfap2b$^{-/lox}$* mice (AP-2β NCC KO), as well as littermate controls. Additionally, for lineage tracing of NCCs, a tdTomato reporter strain

(B6;129S6-Gt(ROSA)26Sortm14(CAG-tdTomato)Hze/J, Jackson Lab) was used (Madisen et al., 2010). In this strain, tdTomato protein expression does not occur unless a loxP flanked stop cassette is removed by Cre recombinase. Male *Wnt1Cre$^{+/-}$; Tfap2b$^{+/-}$* mice were bred with female *Tfap2b$^{lox/lox}$; tdTomato$^{lox/lox}$* mice to generate *Wnt1Cre$^{+/-}$; Tfap2b$^{-/lox}$; tdTomato$^{lox/+}$* mice (AP-2β NCC KOs) and age-matched control littermates, both of which are Wnt1Cre-positive, and express tdTomato in NCCs and their derivatives (Madisen et al., 2010) (Fig. 2.1). All genotyping was carried out using standard PCR protocols (Martino et al., 2016). Inbreeding between mouse lines used for the final cross was avoided. C57BL/6J was the background strain used for all genetic crosses (Charles River, Wilmington, MA).

2.2.2. Histology

Eyeballs were enucleated from euthanized mice, and either fixed in neutral buffered formalin for 24-48 hours followed by preservation in 70% ethanol for paraffin sections, or fixed in 4% paraformaldehyde (PFA) for 2 hours, washed in PBS and incubated overnight in 30% sucrose for frozen sections. Subsequently, the eyes were processed and embedded in paraffin wax or optimal cutting temperature medium. Paraffin blocks were sectioned at a thickness of 4 μm for hematoxylin and eosin (H&E) staining or immunohistochemistry, and frozen tissue blocks were sectioned at a thickness of 10 μm (Bassett et al., 2007).

2.2.3. Immunohistochemistry

Paraffin sections were deparaffinised in xylene and hydrated in decreasing concentrations of ethanol, and then finally washed in water. The sections were heated to a temperature between 80-90°C in 10 mM sodium citrate at pH 6.0 for 20 minutes to unmask the protein epitope, followed

by incubation in blocking serum from the host animal of the secondary antibody to block non-specific staining. All sections were incubated in the appropriate dilution of primary antibodies in 1xPBS overnight at 4ºC (Bassett et al., 2007). Primary antibodies included phospho-histone H3 (PH3, 1:50, Millipore, Etobicoke, CA), αSMA (1:100, Sigma Aldrich, Oakville, CA), myocilin (1:200, FabGennix, Frisco, TX) and endomucin (1:100, eBioscience, Cedarlane, Burlington, CA). Apoptosis was measured using the ApopTag Plus Fluorescein In Situ Apoptosis Detection Kit (Chemicon International, Bellirica, MA). The next day, Alexa Fluor secondary antibodies (Invitrogen, Molecular Probes, Burlington, CA) were added to the sections and stored for 1 hour at room temperature, following by washing three times in 0.1% Tween-20 solution for 5 minutes per wash, and then mounting with ProLong Gold containing DAPI (Invitrogen, Molecular Probes, Burlington, CA) (Bassett et al., 2007). To analyze tdTomato expression for the NCC lineage tracing experiments, frozen sections of control and AP-2β NCC KO mice crossed with the tdTomato reporter strain were used. All sections were imaged with a Leica microscope using either a bright-field attachment or a fluorescence attachment, and images were acquired using a high-resolution camera, along with LasX imaging software.

2.2.4. Toluidine Blue Staining of Plastic Sections and Electron Microscopy

Enucleated eyes obtained from euthanized mice were fixed in a solution of 4% PFA and 2% glutaraldehyde for 24 h at 4º Celsius, and sent to the McMaster Electron Microscopy Facility for post-fixation in 2% aqueous OsO_4 and 0.1 M Cacodylate buffer for 1 h. The samples were then dehydrated in an acetone series of increasing concentration, after which samples were embedded in EPON resin, sectioned with a diamond knife, and stained using toluidine blue (Martino et al., 2016). For electron microscopy (EM), ultrathin sections were placed on copper grids, stained with

uranyl acetate and lead citrate, and visualized using a transmission electron microscope (TEM) (EM Facility, McMaster University) (Smith et al., 2001).

2.2.5. Statistical Analysis

Cell counts of αSMA-positive cells and of αSMA–PH3 double positive cells in control and AP-2β NCC KO eye sections were conducted using the manual Cell Counter plugin on ImageJ. The sections evaluated for the statistical analyses were matched based on the level of the section (e.g., equal diameter of the ocular lens). 2-3 sections were evaluated per eye, and 1-2 cell count measurements were obtained from each section. Differences in cell counts between control and NCC KO animals were analyzed using the student's t-test on GraphPad 6.0.

2.3. Results

Our original investigation of conditional deletion of AP-2β in the NCC-derived POM of the murine eye (AP-2β NCC KO mice) had shown that mutants exhibited multiple anterior segment defects accompanied by increased IOP and loss of RGCs (Martino et al., 2016). The AP-2β NCC KO mice (Fig. 2.1) generated for the current study exhibited the same phenotype as previously shown, including a closed iridocorneal angle phenotype along with abnormalities in the ciliary body and cornea (Fig. 2.2). At E18.5, there was no marked difference between the control and KO POM associated with the angle (Fig. 2.2A-B, POM marked using square brackets; insets show higher magnification images of the POM). POM cells are present in approximately the same location near the anterior rim of the developing neural retina in both control and KO animals (Fig. 2.2A-B, square brackets), and higher magnification insets showed that the control and KO POM cells appeared similar (Fig. 2.2A-B; insets). However, there were already defects associated with

the NCC-derived corneal tissues apparent at this time in the KO, including the presence of blood vessels in the stroma (Fig. 2.2B, black chevron). By 2 to 3 months of age, while the control mice displayed an open iridocorneal angle, with trabecular meshwork cells (Fig. 2.2C inset; closed red arrowhead) and a Schlemm's canal (Fig. 2.2C inset; open white arrowhead), the KO mice had a closed iridocorneal angle without an obvious trabecular meshwork or Schlemm's canal (Fig. 2.2D inset; asterisk).

Since the defects in the AP-2β NCC KO mice became apparent during embryogenesis, we set out to determine if there were any alterations in the overall contribution of the NCC KO cells to the POM in the anterior region in the mutant mice throughout the critical developmental window between E15.5 and P14. To do so, we incorporated the tdTomato allele into the genetic background of both experimental and control mice (Madisen et al., 2010). Thus, by studying tdTomato expression, we were able to fate map NCCs in the AP-2β NCC KO mice during development. At E15.5, both the control and mutant animals demonstrated similar levels of specific tdTomato expression in the corneal stroma, indicating that migration of NCCs giving rise to corneal cell types had occurred successfully (Fig. 2.3A-B). However, as we have shown previously, these cells are not able to form the corneal endothelium (Chen et al., 2016; Hara et al., 2018; Martino et al., 2016). By P1, the specific sub-population of POM cells that give rise to the future trabecular meshwork cells (Fig. 2.3C-D) also appeared similar in both the KOs and controls. This demonstrated that migration of the POM during embryonic development was not affected by the deletion of AP-2β. However, by P7 (Fig. 2.3E/F/I; n=3 eyes; p<0.01; analyzed region in white dashed lines) and P14 (Fig. 2.3G/H/J; n=4 eyes; p<0.0001; analyzed region in white dashed lines), significantly fewer tdTomato-positive cells were observed in the iridocorneal angle of AP-2β NCC KO mice, when compared with control mice. In addition, at P7 and P14, the cells of the control

iridocorneal angle consisted of multiple cell layers that were spread over a larger area, whereas there were fewer labeled cells in the KO angle, and these cells were more closely spaced (Fig. 2.3E-H).

To investigate whether proliferative or apoptotic changes had contributed to the observation of fewer POM cells in the iridocorneal angle of AP-2β NCC KO mice during development, we employed PH3 as a proliferative marker, as well as a TUNEL assay for apoptotic changes. No difference in apoptosis was observed in the angle of the AP-2β NCC KO mice versus controls at all stages examined, which included E15.5, P1, P7 and P14 (Fig. 2.S1-2.S2). Moreover, there were no changes observed in proliferation as indicated by PH3 staining at E15.5 and E18.5 (data not shown). However, at P7 (Fig. 2.4A-D), there was a significant reduction observed in PH3 staining in the trabecular meshwork region of AP-2β NCC KO mice, as indicated by the reduced number of cells positive for both PH3 and αSMA, the latter being a trabecular meshwork marker (Fig. 2.4I; n=3 eyes; p<0.05; analyzed region outlined with white dashed lines) (Ko & Tan, 2013; Overby et al., 2014). By P14 (Fig. 2.4E-H), the reduction in the number of proliferating trabecular meshwork cells in the KO versus control mice remained significant, as determined by cell counts of PH3 and αSMA double positive cells (Fig. 2.4J; n=4 eyes; p<0.001; analyzed region outlined with white dashed lines).

To further determine whether the trabecular meshwork region was differentiating appropriately in the AP-2β NCC KO mice, we examined the expression of myocilin, a known trabecular meshwork marker, along with αSMA, at early postnatal and adult stages (Overby et al., 2014; Robertson et al., 2013). At both P14 (Fig. 2.S3) and adult stages (2-3 months) (Fig. 2.5) there was a reduction in expression of myocilin in the angle of the mutant mice when contrasted with controls. In addition, at 2 to 3 months of age, a reduction in expression of αSMA was observed

in the trabecular region of KO mice compared to controls (Fig. 2.5). When quantified, the number of αSMA-positive cells was significantly reduced in the NCC KO animals (Fig. 2.5E; n=4 eyes, p<0.001; analyzed region outlined with dashed lines in A-B) in the trabecular region (Fig. 2.5B, asterisk) when compared to control littermates (Fig. 2.5A; TM). In order to examine development of Schlemm's canal, another important outflow structure, immunohistochemistry was performed for endomucin, a marker of this structure (Kizhatil et al., 2014). At P7 (Fig. 2.6A-B; n=3 eyes), endomucin expression was low in the iridocorneal angle of both control and KO mice. However, at P14 (Fig. 2.6C-D; n=4 eyes) and 2-3 months of age (Fig. 2.6E-F; n=3 eyes), endomucin expression was prominent in the Schlemm's canal endothelium of control mice (Fig. 2.6C & E; SC, demarcated with open white arrowheads), whereas a similar pattern of staining appeared to be absent in the NCC KO iridocorneal angle (Fig. 2.6D & F).

We next examined the morphology of the angle region in AP-2β NCC KO mice and age-matched control littermates in detail using plastic and ultrastructural sections at P14 (Fig. 2.7). While control animals exhibited normal roughly alternating layers of trabecular beams and trabecular meshwork cells in toluidine blue-stained sections (Fig. 2.7A, arrowheads), the AP-2β NCC KO animals did not show clear spacing between adjacent iridocorneal angle cells, with the entire angle region appearing compact (Fig. 2.7B; arrowheads). Ultrastructural analysis showed that at P14 in control mice, trabecular beams (Fig. 2.7C, marked with red arrowheads; Fig. 2.7E, higher magnification image of Fig. 2.7C) presented as a collection of collagen fibrils interspersed with elastin fibres, and these beams were typically surrounded by trabecular meshwork cells (Fig. 2.7C & E, trabecular meshwork). In contrast, the iridocorneal angle was closed in the AP-2β NCC KO mice, and the angle tissue could not easily be distinguished from the corneal stroma. Importantly, there were no obvious trabecular beams in the mutant angle (Fig. 2.7D; Fig. 2.7F,

higher magnification image of Fig. 2.7D). These observations are consistent with the fact that fewer POM-derived cells were observed in the angle of the AP-2β NCC KO mutants, since these are the cells responsible for secreting the extracellular matrix components required for proper trabecular beam formation (Acott & Kelley, 2008).
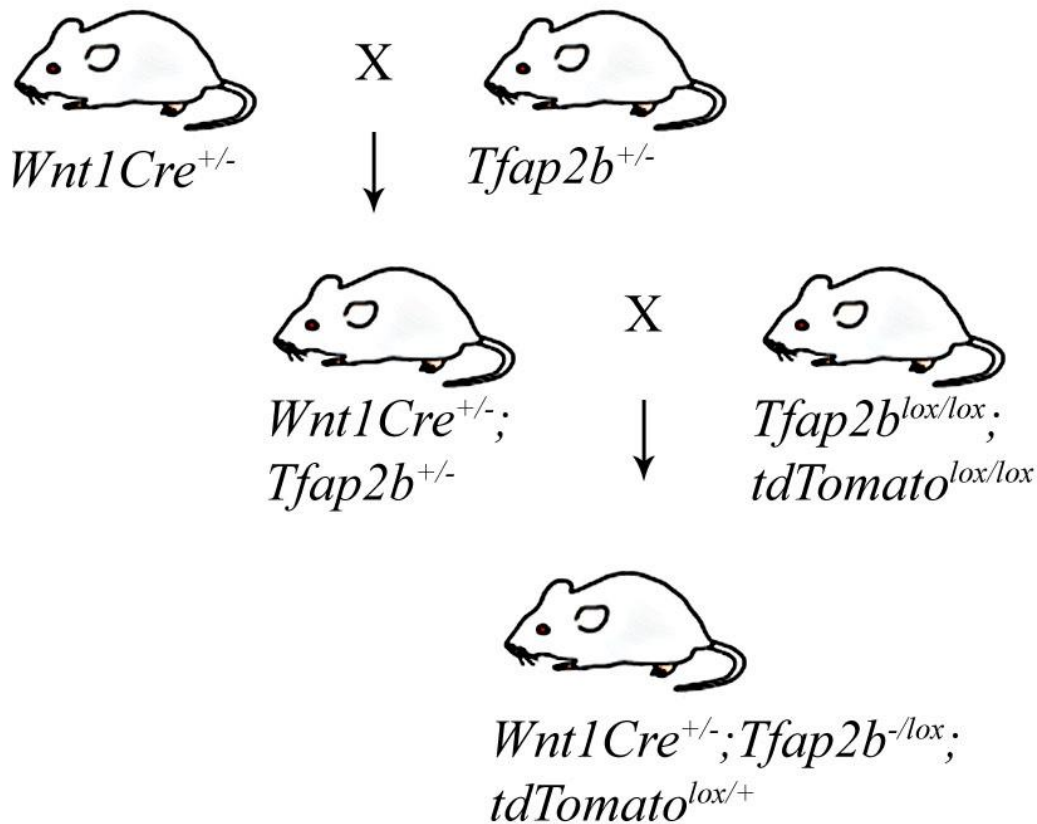
Fig. 2.1. Breeding scheme for AP-2β NCC KO mice. Mice heterozygous for the *Wnt1Cre*^{+/-} genotype were bred with heterozygous *Tfap2b*^{+/-} gene deletion mutants. The progeny were bred with mice containing the *Tfap2b*[lox/lox]; *tdTomato*[lox/lox] genotype to ensure that Cre recombinase binds to the loxP sites flanking the AP-2β gene to ensure deletion specifically in the NCCs. Adapted from Hicks (2017).
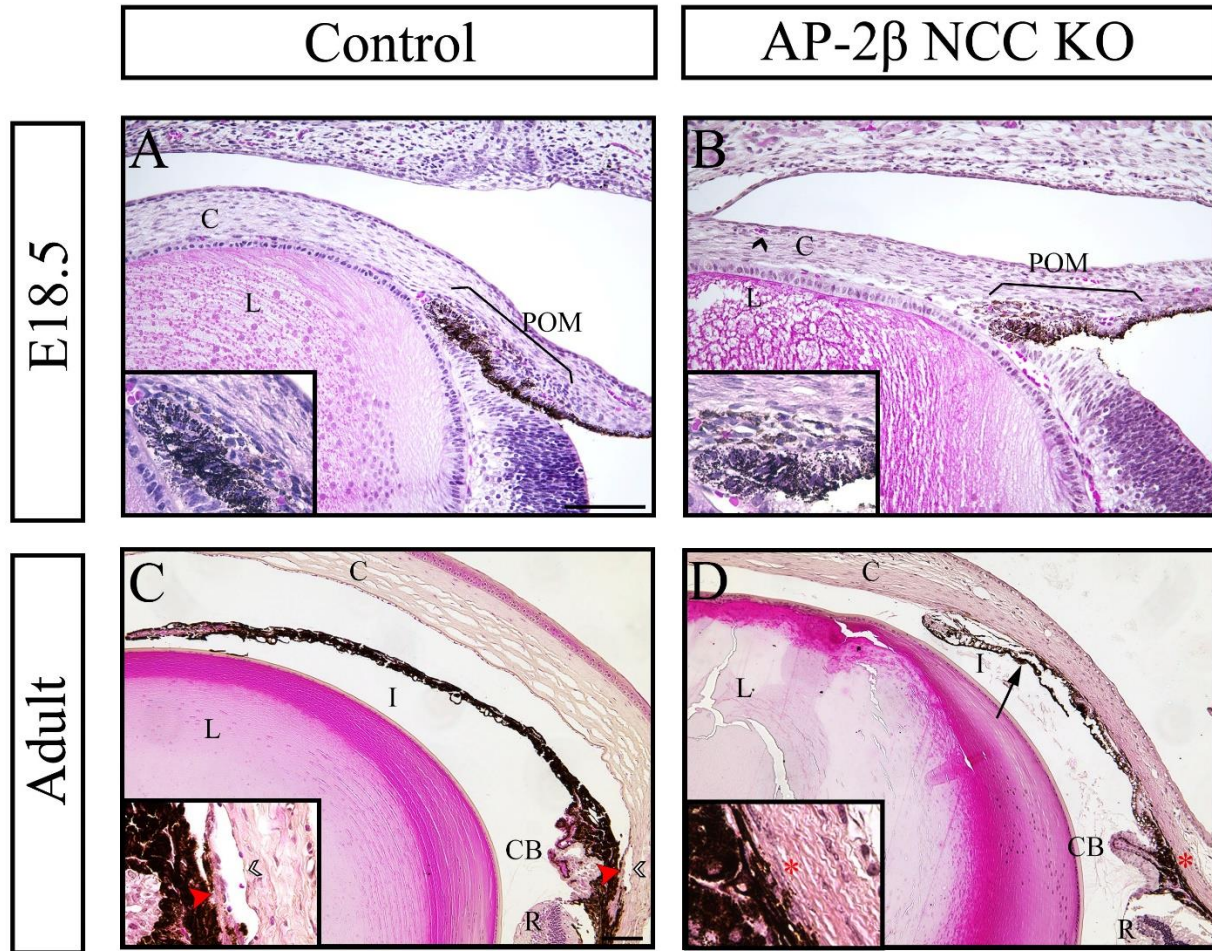
Fig. 2.2. H&E stained sagittal sections of control (A, C) and AP-2β NCC KO (B, D) eyes at E18.5 (A, B) and adult stages (C, D). A-B) At E18.5, the AP-2β NCC KO mouse does not have overt defects in the POM region when compared with control animals (POM region marked with square brackets; insets are higher magnification images of the POM). POM cells are present in approximately the same location near the anterior rim of the developing neural retina in both control and KO animals, and the control POM cells also appear similar to the KO POM cells (A-B, insets). However, blood vessels are present in the corneal stroma of KO animals (B, open black arrowhead) when compared with the control cornea (A). C-D) The adult AP-2β NCC KO mouse displays a closed iridocorneal angle phenotype (D, black arrow), along with other anterior segment defects, including abnormalities in the ciliary body and cornea. Additionally, while the control

animals contain fully formed iridocorneal angle structures, including the trabecular meshwork (C, inset; closed red arrowhead) and Schlemm's canal (C, inset; open white arrowhead), the KO mice do not have obvious iridocorneal angle structures (D, inset; asterisk). C, cornea; POM, periocular mesenchyme; I, iris; CB, ciliary body; L, lens; R, retina. Scale bars represent 100 μm.
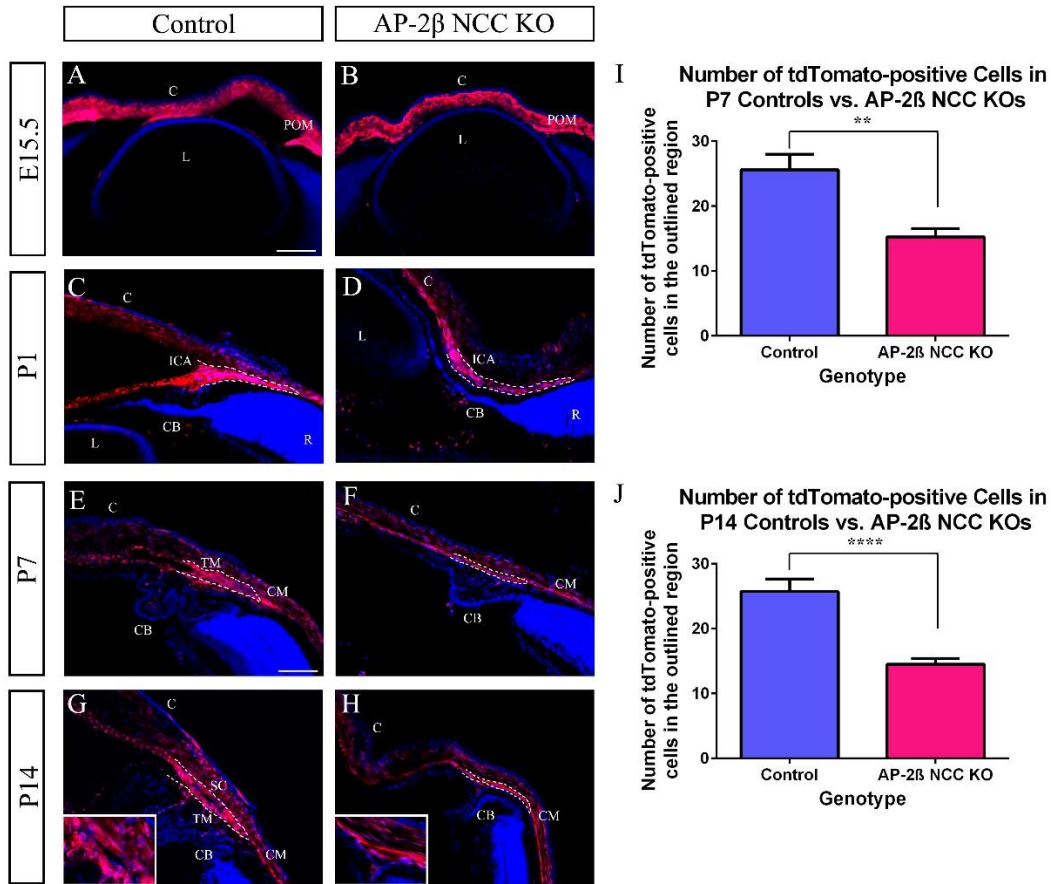
Fig. 2.3. Fluorescent imaging of tdTomato expression in transverse sections of E15.5 eyes, and sagittal sections of P1, P7 and P14 eyes. A-B) At E15.5 (n=3 eyes), there appears to be no difference in the NCC contribution to the anterior segment between control and AP-2β NCC KO mice, as indicated by tdTomato expression (red). C-D) At P1 (n=3 eyes), there is no major difference in the number of POM cells found in the iridocorneal angle of KO versus control mice. E-H) At both P7 (n=3 eyes) and P14 (n=4 eyes), there appear to be fewer neural crest-derived cells

marked by tdTomato expression in the iridocorneal angle region of AP-2β NCC KO mice when compared with control mice. Furthermore, the cells of the control iridocorneal angle at both stages consist of multiple cell layers that are spread over a larger area (E & G), unlike the KO angle, which contains fewer layers of cells that are closely spaced together (F & H). Insets in panels G-H are higher magnification images of the iridocorneal angle region in the P14 control and KO mice, respectively. I-J). At both P7 (I, n=3 eyes) and P14 (J, n=4 eyes) there is a significant decrease in the number of tdTomato-positive cells in the iridocorneal angle region of KO mice when compared with control mice (** signifies a p-value<0.01; **** p-value<0.0001; error bars represent standard deviation; analyzed region in dashed lines; 2-3 sections were evaluated per eye, and 1-2 cell count measurements were acquired per section). DAPI staining (blue) was used to visualize nuclei. C, cornea; POM, periocular mesenchyme; ICA, iridocorneal angle; CB, ciliary body; L, lens; R, retina; CM, ciliary muscle; trabecular meshwork, trabecular meshwork; SC, Schlemm's canal. Scale bars represent 100 µm.
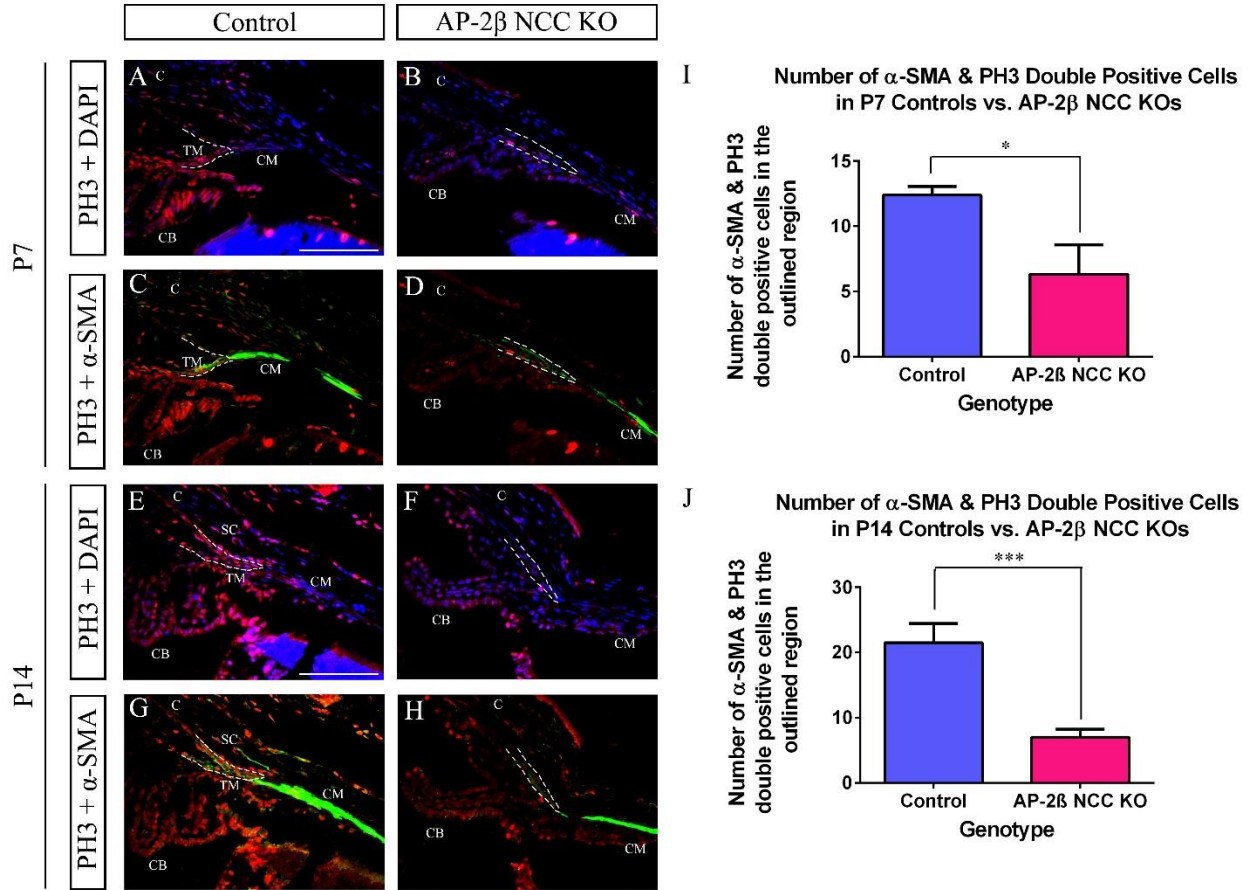
Fig. 2.4. αSMA–PH3 co-staining of P7 and P14 sagittal sections. A-D) At P7, there is a reduction in the number of αSMA (green) and PH3 (red) double positive cells in the trabecular meshwork region (white dashed lines) of AP-2β NCC KO animals compared with controls. E-H) At P14, there continues to be a reduction in the number of αSMA and PH3 double positive cells in the trabecular meshwork region in the AP-2β NCC KO mice, as compared with control mice. I-J). Quantification of double positive cells at P7 (I, n=3 eyes) and P14 (J, n=4 eyes) confirms a significant reduction of proliferation in the AP-2β NCC KO trabecular meshwork (* signifies a p-value<0.05; *** signifies a p-value<0.001; error bars represent standard deviation; analyzed region marked with white dashed lines; 2-3 sections were evaluated per eye, and 1-2 cell count measurements were obtained from each section). However, at both P7 and P14, there is no difference in αSMA or PH3 expression in the ciliary muscle region. DAPI staining (blue) was used

to visualize nuclei. TM, trabecular meshwork; C; cornea; CB, ciliary body; CM, ciliary muscle; SC, Schlemm's canal. Scale bars represent 100 μm.
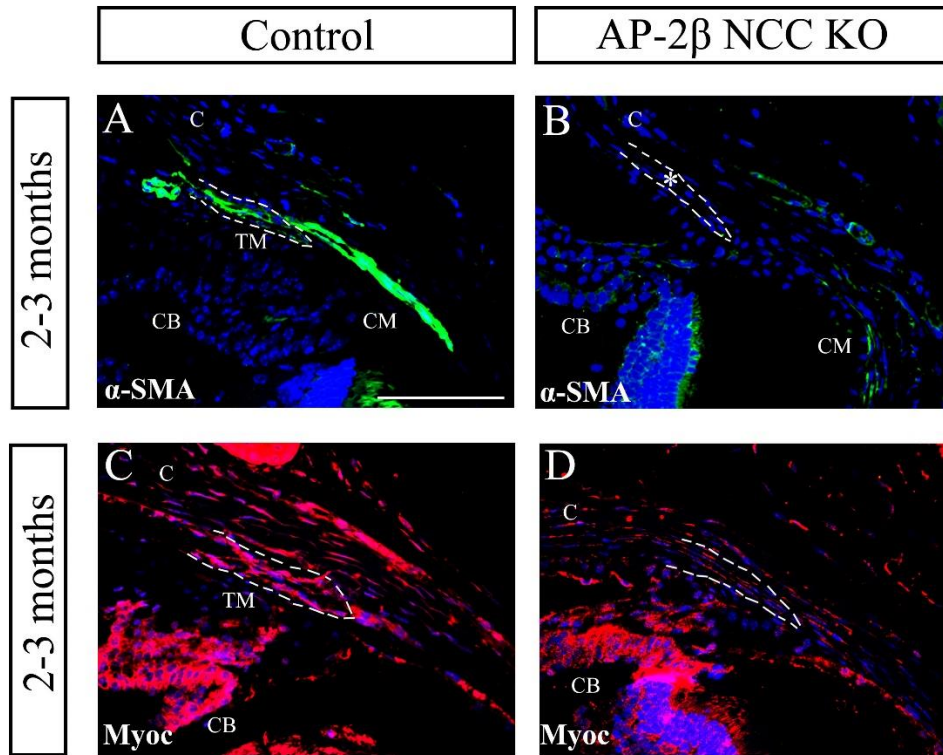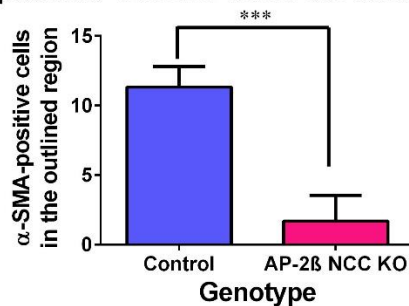
Fig. 2.5. αSMA and myocilin staining using sagittal sections of 2 to 3 month-old eyes. (A-B) αSMA expression (green) is reduced in NCC KO animals, both in the trabecular meshwork region (B, asterisk) and ciliary muscle region (B, CM), when compared to control littermates (A; trabecular meshwork & CM). C-D). At 2 to 3 months of age, there is a reduction in expression of

myocilin (red) in the iridocorneal angle region of AP-2β NCC KO mice compared with controls (C & D, dashed lines). E) There is a significant reduction in the number of αSMA-positive cells in the trabecular meshwork region of NCC KOs when compared with control animals (n=3 eyes; *** signifies a p-value<0.001; error bars show standard deviation; analyzed regions outlined with dashed lines in A-B; 2-3 sections were evaluated per eye, and 1-2 cell count measurements were obtained from each section). DAPI staining (blue) was used to visualize nuclei. TM, trabecular meshwork; CM, ciliary muscle; C, cornea; CB, ciliary body. Scale bar represent 100 μm.
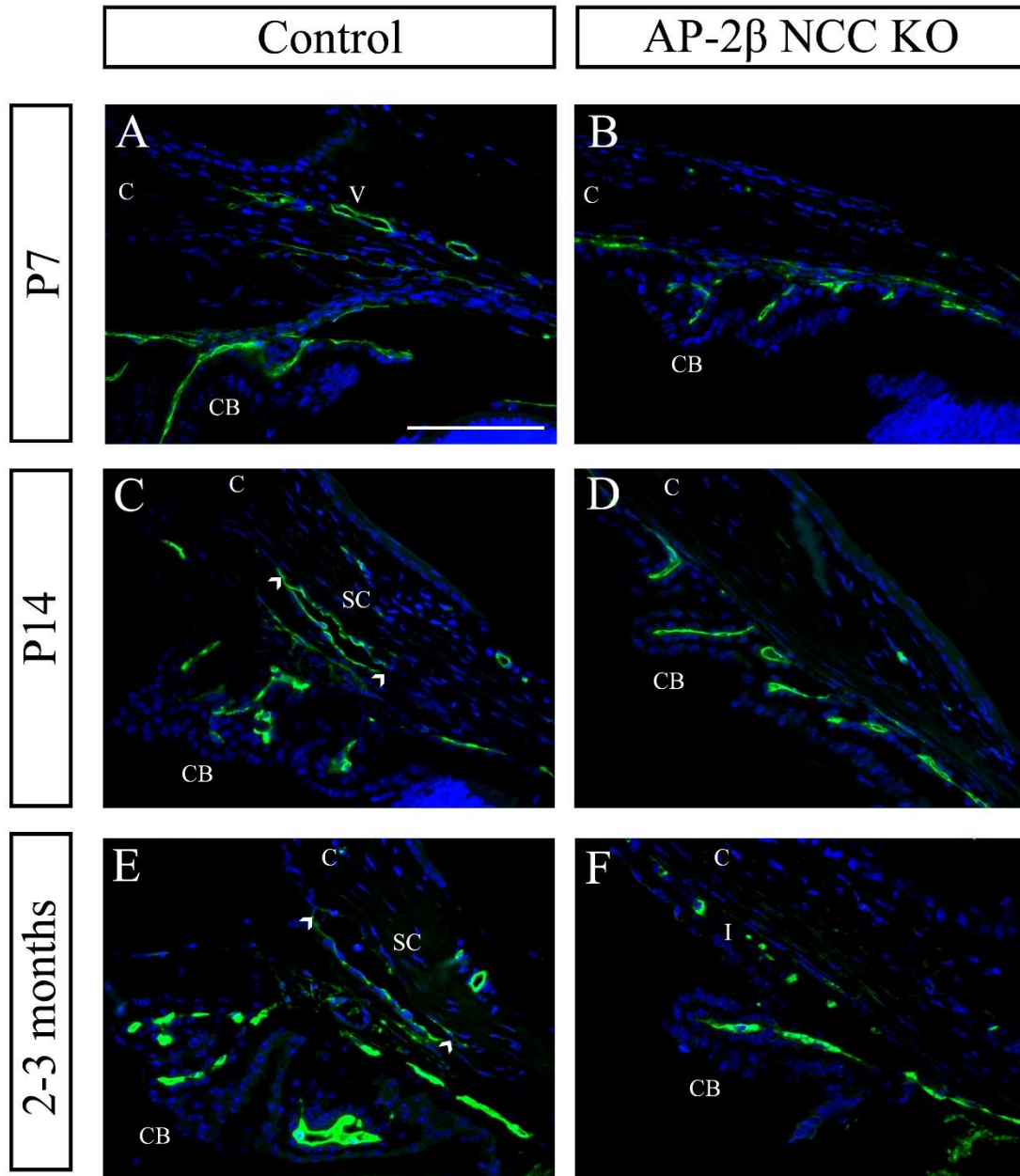
Fig. 2.6. Endomucin staining of the Schlemm's canal in sagittal sections of P7, P14 and 2-3 month-old mice. A-F) At P7 (A-B; n=3 eyes), endomucin expression is low in the developing iridocorneal angle of both control (A) and KO (B) mice. However, at P14 (C-D; n=4 eyes) and 2-3 months of age (E-F; n=3 eyes), endomucin expression is prominent in the Schlemm's canal endothelium of control mice (C & E; SC, arrowheads), whereas a similar pattern of staining appears to be absent in the AP-2β NCC KO iridocorneal angle (D & F). DAPI staining (blue) was

used to visualize nuclei. C, cornea; CB, ciliary body; SC, Schlemm's canal; I, iris; V, blood vessels. Scale bars represent 100 μm.
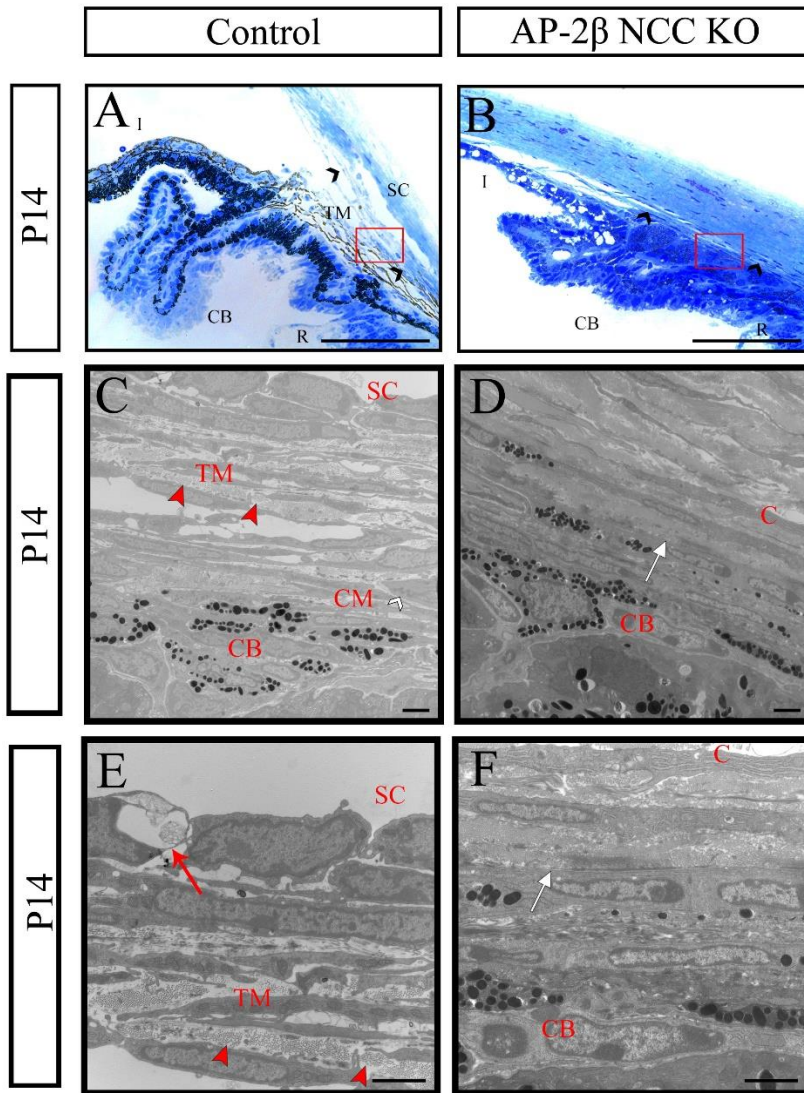
Fig. 2.7. Transmission electron micrographs of the P14 trabecular meshwork region, sectioned in the sagittal plane. A-B) The top 2 panels are toluidine blue stained plastic sections of the P14 iridocorneal angle, with the approximate areas captured by TEM in C-D outlined with red boxes. The black arrowheads mark the extent of the angle. C) The control iridocorneal angle contains trabecular beams (closed red arrowheads) that are surrounded by trabecular meshwork

cells. The tip of a ciliary muscle cell is visible (open white arrowhead). D) The NCC KO iridocorneal angle is closed so that the corneal stroma, angle tissue, and outer ciliary body epithelium (OCE) are all juxtaposed. The boundary between the corneal stroma and angle tissue is not distinct. The OCE can be distinguished from the angle tissue by the presence of melanin granules (boundary marked by open white arrow). E) A higher magnification image of the trabecular meshwork region from Panel C contains trabecular beams (red arrowheads), typified by the presence of collagen fibrils and elastin fibers. A giant vacuole is present in the Schlemm's canal endothelium (red arrow). F) In a higher magnification image of Panel D, there are no obvious trabecular meshwork beams, although presumptive angle tissue cell nuclei can be observed above the OCE. CB, ciliary body; TM, trabecular meshwork; SC, Schlemm's canal; I, iris; R, retina; C, cornea; CM, ciliary muscle. Scale bars in A-B represent 100 µm, and scale bars in C-F represent 2 µm.
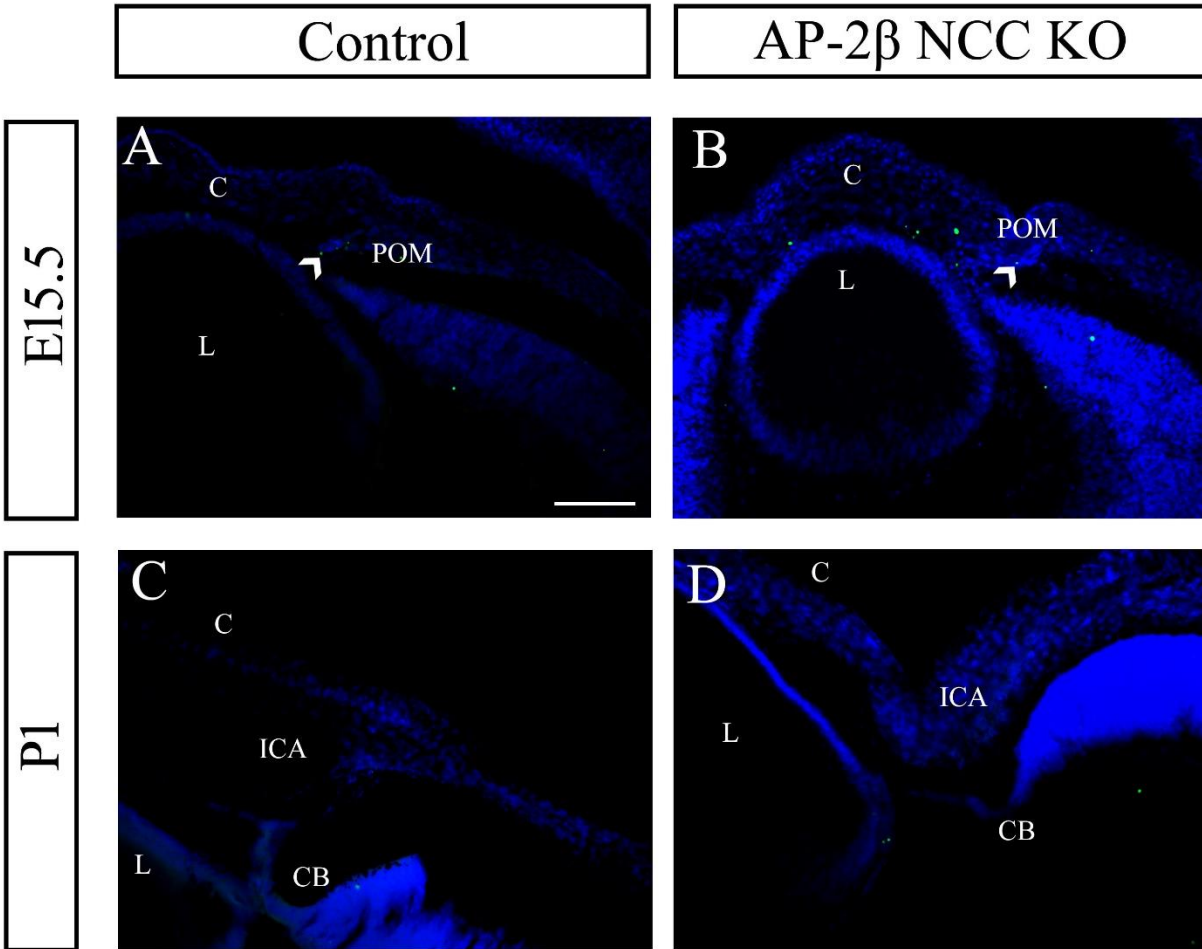
Fig. 2.S1. TUNEL staining at E15.5 and P1. A-D) At both E15.5 and P1, there is no observable difference in TUNEL staining (green) between control and AP-2β NCC KO animals (n=3). White arrowheads highlight TUNEL staining in the POM. DAPI staining (blue) was used to visualize nuclei. POM, periocular mesenchyme; ICA, iridocorneal angle; CB, ciliary body; C, cornea; L, lens. Scale bars represent 100 μm.
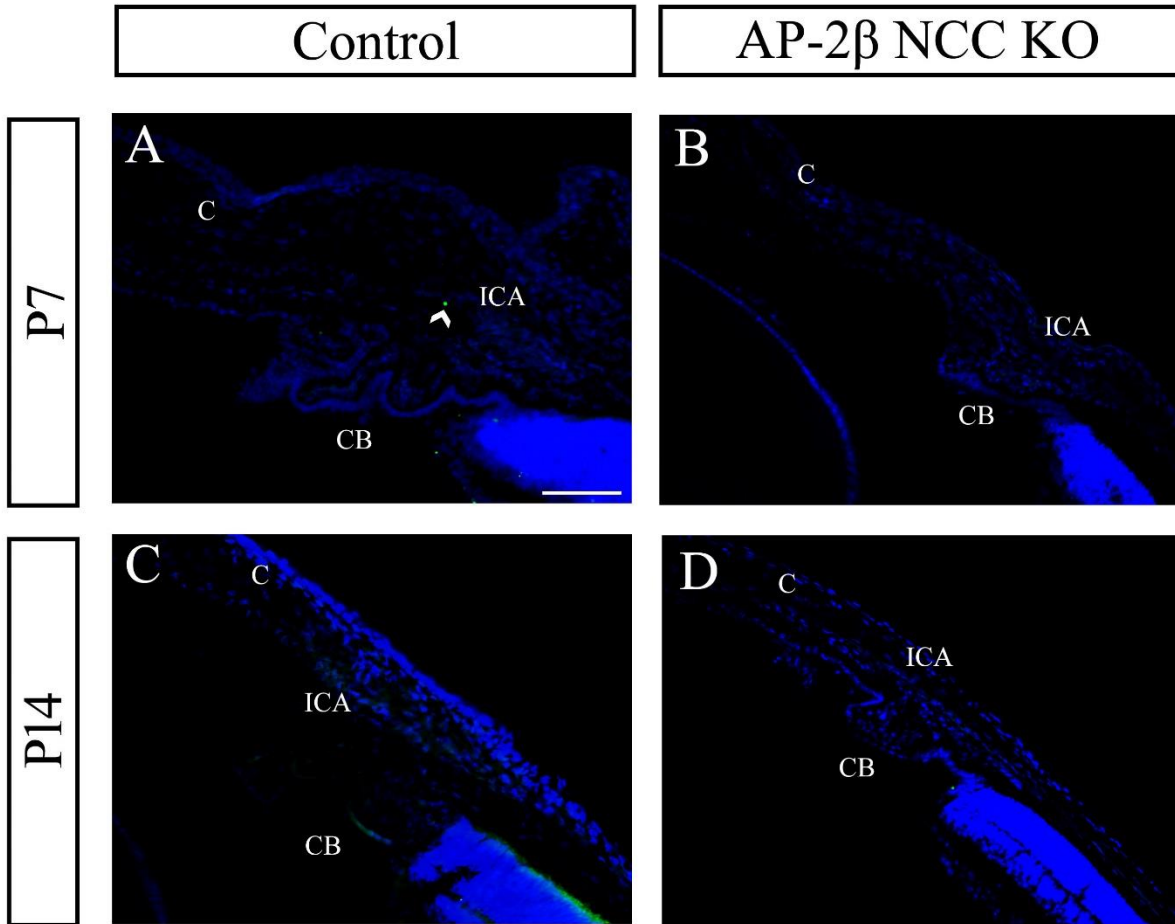
Fig. 2.S2. TUNEL staining at P7 and P14. A-D) At P7 and P14, there is no observable difference in TUNEL staining (green) between control and AP-2β NCC KO animals (n=3). The white arrowhead highlights occasional TUNEL staining in the POM. DAPI (blue) was used to visualize nuclei. ICA, iridocorneal angle; CB, ciliary body; C, cornea. Scale bars represent 100 μm.
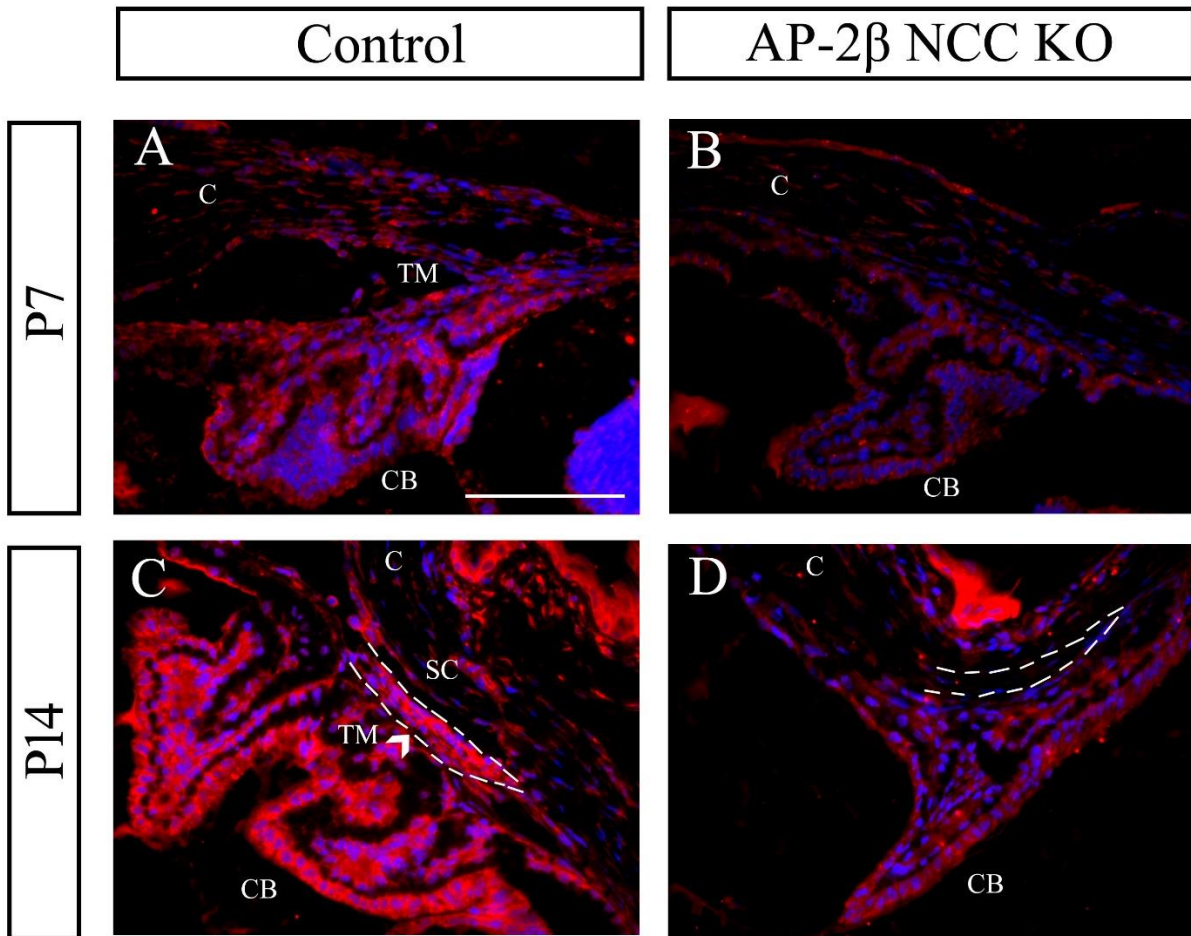
Fig. 2.S3. Myocilin staining at P7 and P14 using sagittal sections. (A-B) At P7 (n=3), there is very little expression of myocilin (red) in the iridocorneal angle region of both control and AP-2β NCC KO mice. C-D) By P14 (n=3), control animals exhibit significant myocilin expression in the iridocorneal angle region (white arrowhead), but this is not apparent in the AP-2β NCC KO (C & D, dashed lines). DAPI staining (blue) was used to visualize nuclei. TM, trabecular meshwork; CB, ciliary body; C, cornea; SC, Schlemm's canal. Scale bar represent 100 μm.

2.4. Discussion

Anterior segment dysgenesis involves improper development of several anterior ocular structures and contributes to vision loss. The trabecular meshwork and the ciliary body are both

anterior segment tissues that develop postnatally and are important for the maintenance of IOP. The trabecular meshwork, ciliary body and cornea all receive contributions from the POM, and several genes have been shown to play a role in their development (Chen, 2016; Chen et al., 2016; Cvekl & Tamm, 2004; Liu & Johnson, 2010; Smith et al., 2000). One such gene, *Tfap2b* encoding AP-2β, is expressed during eye development, and conditional deletion of AP-2β from NCCs has been shown to lead to corneal opacity and increased IOP, associated with defects of anterior segment structures (Martino et al., 2016). Consequently, in this study, the requirement for AP-2β within the NCC-derived POM of the eye and the tissues to which it gives rise was further investigated. Using Wnt1Cre-mediated conditional deletion of AP-2β in mice, this transcription factor was shown to be required for proper differentiation of a number of POM-derived tissues including the trabecular meshwork and Schlemm's canal. The AP-2β NCC mutants exhibited defects in the angle region that arose during postnatal development, involving a reduction in proliferation of POM cells and a lack of appropriate differentiation markers used to identify the trabecular meshwork and Schlemm's canal. Since these structures are key in regulating aqueous humour outflow, it is likely that their absence contributed to the elevated IOP previously reported in the AP-2β NCC KO mice (Chen et al., 2016; Hara et al., 2018; Martino et al., 2016).

Our examination of the fate of NCC-derived POM in the AP-2β NCC KO mice using the tdTomato allele revealed no difference between controls in the appearance of the POM cells contributing to the anterior segment tissues during the early developmental stages examined (Fig. 2.3). This suggested that defects in early migration and/or population of NCC-derived POM into the eye likely did not contribute to the defects observed. However, a significant reduction in proliferation of the POM cells in the region of the trabecular meshwork was observed postnatally in the mutants compared to controls. Interestingly, *Tfap2b* has been shown to play a role in

regulating proliferation in other systems, such as breast cancer cells (Raap et al., 2018). Thus, AP-2β may be required in order to maintain cell proliferation in the trabecular meshwork region during postnatal development.

The trabecular meshwork consists of trabecular beams, composed of collagen fibrils intermixed with elastin fibres and other extracellular matrix components that form long beams covered by trabecular meshwork cells, an endothelial-like cell type (Acott & Kelley, 2008). The trabecular meshwork cells normally secrete the extracellular matrix components required for trabecular beam formation (Cvekl & Tamm, 2004), and the lack of structurally defined trabecular beams in the AP-2β NCC KO, compared with the defined beams that were surrounded by trabecular meshwork cells in control animals, may be reflective of the reduced number of trabecular meshwork cells observed during postnatal development in the KO. Alternatively, the absence of trabecular beams may indicate a defect in differentiation and/or function of these cells. In this context, POM cells that remained in the trabecular meshwork region of the mutant eyes did not express two previously identified trabecular meshwork markers, αSMA and myocilin (Overby et al., 2014; Robertson et al., 2013).

It is possible that the defect in differentiation occurred because AP-2β plays a direct, cell-autonomous role in regulating trabecular meshwork cell differentiation. Indeed, our laboratory has shown a cell-autonomous requirement for AP-2β in other ocular tissues (Bassett et al., 2012; West-Mays et al., 1999). Moreover, as shown in our previous study (Martino et al., 2016), corneal endothelial cells do not differentiate in the absence of AP-2β, further supporting the possibility that AP-2β plays a direct role in differentiation of POM derivatives, such as trabecular meshwork cells. However, it is also possible that the closed iridocorneal angle may have prevented the POM cells from proliferating and differentiating properly in the AP-2β NCC KO mice. For example, it

has been suggested that an open iridocorneal angle in the developing postnatal mouse eye is required for proper trabecular meshwork development (Cvekl & Tamm, 2004). The open angle is thought to provide space for dynamic remodeling of the POM cells that may be important for differentiation into functional trabecular meshwork cells. Furthermore, a closed iridocorneal angle may prevent the developing POM cells from accessing growth factors and molecules secreted into the aqueous humour by the ciliary body that are required for trabecular meshwork proliferation and differentiation (Smith et al., 2000). Further studies are required to distinguish between a cell-autonomous versus a non-cell-autonomous role for AP-2β in trabecular meshwork cell differentiation by utilizing more specific Cre tools to delete AP-2β from the trabecular meshwork.

On the other hand, the absence of expression of the Schlemm's canal marker, endomucin, is most likely a non-cell-autonomous effect of AP-2β deletion, since the Schlemm's canal is derived from the paraxial mesoderm cell population of the POM, and not the NCC population. Although the Schlemm's canal is not derived from NCCs, the lack of formation of this structure appears to be a consistent effect in the NCC KO mice, as multiple H&E and toluidine blue-stained sections of numerous NCC KO animals at various ages have been examined, and the Schlemm's canal has not been observed (data not shown). One possible explanation for the absence of a Schlemm's canal in these mutants is that AP-2β expression in NCCs may be acting in a non-cell-autonomous manner on mesoderm cells to affect development of mesoderm-derived structures, such as the Schlemm's canal. The second possible explanation is that the closed iridocorneal angle may be preventing remodeling of the POM cells early during postnatal development, as mentioned above, which could then be resulting in the lack of formation of a Schlemm's canal (Smith et al., 2001).

Additional transcription factors presumed to be in a similar genetic cascade as AP-2β have also been implicated in regulating development of the trabecular meshwork. For example, previous

research has shown that *Pitx2* lies upstream of *Tfap2b* (Chen et al., 2016), and heterozygous Pitx2-null mice exhibit defects in the trabecular meshwork region when compared with control mice, similar to the results observed here using AP-2β NCC KO mice (Chen, 2016). Foxc1 is a suspected downstream effector of AP-2β, the deletion of which also leads to abnormal development of the trabecular meshwork (Chen et al., 2016; Smith et al., 2001). Deletion of the transcription factor, Lmx1b, in mice results in a hypoplastic trabecular meshwork and other anterior segment defects similar to those observed in the AP-2β NCC KO mice (Cross et al., 2014; Liu & Johnson, 2010). As the trabecular meshwork is a crucial tissue for aqueous humour outflow and IOP maintenance, elucidating the gene regulatory network in which *Tfap2b*, *Pitx2*, *Foxc1* and *Lmx1b* participate to control trabecular meshwork cell proliferation and differentiation will be an important next step.

References

Acott, T. S., & Kelley, M. J. (2008). Extracellular matrix in the trabecular meshwork. *Exp Eye Res., 86*(4), 543-561.

Barzago, M. M., Kurosaki, M., Fratelli, M., Bolis, M., Giudice, C., Nordio, L., . . . Garattini, E. (2017). Generation of a new mouse model of glaucoma characterized by reduced expression of the AP-2β and AP-2δ proteins. *Sci Rep., 7*, 11140.

Bassett, E., Korol, A., Deschamps, P., Buettner, R., Wallace, V., Williams, T., & West-Mays, J. (2012). Overlapping expression patterns and redundant roles for AP-2 transcription factors in the developing mammalian retina. *Dev Dyn., 241*(4), 814-829.

Bassett, E., Pontoriero, G., Feng, W., Marquardt, T., Fini, M., Williams, T., & West-Mays, J. (2007). Conditional deletion of activating protein 2alpha (AP-2alpha) in the developing

retina demonstrates non-cell-autonomous roles for AP-2alpha in optic cup development. *Mol Cell Biol., 27*(21), 7497-7510.

Bassett, E., Williams, T., Zacharias, A., Gage, P., Fuhrmann, S., & West-Mays, J. (2010). AP-2alpha knockout mice exhibit optic cup patterning defects and failure of optic stalk morphogenesis. *Hum Mol Genet., 19*(9), 1791-1804.

Chen, L., & Gage, P. J. (2016). Heterozygous Pitx2 Null Mice Accurately Recapitulate the Ocular Features of Axenfeld-Rieger Syndrome and Congenital Glaucoma. *IOVS, 57*, 5023-5030.

Chen, L., Martino, M., Dombkowski, A., Williams, T., West-Mays, J., & Gage, P. J. (2016). AP-2β is a downstream effector of PITX2 required to specify endothelium and establish angiogenic privilege during corneal development. *Invest Ophthalmol Vis Sci., 57*(3), 1072–1081.

Chograni, M., Derouiche, K., Chaabouni, M., Lariani, I., & Bouhamed, H. C. (2014). Molecular analysis of the PAX6 gene for aniridia and congenital cataracts in Tunisian families. *Human Genome Variation, 1*(14008).

Cross, S., Macalinao, D., McKie, L., Rose, L., Kearney, A., Rainger, J., . . . IJ, J. (2014). A dominant-negative mutation of mouse Lmx1b causes glaucoma and is semi-lethal via LDB1-mediated dimerization. *PLoS Genet., 10*(5), e1004359.

Cvekl, A., & Tamm, E. (2004). Anterior eye development and ocular mesenchyme: new insights from mouse models and human diseases. *Bioessays, 26*(4), 374-386.

Eckert, D., Buhl, S., Weber, S., Jäger, R., & Schorle, H. (2005). The AP-2 family of transcription factors. *Genome Biology, 6*(13), 246.

Gage, P., Rhoades, W., Prucka, S., & Hjalt, T. (2005). Fate maps of neural crest and mesoderm in the mammalian eye. *Invest Ophthalmol Vis Sci., 46*(11), 4200-4208.

Garcia-Montalvo, I. A., Pelcastre-Luna, E., Nelson-Mora, J., Buentello-Volante, B., Miranda-Duarte, A., & Zenteno, J. C. (2014). Mutational screening of FOXE3, GDF3, ATOH7, and ALDH1A3 in congenital ocular malformations. Possible contribution of the FOXE3 p.VAL201MET variant to the risk of severe eye malformations. *Ophthalmic Genetics, 35*(3), 190–192.

Gould, D., Smith, R., & John, S. (2004). Anterior segment development relevant to glaucoma. *Int J Dev Biol., 48*(8-9), 1015-1029.

Gould, D. B., & John, S. W. (2002). Anterior segment dysgenesis and the developmental glaucomas are complex traits. *Hum Mol Genet., 11*(10), 1185-1193.

Hara, S., Kawasaki, S., Yoshihara, M., Winegarner, A., Caleb, B., Tsujikawa, M., & Nishida, K. (2018). Transcription factor TFAP2B up-regulates human corneal endothelial cell–specific genes during corneal development and maintenance. *Journal of Biol. Chem., 294*, 2460–2469.

Hicks, E. A. (2017). *THE ROLE OF AP-2α AND AP-2β IN RETINAL DEVELOPMENT.* (M. Sc.), McMaster University, Hamilton.

Kerr, C., Zaveri, M., Robinson, M., Williams, T., & West-Mays, J. (2014). AP-2α is required after lens vesicle formation to maintain lens integrity. *Developmental Dynamics, 243*(10), 1298–1309.

Kizhatil, K., Ryan, M., Marchant, J. K., Henrich, S., & John, S. W. M. (2014). Schlemm's Canal Is a Unique Vessel with a Combination of Blood Vascular and Lymphatic Phenotypes that Forms by a Novel Developmental Process. *PLOS Biology, 12*(7), e1001912.

Ko, M., & Tan, J. (2013). Contractile markers distinguish structures of the mouse aqueous drainage tract. *Mol Vis., 19*, 2561–2570.

Lewis, A., Vasudevan, H., O'Neill, A., Soriano, P., & Bush, J. (2013). The widely used Wnt1-Cre transgene causes developmental phenotypes by ectopic activation of Wnt signaling. *Dev Biol., 379*(2), 229-234.

Liu, P., & Johnson, R. (2010). Lmx1b is required for murine trabecular meshwork formation and for maintenance of corneal transparency. *Dev Dyn., 239*(8), 2161-2171.

Madisen, L., Zwingman, T., Sunkin, S., Oh, S., Zariwala, H., Gu, H., . . . Zeng, H. (2010). A robust and high-throughput Cre reporting and characterization system for the whole mouse brain. *Nat Neurosci., 13*(1), 133-140.

Martino, V. B., Sabljic, T., Deschamps, P., Green, R. M., Akula, M., Peacock, E., . . . West-Mays, J. A. (2016). Conditional deletion of AP-2β in the cranial neural crest results in anterior segment dysgenesis and early-onset glaucoma. *Disease Models & Mechanisms, 9*(8), 849–861.

Moser, M., Pscherer, A., Roth, C., Becker, J., Mücher, G., Zerres, K., Dixkens, C., Weis, J., Guay-Woodford, L., Buettner, R., & Fässler, R. (1997). Enhanced apoptotic cell death of renal epithelial cells in mice lacking transcription factor AP-2β. *Genes Dev., 11*(14), 1938–1948.

Napier, H., & Kidson, S. (2005). Proliferation and cell shape changes during ciliary body morphogenesis in the mouse. *Dev Dyn., 233*(1), 213-223.

Overby, D., Bertrand, J., Schicht, M., Paulsen, F., Stamer, W., & Lütjen-Drecoll, E. (2014). The structure of the trabecular meshwork, its connections to the ciliary muscle, and the effect of pilocarpine on outflow facility in mice. *Invest Ophthalmol Vis Sci., 55*(6), 3727-3736.

Pontoriero, G., Deschamps, P., Ashery-Padan, R., Wong, R., Yang, Y., Zavadil, J., . . . West-Mays, J. (2008). Cell autonomous roles for AP-2alpha in lens vesicle separation and maintenance of the lens epithelial cell phenotype. *Dev Dyn., 237*(3), 602-617.

Raap, M., Gronewold, M., Christgen, H., Glage, S., Bentires-Alj, M., Koren, S., . . . Christgen, M. (2018). Lobular carcinoma in situ and invasive lobular breast cancer are characterized by enhanced expression of transcription factor AP-2β. *Lab Invest., 98*(1), 117-129.

Robertson, J. V., Siwakoti, A., & West-Mays, J. A. (2013). Altered expression of transforming growth factor beta 1 and matrix metalloproteinase-9 results in elevated intraocular pressure in mice. *Mol Vis., 19*, 684–695.

Romero, P., Sanhueza, F., Lopez, P., Reyes, L., & Herrera, L. (2011). c.194 A>C (Q65P) mutation in the LMX1B gene in patients with nail-patella syndrome associated with glaucoma. *Molecular Vision, 17*, 1929–1939.

Smith, R., Zabaleta, A., Kume, T., Savinova, O., Kidson, S., Martin, J., . . . John, S. (2000). Haploinsufficiency of the transcription factors FOXC1 and FOXC2 results in aberrant ocular development. *Hum Mol Genet., 9*(7), 1021-1032.

Smith, R., Zabaleta, A., Savinova, O., & John, S. (2001). The mouse anterior chamber angle and trabecular meshwork develop without cell death. *BMC Dev Biol., 1*(3).

Summers, K. M., Withers, S. J., Gole, G. A., Piras, S., & Taylor, P. J. (2008). Anterior segment mesenchymal dysgenesis in a large Australian family is associated with the recurrent 17 bp duplication in PITX3. *Molecular Vision, 14*, 2010–2015.

Tümer, Z., & Bach-Holm, D. (2009). Axenfeld–Rieger syndrome and spectrum of PITX2 and FOXC1 mutations. *European Journal of Human Genetics, 17*(12), 1527–1539.

Van Otterloo, E., Li, H., Jones, K. L., & Williams, T. (2018). AP-2α and AP-2β cooperatively orchestrate homeobox gene expression during branchial arch patterning. *Development, 145*. doi:doi: 10.1242/dev.157438

West-Mays, J. A., Zhang, J., Nottoli, T., Hagopian-Donaldson, S., Libby, D., Strissel, K. J., &

Williams, T. (1999). AP-2alpha transcription factor is required for early morphogenesis of

the lens vesicle. *Developmental Biology, 206*(1), 46–62.

3. Chapter 3: Deletion of Transcription Factor AP-2β from the Developing Trabecular Meshwork Region Leads to Progressive Glaucomatous Changes

I helped design the experiments, completed all experiments, data analyses and manuscript writing. Dr. Aftab Taiyab was involved in research design, assisting with experiments and data analysis, and manuscript writing, while Japnit Dham assisted with experiments. Dr. Judith West-Mays was involved in research design, providing reagents and writing the manuscript. Dr. Teresa Borrás was involved in experimental design, providing the *Mgp*-Cre.KI mice and manuscript writing, while Dr. Trevor Williams was involved in research design, providing the *Tfap2b*[lox/lox] mice and writing the manuscript. The results for Chapter 3 were extracted from a manuscript in preparation, the details for which are given below:

Monica Akula[1*] Aftab Taiyab[1*], Japnit Dham[1], Paula Deschamps[1], Heather Sheardown[2], Trevor Williams[3], Teresa Borras[4], & Judith A. West-Mays[1]

1. McMaster University, Health Sciences Centre

2. McMaster University, Department of Chemical Engineering

3. University of Colorado, Craniofacial Biology

4. University of North Carolina School of Medicine, Department of Ophthalmology

*First co-authors

Status of paper: The manuscript is in the process of being submitted to a suitable journal.

Abstract

ASD is a group of disorders stemming from anomalies in anterior structures of the eye, including the trabecular meshwork and Schlemm's canal. Transcription factors including AP-2β have important roles in anterior segment development and maintenance, but genetic tools to assess the critical tissues in which these regulators act have been limited. Here, we show that the recently described *Mgp*-Cre knock-in (*Mgp*-Cre.KI) transgenic mouse line can be used to target the embryonic POM that gives rise to the trabecular meshwork and Schlemm's canal. Subsequently, we show that deletion of AP-2β specifically from this developing trabecular meshwork region causes defects in aqueous humor outflow pathway structures and progressive development of glaucomatous features. Fate mapping indicates that AP-2β loss causes a decrease in cells derived from *Mgp*-Cre.KI expressing populations in the iridocorneal angle region compared to controls. Moreover, PAS adhesions occur in the AP-2β TMR mutants, accompanied by a decrease in expression of markers of the trabecular meshwork and Schlemm's canal. In adult AP-2β TMR mutant mice, IOP was significantly higher when compared with control eyes, correlating with reduced retinal thickness and a progressive, significant loss of RGCs. Further, retinal function was reduced in AP-2β TMR mutants in comparison to controls, reflecting pathology described in patients with late-stage glaucoma. Taken together, these findings demonstrate that AP-2β is critical for development of the trabecular meshwork and Schlemm's canal, and indicate that these mutant mice can serve as a model for understanding and treating progressive glaucoma.

3.1. Introduction

Glaucoma is one of the leading causes of irreversible blindness worldwide, with 111.8 million individuals projected to be affected by the end of 2040 (Quigley & Broman, 2006; Tham et al., 2014). There are two major types of glaucoma, which are primary open angle glaucoma and primary angle closure glaucoma, with increased IOP being a risk factor for both types (Weinreb et al., 2014). IOP results from the balance between aqueous humor secretion from the ciliary body found posterior to the iris (Civan & Macknight, 2004) and aqueous humor outflow through the drainage structures in the iridocorneal angle that include the trabecular meshwork and Schlemm's canal (Civan & Macknight, 2004). Blockade of outflow can lead to elevated IOP (Lee et al., 2006), which can put mechanical stress on the optic nerve head, causing progressive degeneration of RGCs (Gould & John, 2002) and eventual vision loss. Obstruction of aqueous humor outflow can arise from adhesions between the iris and cornea, such as a peripheral iridial adhesion to the cornea, also known as PAS (Lee et al., 2006).

Primary angle closure glaucoma can result from anterior segment dysgenesis, in which structures found in the anterior segment of the eye, including the lens, ciliary body, iris, cornea, trabecular meshwork and Schlemm's canal, develop abnormally (Gould & John, 2002; Wright et al., 2016). The embryonic tissue types that contribute to these structures include the surface ectoderm and the POM consisting of cranial NCCs and paraxial mesoderm cells (Gage et al., 2005; Gould et al., 2004). Of particular importance for glaucoma are the trabecular meshwork and Schlemm's canal, since they regulate aqueous outflow (Gould et al., 2004). In mice at embryonic day (E) 15.5, POM cells migrate into the region between the anterior rim of the optic cup and the developing corneal endothelium, with this population of cells giving rise to the stroma of the iris and ciliary body, as well as the trabecular meshwork and Schlemm's canal (Cvekl & Tamm, 2004).

Between postnatal day (P) 1 and P4, POM cells can be found at the iridocorneal angle between the newly forming iris and cornea (Cvekl & Tamm, 2004; Smith et al., 2001). Between P4 and P10, POM cells elongate, flatten and begin differentiating into trabecular meshwork cells that secrete extracellular matrix components, while blood vessels form in the scleral region (Cvekl & Tamm, 2004; Smith et al., 2001). By P14, extracellular matrix fibres secreted by the developing trabecular meshwork cells form beams, with these cells wrapping around the beams and the blood vessels at the iridocorneal angle adjacent to the sclera fusing to form Schlemm's canal, both of which play a vital role in aqueous humor outflow (Cvekl & Tamm, 2004; Kizhatil et al., 2014).

A number of genes have been shown to regulate development of the anterior segment in mice (Chen, 2016; Cross et al., 2014; Liu & Johnson, 2010; Romero et al., 2011b; Smith et al., 2000; Tümer & Bach-Holm, 2009), including the AP-2 transcription factor family encompassing AP-2α, AP-2β, AP-2γ, AP-2δ and AP-2ε (Barzago et al., 2017; Bassett et al., 2012; Bassett et al., 2007; Bassett et al., 2010; Chen et al., 2016; Kerr et al., 2014; Pontoriero et al., 2008; West-Mays et al., 1999). Specifically, AP-2β, encoded by the *Tfap2b* gene, is expressed in the mouse POM cells that migrate into the region between the anterior rim of the optic cup and cornea, and that also give rise to the trabecular meshwork and Schlemm's canal (Bassett et al., 2012; Martino et al., 2016). AP-2β null mice show eye defects; however, since these mice do not survive postnatally, they do not allow assessment of pathology that arises at later stages (Moser et al., 1997a). Therefore, we previously used the Wnt1Cre transgenic line to conditionally delete AP-2β from cranial NCCs (AP-2β NCC KOs) allowing such mutant mice to be followed into adulthood (Martino et al., 2016). The resulting mice showed anterior segment defects, including the loss of a corneal endothelium, a peripheral to central iridocorneal adhesion, and absence of formation of a trabecular meshwork region (TMR) and Schlemm's canal (Chapter 2), in addition to increased

IOP and glaucomatous features (Martino et al., 2016). However, it was unclear whether the peripheral to central iridocorneal adhesion, or the lack of a trabecular meshwork and Schlemm's canal due to AP-2β deletion, contributed to the increased IOP and glaucomatous features. This study sets out to distinguish between a cell-autonomous versus a non-cell-autonomous role for AP-2β in trabecular meshwork cell development by using a more specific Cre mouse line to delete AP-2β from the TMR. The matrix GLA protein (Mgp) Cre mouse line expresses Cre in the iridocorneal angle region in the adult mouse, in addition to the peripapillary scleral region and retinal vascular bed (Asokan et al., 2018; Borrás et al., 2015). Due to this specific localization of Cre expression to the iridocorneal angle region, the *Mgp*-Cre knock-in (*Mgp*-Cre.KI) mouse line was used to study the effect of AP-2β deletion from the TMR. Mutant mice, termed the AP-2β trabecular meshwork region knockouts (AP-2β TMR KOs), underwent normal POM cell migration, but displayed absence of a morphologically distinct TMR, in addition to partial angle closure and a reduction in expression of the trabecular meshwork markers, αSMA and myocilin, and Schlemm's canal markers, Prox1 and endomucin. These mice further developed increased IOP at one month of age, accompanied by a significant reduction in the number of RGCs and reduced retinal function, making this a model of human primary angle closure glaucoma.

3.2. Methods

3.2.1. Animal Husbandry

All procedures were conducted in accordance with the ARVO Statement for the Use of Animals in Ophthalmic and Vision Research. In the AP-2β TMR KO and AP-2β NCC KO mouse models used in the current study, the *Tfap2b* gene was deleted using either a Cre transgene under control of the *Mgp* gene (Borrás et al., 2015) or the *Wnt1* gene ($H2az2^{Tg(Wnt1-cre)11Rth}$ Tg(Wnt1-

GAL4)11Rth/J, Jackson Lab, Bar Harbor, ME). Either male *Mgp*-Cre.KI$^{+/-}$*; Tfap2b$^{+/-}$* mice or male *Wnt1Cre$^{+/-}$; Tfap2b$^{+/-}$* mice were bred with female *Tfap2b$^{lox/lox}$* to generate *Mgp*-Cre.KI$^{+/-}$*; Tfap2b$^{-/lox}$* mice (AP-2β TMR KOs) and *Wnt1Cre$^{+/-}$; Tfap2b$^{-/lox}$* mice (AP-2β NCC KOs), respectively, as well as age-matched control littermates. In addition, male *Mgp*-Cre.KI$^{+/-}$*; Tfap2b$^{+/-}$* mice were bred with *Tfap2b$^{lox/lox}$; tdTomato$^{lox/lox}$* mice (the tdTomato reporter was the B6; 129S6-Gt (ROSA)26Sortm14(CAG-tdTomato)Hze/J strain from the Jackson Lab) to generate *Mgp*-Cre.KI$^{+/-}$*; Tfap2b$^{-/lox}$; tdTomato$^{lox/+}$* mice in order to assess *Mgp*-Cre.KI expression. All genotyping was carried out using standard PCR protocols (Martino et al., 2016). Inbreeding between mouse lines used for the final cross was avoided, and C57BL/6J was the background strain used for all genetic crosses (Charles River, Wilmington, MA).

3.2.2. Histology

Eyes were enucleated from euthanized mice, and fixed in 4% PFA for 24 hours at 4ºC, followed by storage in 70% ethanol for paraffin sections, or in 30% sucrose overnight at 4ºC for frozen sections. The eyes were then processed and embedded in paraffin wax or optimal cutting temperature compound. Paraffin tissue blocks were sectioned at a thickness of 4 μm and subsequently stained using hematoxylin and eosin (H&E), or immunohistochemistry was carried out. Frozen tissue blocks were sectioned at a thickness of 10 μm to assess tdTomato expression (Bassett et al., 2007).

3.2.3. Immunohistochemistry

Immunohistochemistry was performed as previously described (Chapter 2). Primary antibodies included AP-2β (1:50, Cell Signaling, Danvers, MA), α-smooth muscle actin (αSMA,

1:100, Sigma Aldrich, Oakville, ON), myocilin (1:200, FabGennix, Frisco, TX), endomucin (1:100, eBioscience, San Diego, CA), Prox1 (1:100, Covance, Princeton, NJ), N-cadherin (1:100, BD Transduction, San Jose, CA) and Brn3a (1:100, Santa Cruz, CA). Alexa Fluor secondary antibodies (Invitrogen, Molecular Probes, Burlington, ON) were used to detect the primary antibodies, and slides were mounted with ProLong Gold containing DAPI (Bassett et al., 2007). To analyze tdTomato expression for the fate mapping experiments, frozen sections of eyes from control and AP-2β TMR KO mice crossed with the tdTomato mouse line were used. All sections were imaged using a Leica DM6 B microscope with a bright-field or fluorescence attachment, and images were acquired using a high-resolution camera and LasX imaging software.

3.2.4. Immunohistochemistry of Flat Mounted Retinas

Eyes were fixed in 4% PFA for 2 hours at room temperature and washed 3 times for 10 minutes per wash in PBS, after which retinas were dissected out and permeabilized overnight in a solution of 0.3% Triton-X mixed in PBS (PBST) (Hicks et al., 2018). Retinas were blocked in normal serum with PBST for 3 hours at room temperature, and agitated in a 1:100 dilution of Brn3a antibody (Santa Cruz, CA) mixed with 1% DMSO and 5% normal serum in PBST for 72 hours at 4ºC. Retinas were then washed in PBST and agitated in secondary antibody at a 1:200 dilution along with 1% DMSO and 2.5% normal serum in PBST for 4 hours at room temperature, after which retinas were washed in PBS, flat mounted using mounting medium containing DAPI and coverslipped.

3.2.5. IOP Measurement

Eye drops (Alcon, Mississauga, CA) were applied to the corneas of anesthetized mice to prevent them from drying, and a minimum of 6 IOP values were acquired from each eye using a rebound tonometer (TonoLab, Vantaa, Finland), with each value being an average of 6 measurements (Martino et al., 2016).

3.2.6. Electroretinograms (ERGs)

P45 and 2-3 month-old control and AP-2β TMR KO mice were used to perform scotopic full field ERGs (Phoenix Research Laboratories, Pleasanton, CA). Animals were anesthetized as described, their pupils dilated with 0.5% tropicamide (AKORN, Lake Forest, IL) and eye drops applied to prevent the cornea from drying. A ground electrode was placed in the tail, while a reference electrode was placed in the scalp, and the eye was positioned such that the cornea made contact with the corneal electrode (Hicks et al., 2018). The retinal responses to 2 ms flashes of LED light (504 nm) at light intensities between -0.2 and 2.5 cd·s/m^2 (on a log scale) were recorded, and 20 responses were measured for the lowest intensity, while 5 were measured for the highest intensity.

3.2.7. Statistical Analysis

Cell counts of Brn3a-positive cells in control and AP-2β TMR KO mice were carried out using the manual cell counter plugin on ImageJ. Furthermore, thickness of the total retina, the outer nuclear layer, the inner nuclear layer and the inner plexiform layer were measured using the line tool on ImageJ. The sections used for the statistical analyses were matched by the level of the section, including by diameter of the ocular lens, and 3 sections were evaluated per eye for all

analyses. For analysis of retinal thickness and Brn3a cell counts in sections, 3 measurements were acquired per section, which included one measurement at each peripheral region and one in the central retina, which were averaged for each section. For flat mounted retinas, Brn3a-positive cells were counted in three separate regions, which included the region adjacent to the optic nerve head, the mid periphery and the peripheral retina, and these measurements were acquired in 4 different retinal petals and averaged (Fig. 3.7). Differences in IOP, cell count in flat mounted retinas and retinal sections, as well as thickness of retinal layers between control and AP-2β TMR KO animals were analyzed using a t-test, while differences in the a-wave and b-wave amplitudes were analyzed using either a two-way repeated measures ANOVA or a mixed model on GraphPad Prism software, and if significance was found, multiple comparisons was performed using the Bonferroni method.

3.3. Results

The *Mgp*-Cre.KI mouse line has previously been characterized for its function in the adult eye, where it has been shown to target cells in the iridocorneal angle region, as well as the peripapillary scleral region and retinal vascular bed (Asokan et al., 2018; Borrás et al., 2015). Mgp is also expressed in embryonic mouse tissues (Luo et al., 1995), and we therefore reasoned that *Mgp*-Cre.KI might be active during the perinatal period of mouse eye development. To test this hypothesis, male *Mgp*-Cre.KI mice were crossed with tdTomato females, and the expression of the Cre activated tdTomato reporter was tracked beginning at E15.5 when the POM that gives rise to the trabecular meshwork during ocular development is being populated by the neural crest (Cvekl & Tamm, 2004). At E15.5, mice heterozygous for the *Mgp*-Cre.KI transgene expressed tdTomato in the developing POM region at the anterior rim of the optic cup (Fig. 3.2A). At P1

(Fig. 3.2C), tdTomato expression was present in the iridocorneal angle region of control mice, and there was a similar pattern of expression at P4, P7 and P10 (Fig. 3.2E, G & I). Notably, though, neither the corneal endothelium nor stroma, additional derivatives of the NCC-derived POM, are strongly marked by *Mgp*-Cre.KI in contrast to the results obtained using the Wnt1Cre transgene which also targets these tissues (Chapter 2) (Martino et al., 2016).

Next, the *Mgp*-Cre.KI mouse line was used to delete AP-2β from the iridocorneal angle region and examine the effect of AP-2β deletion on trabecular meshwork development. In this instance, fate mapping showed that there was no overt difference in tdTomato cell populations between the AP-2β TMR KO compared with control mice at either E15.5 or P1 (Fig. 3.2A-D; n=3 eyes). However, by P4 (n=3 eyes), P7 (n=3 eyes) and P14 (n=3 eyes), there was a reduction in tdTomato expression in the iridocorneal angle region of TMR KO mice (Fig. 3.2F, H & J, asterisks), when compared with the developing angle of control mice (Fig. 3.2E, G & I). These findings indicate that AP-2β is required for appropriate development and/or maintenance of these iridiocorneal angle populations.

The overall morphology of the AP-2β TMR KO eyes at P14, as shown by H&E stained sections, revealed partial iridocorneal angle closure due to PAS of the iris to the cornea (Fig. 3.3A-B). There was also a small amount of variability in the degree of angle closure within the same eye (Fig. 3.3). Since the absence of a corneal endothelium is known to contribute to adherence of the iris to the cornea (Reneker et al., 2000; Waring et al., 1982) immunohistochemistry for N-cadherin was performed, and this experiment demonstrated that the corneal endothelium was present in the TMR KO mice, although its appearance was more discontinuous than in controls (Fig. 3.3G-H; n=3 eyes). Additionally, at P14, a distinct trabecular meshwork region was not visible in the AP-2β TMR KO eyes (Fig. 3.3D & F, arrowhead) when compared to control eyes

(Fig. 3.3C & E). To assess the deletion of AP-2β in the trabecular meshwork, immunohistochemistry was performed using antibodies specific for AP-2β and αSMA, a marker of the trabecular meshwork. AP-2β was observed to be completely absent in the trabecular meshwork region of P14 AP-2β TMR KO mice (Fig. 3.4A, TMR KO panel, brackets, inset) when compared to control mice (Fig. 3.4A, panel marked "control"; brackets; n=3 eyes). Furthermore, a marked reduction in αSMA expression was observed in the TMR KO when compared with control mice. There was also a prominent reduction in expression of myocilin, another trabecular meshwork marker, in the iridocorneal angle of TMR KO eyes (Fig. 3.4B; n=3 eyes) compared with control eyes. In addition to the trabecular meshwork, Schlemm's canal is also part of the conventional outflow pathway that is blocked in primary angle closure glaucoma. Consequently, immunohistochemistry was carried out for markers of Schlemm's canal, and TMR KOs showed reduced expression of Schlemm's canal markers, Prox1 (Fig. 3.4C; arrowheads) and endomucin (Fig. 3.4C; arrows), when compared with controls.

To determine whether abnormalities in the trabecular meshwork are leading to an increase in IOP, measurements were acquired from both TMR KO and control mice at P30. There was a significant increase in IOP in TMR KOs when compared with controls at P30 (n=6 eyes; $p<0.0001$) (Fig. 3.5A). To investigate whether the increased IOP observed in the AP-2β TMR KO mice is correlated with additional glaucomatous changes, immunohistochemistry was performed for Brn3a, a marker of RGCs. While there was no difference in expression of Brn3a at P14, by P30 and P40, reduced expression was found in TMR KO sections when compared with controls (Fig. 3.6). Immunohistochemistry studies using flat mounted retinas from the P60 control and TMR KO showed that there was a significant reduction in the number of Brn3a-positive cells in the region adjacent to the optic nerve head, the mid-periphery and peripheral retina (analyzed regions marked

in Fig. 3.7) in TMR KOs when compared to controls (Fig. 3.8C/D; n=6 eyes; p<0.0001 for all 3 regions). Furthermore, analysis of H&E-stained retinal sections revealed a significant reduction in thickness of the total retina, the inner nuclear layer and inner plexiform layer, at both P30 (a minimum of n=3 eyes; total retina, p<0.01; inner nuclear layer, p<0.01; inner plexiform layer, p<0.05) and P40 (a minimum of n=3 eyes; total retina, p<0.05; inner nuclear layer, p<0.05; inner plexiform layer, p<0.01) (Fig. 3.8A, B) as compared to controls. In addition, as seen using a full field scotopic flash ERG, although at P45 there was no difference in a-wave and b-wave amplitudes between TMR KOs and controls (Fig. 3.9), a significant reduction in the a-wave and b-wave amplitudes of 2-3 month-old TMR KO animals was observed when compared with age-matched control animals (Fig. 3.10A-C; a minimum of n=3 mice; p<0.05 for the last 3 flash intensities tested for both the a-wave and b-wave amplitudes).

Mgp-Cre.KI$^{+/-}$ X $Tfap2b^{+/-}$

Mgp-Cre.KI$^{+/-}$; $Tfap2b^{+/-}$ X $Tfap2b^{lox/lox}$; $tdTomato^{lox/lox}$

Mgp-Cre.KI$^{+/-}$; $Tfap2b^{-/lox}$; $tdTomato^{lox/+}$
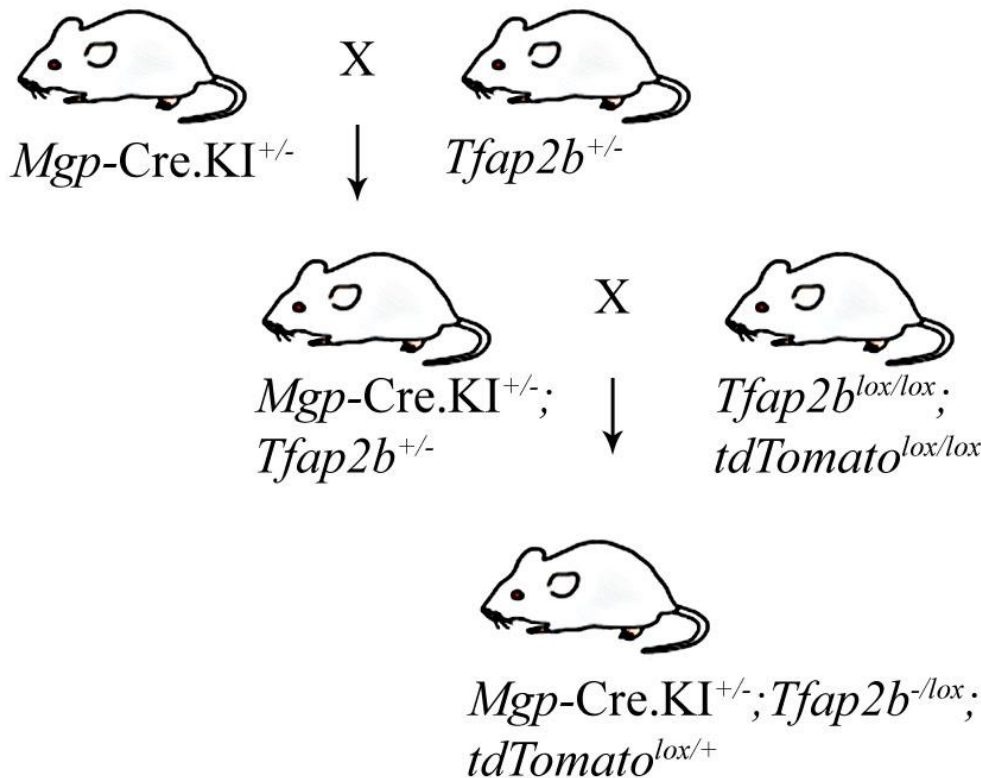
Fig. 3.1. Breeding scheme for AP-2β TMR KO mice. Heterozygous *Mgp*-Cre knock-in (*Mgp*-Cre.KI$^{+/-}$) mice were bred with heterozygous *Tfap2b*$^{+/-}$ gene deletion mutants. The progeny were bred with mice containing the *Tfap2b*$^{lox/lox}$; *tdTomato*$^{lox/lox}$ genotype to ensure that Cre recombinase binds to the loxP sites flanking the AP-2β gene to ensure deletion specifically in the iridocorneal angle, peripapillary scleral region and retinal vascular bed. Adapted from Hicks (2017).
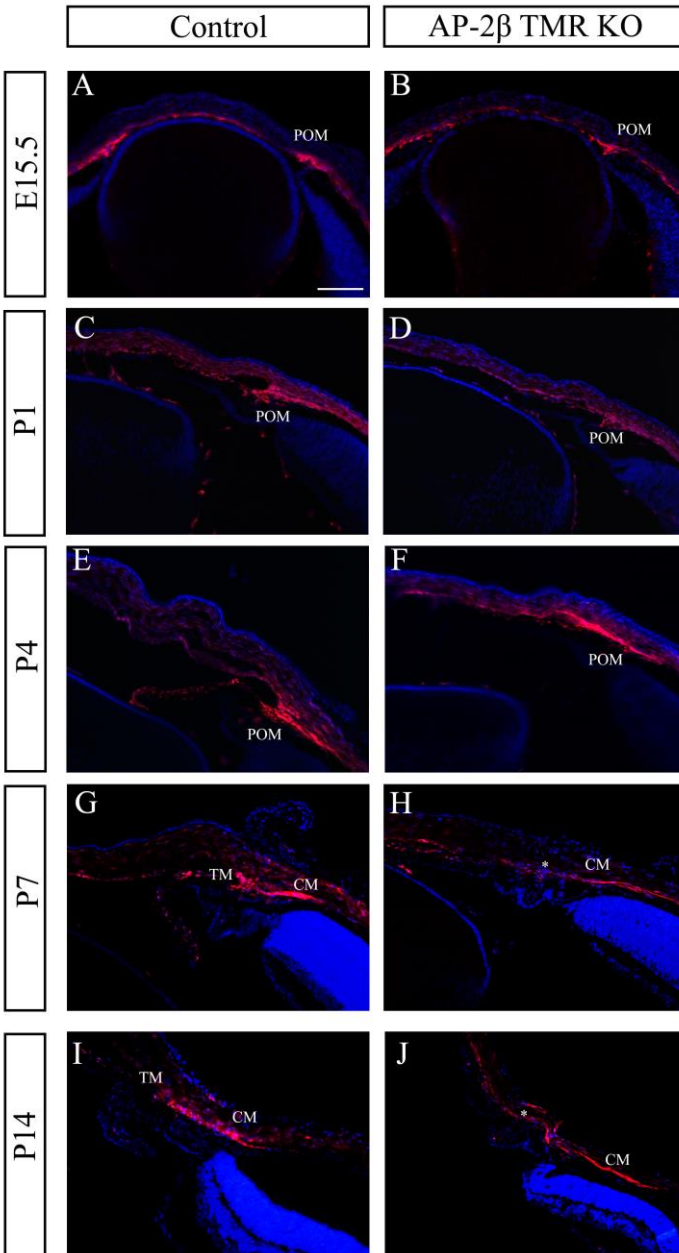
Fig. 3.2. Fate mapping of *Mgp*-Cre.KI using tdTomato expression in embryonic and early postnatal controls versus AP-2β trabecular meshwork region knockouts (AP-2β TMR KOs). A-B) At E15.5 (n=3 eyes), tdTomato – which marks cells expressing *Mgp*-Cre.KI, or the descendants of such cells – is expressed in the developing POM. No observable difference in NCC migration is present between the TMR KO and controls. C-D) At P1 (n=3 eyes), there is also no

difference in tdTomato expression in the iridocorneal angle of the TMR KO mice compared with controls. E-F) At P4 (n=3 eyes), there appears to be a mild decrease in tdTomato expression in the iridocorneal angle region. G-J) At both P7 (n=3 eyes) and P14 (n=3 eyes), there also appears to be a reduction in expression of tdTomato in the iridocorneal angle of the TMR KO mice compared with controls. Asterisks in panels H & J show the prospective iridocorneal angle region. POM, periocular mesenchyme; TM, trabecular meshwork; CM, ciliary muscle. Scale bars represent 100 μm. Images were acquired using a 20x objective lens.
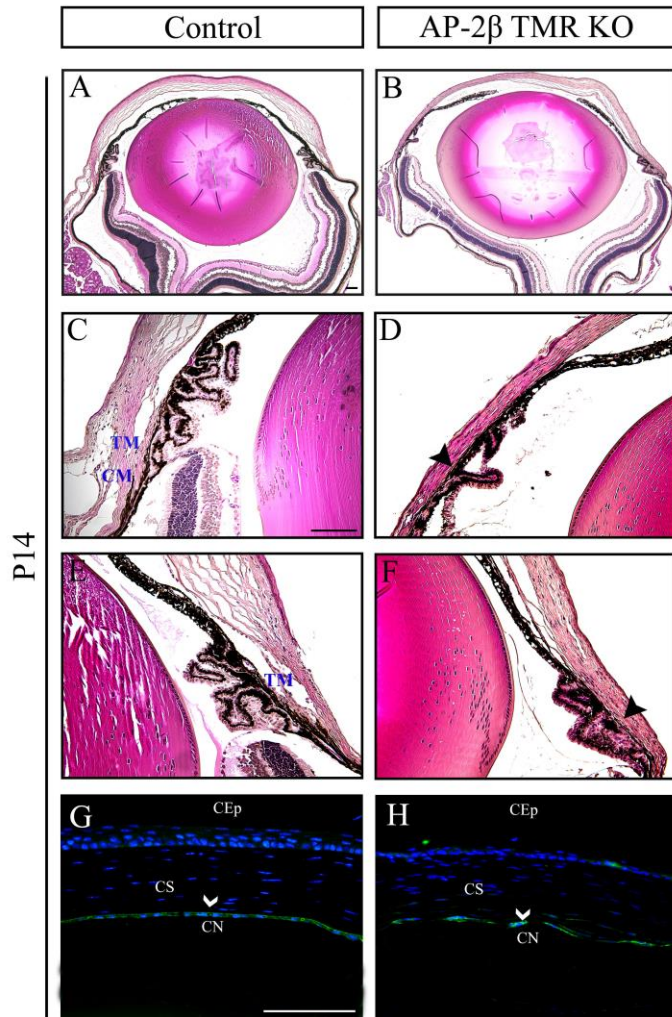
Fig. 3.3. Abnormal morphology of the trabecular meshwork in AP-2β TMR KO mice as compared with control mice. A-B) By P14 (n=3 eyes), the trabecular meshwork region appears to be absent in the TMR KO when compared with control mice. C-F) Higher magnification images of A and B are depicted in C & E and D & F, respectively. G-H) At P14 (n=3 eyes), N-cadherin expression is present in both control and AP-2β TMR KO mice. TM, trabecular meshwork; CM, ciliary muscle; CN, corneal endothelium; CEp, corneal epithelium; CS, corneal stroma. Scale bars in panels A-H represent 100 µm. Images A-B were acquired using a 5x objective lens, images C-F were acquired using a 20x lens, and images G-H were acquired using a 40x objective lens.
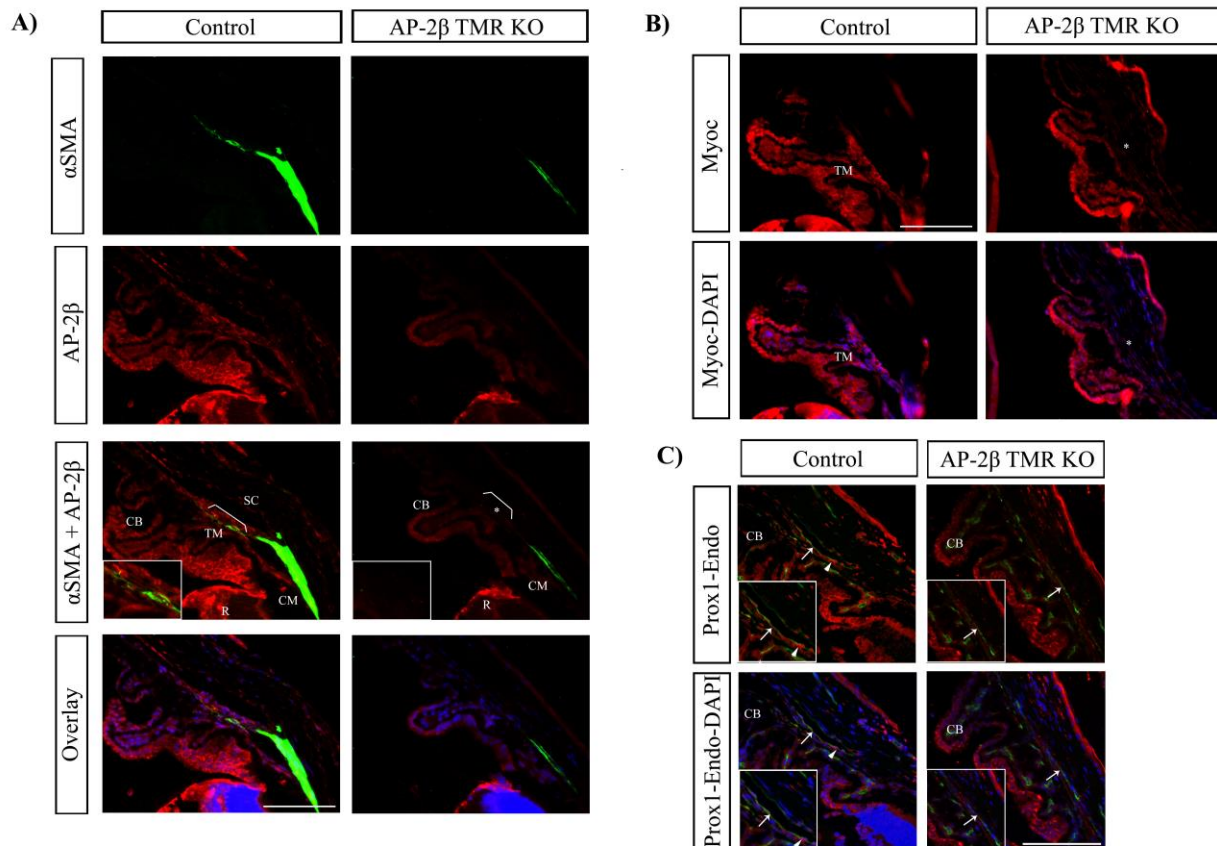
Fig. 3.4. Loss of AP-2β in TMR KOs causes reduced expression of trabecular meshwork and Schlemm's canal markers. A) In P14 control mice, AP-2β is detected in the iridocorneal angle,

as well as the retina (R) and ciliary body (CB). In P14 AP-2β TMR KO animals (n=3 eyes), AP-2β is still observed in the ciliary body and retina but is now absent from the iridocorneal angle (TMR KO panel showing αSMA and AP-2β co-staining, bracketed region also shown as inset). αSMA expression is also reduced in the trabecular meshwork region of TMR KO mice compared with control mice. B) At P14 (n=3 eyes), in controls there is extensive myocilin expression within the angle tissue, the corneal epithelium and the ciliary body, but expression is specifically lost in the angle tissue of TMR KO mice (AP-2β TMR KO panels, asterisks). C) Co-staining of Prox1 (red) and endomucin (green) shows a defined and open Schlemm's canal region in the control angle (control panels; endomucin staining marked by the arrow), whereas the TMR KO angle shows a hypoplastic Schlemm's canal (AP-2β TMR KO panels; endomucin staining marked by the arrow). Furthermore, there appears to be a reduction in Prox1 staining in this region in the TMR KO when compared with the control Schlemm's canal (control panels, insets, Prox1 staining marked by the arrowhead). TM, trabecular meshwork; CM, ciliary muscle; CB, ciliary body; SC, Schlemm's canal; R, retina. Scale bars represent 100 μm. Images were acquired using a 40x objective lens.

A) IOP of P30 Controls vs. AP-2β TMR KOs
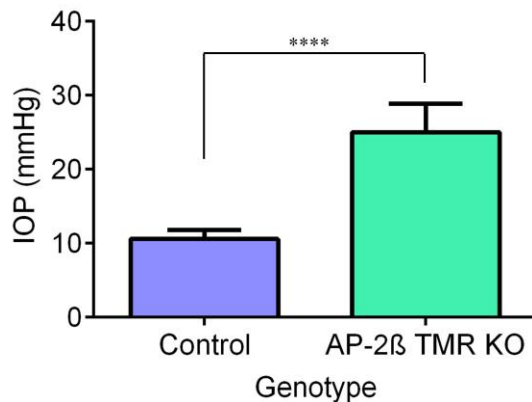
Fig. 3.5. Increased IOP resulting from partial angle closure in AP-2β TMR KO eyes. A) There is a significant increase in IOP in the AP-2β TMR KO mice at P30 (n=6; p<0.0001; all error bars signify standard deviation) when compared with control mice.
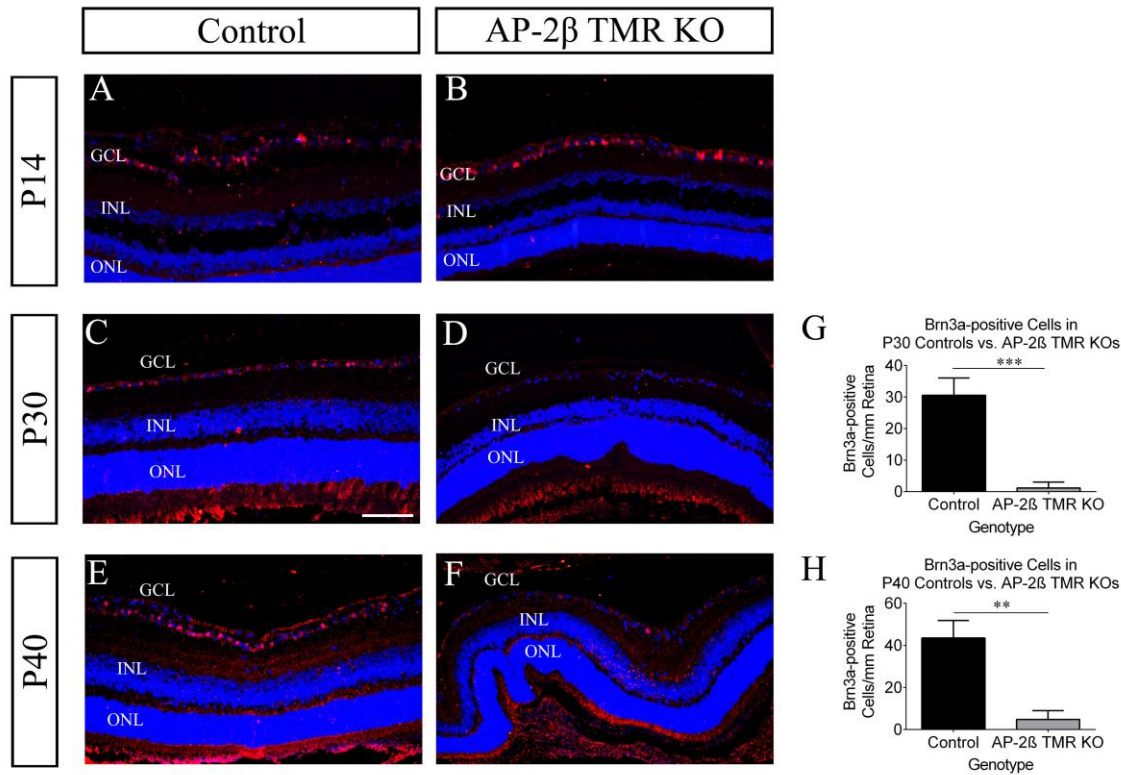
Fig. 3.6. Fewer retinal ganglion cells (RGCs) in the P30 and P40 AP-2β TMR KO retina when compared with the control retina. A-B) At P14, there is no difference in Brn3a expression within the ganglion cell layer of controls and TMR KOs. C-F) At P30 and P40, there is reduced expression of Brn3a in the TMR KO retina when compared with the control retina. G-H) At both P30 (n=3 eyes; p<0.001; all error bars represent standard deviation) and P40 (n=3 eyes; p<0.01), there is a significant reduction in the number of Brn3a-positive cells in TMR KO retinal sections when compared to control sections. GCL, ganglion cell layer; INL, inner nuclear layer; ONL, outer nuclear layer. Scale bars represent 100 μm. Images were acquired using a 20x objective lens.

A)
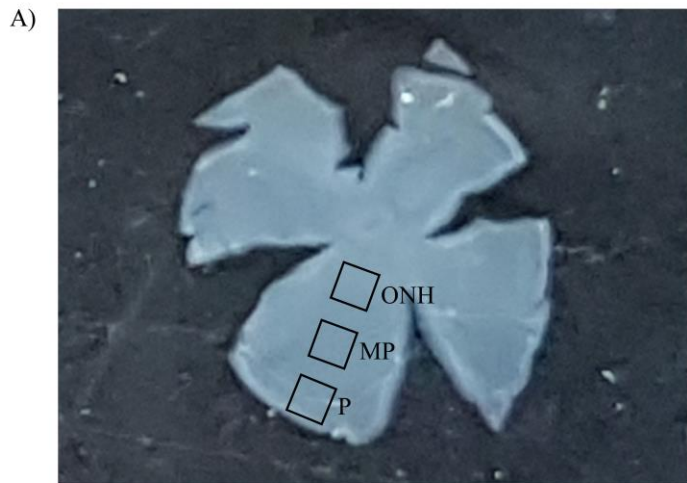
Fig. 3.7. Image of a flat mounted retina marked with the sample regions analyzed in control and AP-2β TMR KO mice. A) This image shows a flat-mounted retina with the regions analyzed in control and AP-2β TMR KO mice marked using black boxes. The three regions analyzed include the area adjacent to the optic nerve head (ONH), the mid-peripheral retina (MP) and the peripheral retina (P), and measurements for each region were acquired in 4 different retinal petals and averaged.
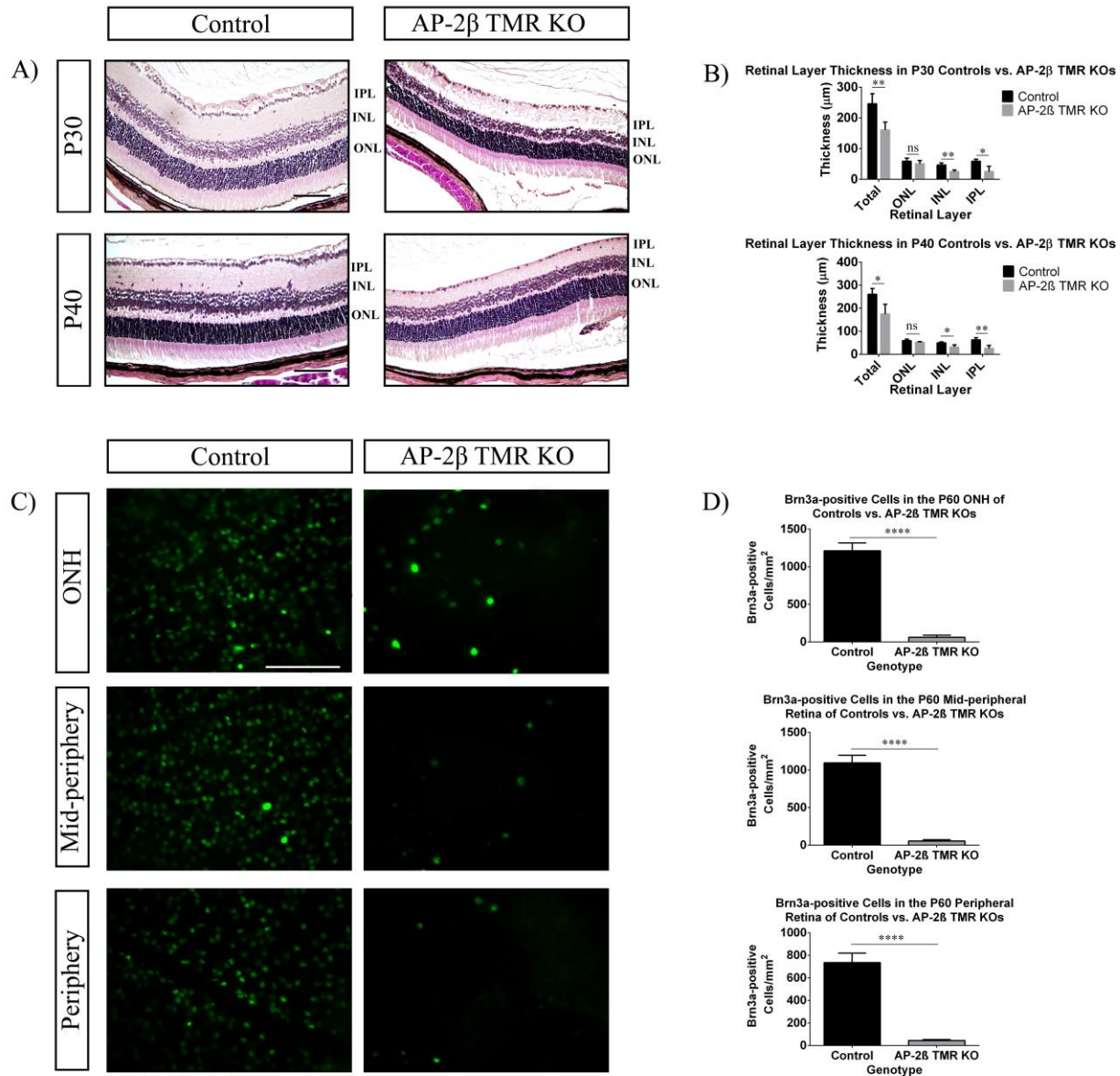
Fig. 3.8. Reduced thickness of the total retina, inner nuclear layer and inner plexiform layer, as well as a reduced Brn3a cell count in flat mounted retinas in the AP-2β TMR KO when compared with controls. A-B) At P30 (a minimum of n=3 eyes), there is a significant reduction in total retinal thickness (p<0.01; all error bars represent standard deviation), as well as thickness of the inner nuclear layer (p<0.01) and inner plexiform layer (p<0.05) in the TMR KOs when compared with controls. At P40 (a minimum of n=3 eyes), there continues to be a significant reduction in total retinal thickness (p<0.05), as well as thickness of the inner nuclear layer (p<0.05)

and inner plexiform layer (p<0.01) in the TMR KOs when compared with controls. C-D) There is a significant reduction in the number of Brn3a-positive cells in flat mounted retinas of TMR KOs when compared with control retinas in the region adjacent to the optic nerve head, mid-periphery and peripheral region of the retina (n=6 eyes; p<0.0001 for all 3 regions). IPL, inner plexiform layer; INL, inner nuclear layer; ONL, outer nuclear layer; ONH, optic nerve head. Scale bars represent 100 μm. Images in (A) were acquired using a 20x objective lens, and images in (C) were acquired using a 40x objective lens.
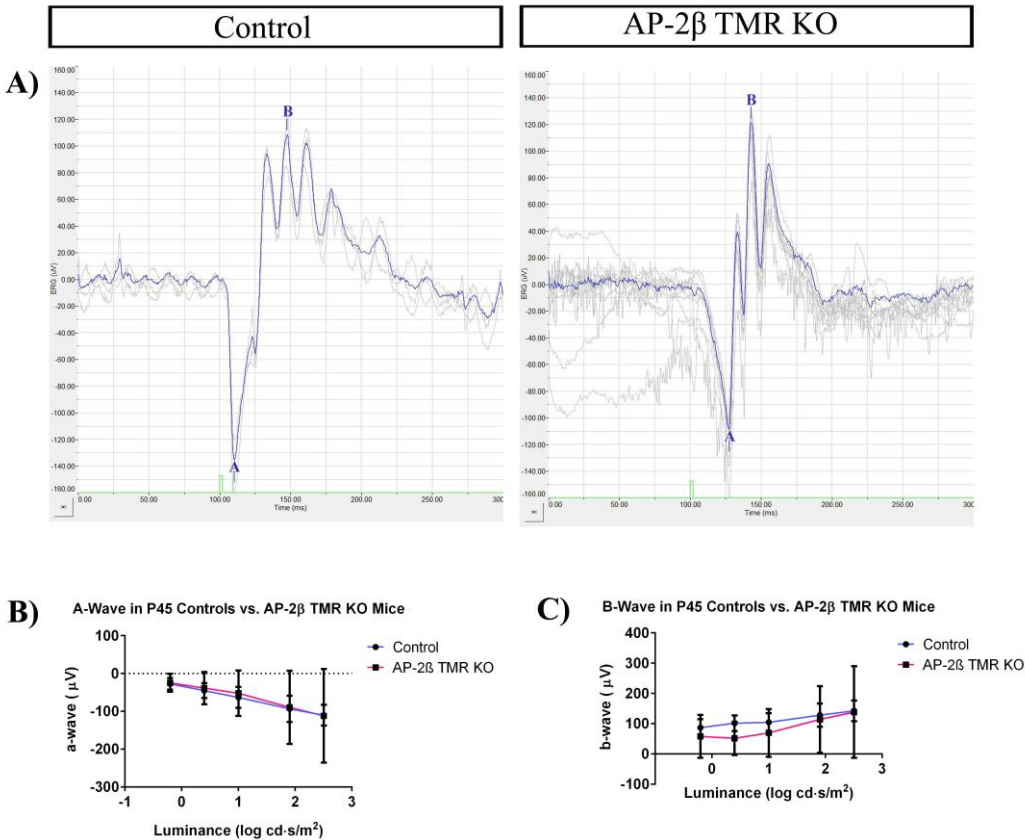
Fig. 3.9. The a-wave and b-wave measured using ERGs in P45 controls and AP-2β TMR KOs. A) Sample ERG traces of the a-wave and b-wave of P45 controls and TMR KOs show that the b-wave peak is similar in appearance in both the control and TMR KO (peaks labelled "B").

C) There is no significant difference in the amplitude of the a-wave in TMR KO mice when compared to control mice in response to 2 ms flashes of light (504 nm) between -0.2 and 2.5 cd·s/m^2 (log scale) in intensity (a minimum of n=3 eyes; all error bars represent standard deviation). C) There is no significant difference in the amplitude of the b-wave in TMR KO mice when compared to control mice in response to 2 ms flashes of light between -0.2 and 2.5 cd·s/m^2 (log scale) in intensity (a minimum of n=3 eyes).
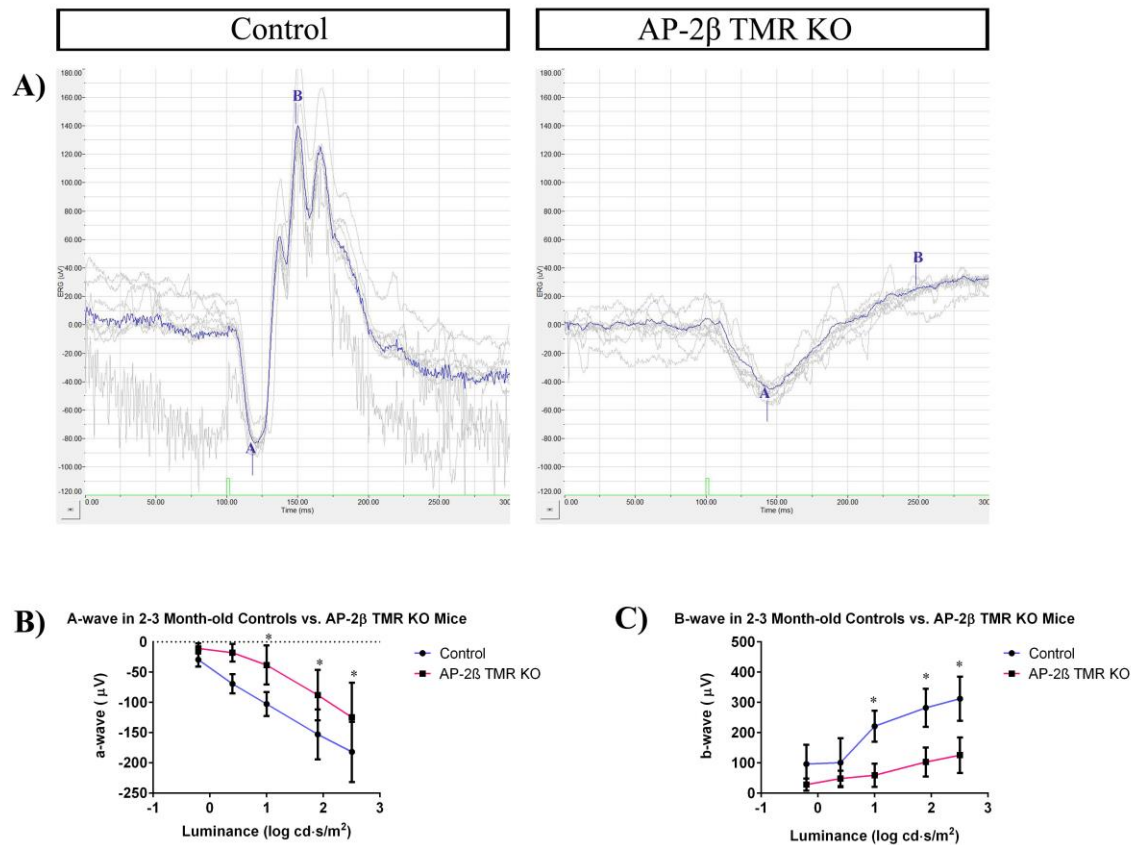
Fig. 3.10. The a-wave and b-wave measured using electroretinograms (ERGs) in controls and AP-2β TMR KOs. A) Sample ERG traces of the a-wave and b-wave of 2-3 month-old controls and TMR KOs show that the b-wave peak is not visible in the KO trace (AP-2β TMR KO panel; region labelled "B"), whereas the control trace shows a b-wave peak (control panel; peak labelled

"B"). B) There is a significant reduction in the amplitude of the a-wave in TMR KO mice when compared to control mice in response to 2 ms flashes of light (504 nm) between 1 and 2.5 cd·s/m^2 (log scale) in intensity (a minimum of n=3 mice; p<0.05 for the last 3 flash intensity values; all error bars represent standard deviation). C) There is a significant reduction in the amplitude of the b-wave in TMR KO mice when compared to control mice in response to 2 ms flashes of light between 1 and 2.5 cd·s/m^2 (log scale) in intensity (a minimum of n=3 mice; p<0.05 for the last 3 flash intensity values).

3.4. Discussion

Glaucoma is the leading cause of irreversible blindness worldwide. Thus, understanding the mechanisms underlying this disease are important and necessary in order to develop treatments. Primary angle closure glaucoma is typically a disorder involving dysgenesis of anterior segment structures required for regulating IOP either through the conventional pathway, including the trabecular meshwork and Schlemm's canal, or the unconventional pathway that includes the ciliary muscle (Gould et al., 2004; Gould & John, 2002). Therefore, it is imperative to understand the role of genes that regulate the development of anterior angle structures. The AP-2β TMR KO mice with AP-2β deleted from the developing iridocorneal angle region not only showed abnormal development of the trabecular meshwork and Schlemm's canal, but also exhibited increased IOP and progressive glaucomatous features, including reduced retinal thickness, RGC loss and reduced retinal function.

Previously, our laboratory had created the AP-2β NCC KO mouse model in which the Wnt1Cre mouse line was used to delete AP-2β from the cranial neural crest (Martino et al., 2016). These mice showed defects in the trabecular meshwork required for aqueous outflow (Chapter 2),

which hinted at a cell-autonomous role for AP-2β in trabecular meshwork development. However, the Wnt1Cre system used to knock out AP-2β was broadly and strongly expressed in multiple neural crest derivatives, including not only the trabecular meshwork but also the corneal stroma and endothelium (Chapter 2). Consequently, it is also possible that the corneal defects leading to the peripheral to central iridocorneal adhesion may have resulted in secondary defects in the trabecular meshwork in AP-2β NCC KO mice (Cvekl & Tamm, 2004). The current study aimed to delineate the role of AP-2β specifically in development of the trabecular meshwork by using a Cre transgenic line *Mgp*-Cre.KI, that was previously shown to target cells in the iridocorneal angle region by adult stages (Borrás et al., 2015) to conditionally delete AP-2β from the developing TMR. *Mgp*-Cre.KI expression was observed in the developing POM giving rise to the trabecular meshwork and Schlemm's canal, but expression in corneal cell types was much more reduced when compared to the Wnt1Cre, suggesting that *Mgp*-Cre.KI can be used to more specifically target trabecular meshwork development. This is the first study to show the developmental expression pattern of *Mgp*-Cre.KI, particularly at early postnatal time points relevant for trabecular meshwork development and expands the genetic tools available for analysis of gene function during development of the anterior segment.

Fate mapping in the AP-2β TMR KO mice using the tdTomato mouse line showed no difference between controls and TMR KOs in the migration of the POM cells contributing to trabecular meshwork tissue prenatally (Fig. 3.2A-B). However, reduced expression of tdTomato in the iridocorneal angle region of TMR KO mice was observed at early postnatal stages (Fig. 3.2E-J) when compared to control mice. The combined observations from fate mapping at postnatal stages and the reduction in expression of trabecular meshwork markers (Fig. 3.4A-B) support the idea that AP-2β is directly involved in trabecular meshwork development. On the other

hand, the reduced expression of Schlemm's canal markers could be attributed to the PAS phenotype observed in the AP-2β TMR KO. It has been shown that development of Schlemm's canal relies on trabecular meshwork-mediated pressure induced expression of transcription factors, such as Klf4 (Choi et al., 2017). Moreover, the trabecular meshwork/conventional outflow pathway was observed to be absent in the TMR mutants, which might be contributing to the hypoplastic appearance of Schlemm's canal, as demonstrated by endomucin staining (Fig. 3.4C). Although the TMR KO model targets trabecular meshwork development more specifically than the NCC KO model, it is possible that PAS in the TMR KO could indirectly lead to abnormal trabecular meshwork development at the iridocorneal angle. Consequently, one way to further target the specific role of AP-2β would be to use temporal Cre mice in which *Tfap2b* is deleted after corneal development is complete and during the developmental window when trabecular meshwork cells begin to develop and differentiate.

The iridocorneal angle defects in AP-2β TMR KO mice were accompanied by significantly increased IOP as compared to littermates, and this is likely due to the fact that the conventional outflow pathway is blocked because of the absence of a trabecular meshwork and hypoplasticity of Schlemm's canal. The trabecular meshwork and Schlemm's canal defects observed in the TMR KO likely resulted in the increased IOP. The significant reduction in the thickness of the retina, the inner nuclear layer and inner plexiform layer, as well as the reduction in the number of Brn3a-positive cells in P60 flat mounted retinas in the TMR KOs when compared with control mice suggest that the elevated IOP is leading to glaucomatous defects in the retina. High IOP in mice has previously been reported to induce thinning of the inner plexiform layer (Martino et al., 2016), and our current results are in agreement with these observations. Previous studies using mouse models in which increased IOP was induced using microbead injections also reported thinning of

the inner nuclear layer combined with a reduction in expression of markers of specific amacrine cell subtypes (Akopian et al., 2019; Gunn et al., 2011), which is one possible explanation for the reduction in the thickness of the inner nuclear layer observed in the TMR KO mice.

In addition to the reduction in the number of RGCs, a reduction in retinal function was also observed in the TMR KOs using a full field scotopic flash ERG. It was previously not possible to carry out ERGs in the AP-2β NCC KO mice, since the central cornea adhered to the lens and caused corneal cataracts (Martino et al., 2016). However, in the TMR KO, the adhesion was absent and the corneas were more transparent, enabling evaluation of retinal function using an ERG. Particularly, there was a reduction in the amplitude of both the a-wave and b-wave that occurred after P45. The a-wave represents the response of photoreceptors to a flash of light in this particular type of ERG, whereas the b-wave represents the depolarization response of inner retinal cells downstream of the photoreceptors, including the bipolar cells and Müller glia, but possibly also the RGCs and amacrine cells (Dong & Hare, 2000; Miura et al., 2009; Smith et al., 2014). The observed decline in b-wave amplitude potentially represents a reduction in RGC function caused by loss of RGCs as assessed by Brn3a staining. Furthermore, since the inner nuclear layer is significantly thinner in TMR KOs, changes in this layer, which includes amacrine cells, may also contribute to the b-wave phenotype. We hypothesize that the reduction in a-wave amplitude results from reduced photoreceptor numbers or a reduction in photoreceptor outer segment length, since the latter is commonly observed in the DBA/2J glaucoma mouse model (Bayer et al., 2001; Harazny et al., 2009). Future studies will be needed to distinguish between these various possibilities.

A number of mouse models of glaucoma, including mechanically-induced models, such as the optic nerve crush model and models that develop spontaneous mutations resulting in

glaucomatous features, such as the DBA/2J model, have been developed to understand the progression of glaucoma (Johnson & Tomarev, 2010). In addition, targeted gene deletion models including mice with mutations in *Sh3pxd2b* (Mao et al., 2011), *Pitx2* (Chen, 2016), *Foxc1*, *Foxc2* (Smith et al., 2000), and *Lmx1b* (Liu & Johnson, 2010), as well as the AP-2β NCC KO mouse established previously in our lab (Martino et al., 2016), all of which have anterior segment dysgenesis, show the role of these genes in the etiology and pathophysiology of glaucoma. Although the DBA/2J model is an effective model of glaucoma, it requires time to develop high IOP and does not always result in a consistent phenotype. Furthermore, the microbead model requires careful experimental manipulation for the best and consistent results (Johnson & Tomarev, 2010). On the other hand, the TMR KO is an acute model of glaucoma that consistently shows increased IOP.

Tfap2b has been associated with a human disorder, Char Syndrome, and while ocular abnormalities have not been reported in this condition, the rarity and severity of this condition could explain the lack of documented ocular defects (Satoda et al., 2000). Moreover, the human *PITX2* gene has been associated with ASD in humans (Tumer & Bach-Holm, 2009), and since in mice, *Tfap2b* has been shown to be a downstream effector of the *Pitx2* gene (Chen et al., 2016), this suggests that the human *TFAP2B* gene may also be associated with human ASD. Here, we demonstrate for the first time that specific deletion of *Tfap2b* from the developing iridocorneal angle using the *Mgp*-Cre.KI (Borrás et al., 2015) leads to partial angle closure and defects in the trabecular meshwork and Schlemm's canal, and the resulting increase in IOP in the TMR KO combined with the progressive loss of RGCs, thinning of the retina and a reduction in retinal function observed makes this a useful animal model of human primary angle closure glaucoma. As a potential model of primary angle closure glaucoma, we also propose that the AP-2β TMR

KO mouse can be employed to investigate the effects and physiological mechanisms of IOP lowering drugs, as well as to study and demonstrate the effect of new and existing neuroprotective strategies.

References

Akopian, A., Kumar, S., Ramakrishnan, H., Viswanathan, S., & Bloomfield, S. A. (2019). Amacrine cells coupled to ganglion cells via gap junctions are highly vulnerable in glaucomatous mouse retinas. *J Comp Neurol, 527*(1), 159-173. doi:10.1002/cne.24074

Barzago, M. M., Kurosaki, M., Fratelli, M., Bolis, M., Giudice, C., Nordio, L., . . . Garattini, E. (2017). Generation of a new mouse model of glaucoma characterized by reduced expression of the AP-2β and AP-2δ proteins. *Sci Rep., 7*, 11140.

Bassett, E., Korol, A., Deschamps, P., Buettner, R., Wallace, V., Williams, T., & West-Mays, J. (2012). Overlapping expression patterns and redundant roles for AP-2 transcription factors in the developing mammalian retina. *Dev Dyn., 241*(4), 814-829.

Bassett, E., Pontoriero, G., Feng, W., Marquardt, T., Fini, M., Williams, T., & West-Mays, J. (2007). Conditional deletion of activating protein 2alpha (AP-2alpha) in the developing retina demonstrates non-cell-autonomous roles for AP-2alpha in optic cup development. *Mol Cell Biol., 27*(21), 7497-7510.

Bassett, E., Williams, T., Zacharias, A., Gage, P., Fuhrmann, S., & West-Mays, J. (2010). AP-2alpha knockout mice exhibit optic cup patterning defects and failure of optic stalk morphogenesis. *Hum Mol Genet., 19*(9), 1791-1804.

Bayer, A. U., Neuhardt, T., May, A. C., Martus, P., Maag, K. P., Brodie, S., . . . Mittag, T. (2001). Retinal morphology and ERG response in the DBA/2NNia mouse model of angle-closure glaucoma. *Invest Ophthalmol Vis Sci, 42*(6), 1258-1265.

Borrás, T., Smith, M., & Buie, L. (2015). A Novel Mgp-Cre Knock-In Mouse Reveals an Anticalcification/Antistiffness Candidate Gene in the Trabecular Meshwork and Peripapillary Scleral Region. *IOVS, 56*(4), 2203–2214.

Chen, L., & Gage, P. J. (2016). Heterozygous Pitx2 Null Mice Accurately Recapitulate the Ocular Features of Axenfeld-Rieger Syndrome and Congenital Glaucoma. *IOVS, 57*, 5023-5030.

Chen, L., Martino, M., Dombkowski, A., Williams, T., West-Mays, J., & Gage, P. J. (2016). AP-2β is a downstream effector of PITX2 required to specify endothelium and establish angiogenic privilege during corneal development. *Invest Ophthalmol Vis Sci., 57*(3), 1072–1081.

Choi, D., Park, E., Jung, E., Seong, Y. J., Hong, M., Lee, S., . . . Hong, Y. K. (2017). ORAI1 Activates Proliferation of Lymphatic Endothelial Cells in Response to Laminar Flow Through Kruppel-Like Factors 2 and 4. *Circ Res, 120*(9), 1426-1439. doi:10.1161/CIRCRESAHA.116.309548

Civan, M., & Macknight, A. (2004). The Ins and Outs of Aqueous Humour Secretion *Exp Eye Res., 78*(3), 625-631.

Cross, S., Macalinao, D., McKie, L., Rose, L., Kearney, A., Rainger, J., . . . IJ, J. (2014). A dominant-negative mutation of mouse Lmx1b causes glaucoma and is semi-lethal via LDB1-mediated dimerization. *PLoS Genet., 10*(5), e1004359.

Cvekl, A., & Tamm, E. (2004). Anterior eye development and ocular mesenchyme: new insights from mouse models and human diseases. *Bioessays, 26*(4), 374-386.

Dong, C. J., & Hare, W. A. (2000). Contribution to the kinetics and amplitude of the electroretinogram b-wave by third-order retinal neurons in the rabbit retina. *Vision Res, 40*(6), 579-589. doi:10.1016/s0042-6989(99)00203-5

Gage, P., Rhoades, W., Prucka, S., & Hjalt, T. (2005). Fate maps of neural crest and mesoderm in the mammalian eye. *Invest Ophthalmol Vis Sci., 46*(11), 4200-4208.

Gould, D., Smith, R., & John, S. (2004). Anterior segment development relevant to glaucoma. *Int J Dev Biol., 48*(8-9), 1015-1029.

Gould, D. B., & John, S. W. (2002). Anterior segment dysgenesis and the developmental glaucomas are complex traits. *Hum Mol Genet., 11*(10), 1185-1193.

Gunn, D. J., Gole, G. A., & Barnett, N. L. (2011). Specific amacrine cell changes in an induced mouse model of glaucoma. *Clin Exp Ophthalmol, 39*(6), 555-563. doi:10.1111/j.1442-9071.2010.02488.x

Harazny, J., Scholz, M., Buder, T., Lausen, B., & Kremers, J. (2009). Electrophysiological deficits in the retina of the DBA/2J mouse. *Doc Ophthalmol, 119*(3), 181-197. doi:10.1007/s10633-009-9194-5

Hicks, E. A. (2017). *THE ROLE OF AP-2α AND AP-2β IN RETINAL DEVELOPMENT.* (M. Sc.), McMaster University, Hamilton.

Hicks, E. A., Zaveri, M., Deschamps, P. A., Noseworthy, M. D., Ball, A., Williams, T., & West-Mays, J. A. (2018). Conditional Deletion of AP-2alpha and AP-2beta in the Developing Murine Retina Leads to Altered Amacrine Cell Mosaics and Disrupted Visual Function. *Invest Ophthalmol Vis Sci, 59*(6), 2229-2239. doi:10.1167/iovs.17-23283

Johnson, T. V., & Tomarev, S. I. (2010). Rodent models of glaucoma. *Brain Res Bull, 81*(2-3), 349-358. doi:10.1016/j.brainresbull.2009.04.004

Kerr, C., Zaveri, M., Robinson, M., Williams, T., & West-Mays, J. (2014). AP-2α is required after lens vesicle formation to maintain lens integrity. *Developmental Dynamics, 243*(10), 1298–1309.

Kizhatil, K., Ryan, M., Marchant, J. K., Henrich, S., & John, S. W. M. (2014). Schlemm's Canal Is a Unique Vessel with a Combination of Blood Vascular and Lymphatic Phenotypes that Forms by a Novel Developmental Process. *PLOS Biology, 12*(7), e1001912.

Lee, J. Y., Kim, Y. Y., & Jung, H. R. (2006). Distribution and characteristics of peripheral anterior synechiae in primary angle-closure glaucoma. *Korean J Ophthalmol, 20*(2), 104-108. doi:10.3341/kjo.2006.20.2.104

Liu, P., & Johnson, R. (2010). Lmx1b is required for murine trabecular meshwork formation and for maintenance of corneal transparency. *Dev Dyn., 239*(8), 2161-2171.

Luo, G., D'Souza, R., Hogue, D., & Karsenty, G. (1995). The matrix Gla protein gene is a marker of the chondrogenesis cell lineage during mouse development. *J Bone Miner Res, 10*(2), 325-334. doi:10.1002/jbmr.5650100221

Mao, M., Hedberg-Buenz, A., Koehn, D., John, S. W., & Anderson, M. G. (2011). Anterior segment dysgenesis and early-onset glaucoma in nee mice with mutation of Sh3pxd2b. *Invest Ophthalmol Vis Sci, 52*(5), 2679-2688. doi:10.1167/iovs.10-5993

Martino, V. B., Sabljic, T., Deschamps, P., Green, R. M., Akula, M., Peacock, E., . . . West-Mays, J. A. (2016). Conditional deletion of AP-2β in the cranial neural crest results in anterior segment dysgenesis and early-onset glaucoma. *Disease Models & Mechanisms, 9*(8), 849–861.

Miura, G., Wang, M. H., Ivers, K. M., & Frishman, L. J. (2009). Retinal pathway origins of the pattern ERG of the mouse. *Exp Eye Res, 89*(1), 49-62. doi:10.1016/j.exer.2009.02.009

Moser, M., Pscherer, A., Roth, C., Becker, J., Mucher, G., Zerres, K., . . . Fassler, R. (1997). Enhanced apoptotic cell death of renal epithelial cells in mice lacking transcription factor AP-2beta. *Genes Dev, 11*(15), 1938-1948. doi:10.1101/gad.11.15.1938

Pontoriero, G., Deschamps, P., Ashery-Padan, R., Wong, R., Yang, Y., Zavadil, J., . . . West-Mays, J. (2008). Cell autonomous roles for AP-2alpha in lens vesicle separation and maintenance of the lens epithelial cell phenotype. *Dev Dyn., 237*(3), 602-617.

Quigley, H. A., & Broman, A. T. (2006). The number of people with glaucoma worldwide in 2010 and 2020. *Br J Ophthalmol, 90*(3), 262-267. doi:10.1136/bjo.2005.081224

Reneker, L. W., Silversides, D. W., Xu, L., & Overbeek, P. A. (2000). Formation of corneal endothelium is essential for anterior segment development - a transgenic mouse model of anterior segment dysgenesis. *Development, 127*(3), 533-542.

Romero, P., Sanhueza, F., Lopez, P., Reyes, L., & Herrera, L. (2011). c.194 A>C (Q65P) mutation in the LMX1B gene in patients with nail-patella syndrome associated with glaucoma. *Molecular Vision, 17*, 1929–1939.

Satoda, M., Zhao, F., Diaz, G. A., Burn, J., Goodship, J., Davidson, H. R., . . . Gelb, B. D. (2000). Mutations in TFAP2B cause Char syndrome, a familial form of patent ductus arteriosus. *Nat Genet, 25*(1), 42-46. doi:10.1038/75578

Smith, B. J., Wang, X., Chauhan, B. C., Cote, P. D., & Tremblay, F. (2014). Contribution of retinal ganglion cells to the mouse electroretinogram. *Doc Ophthalmol, 128*(3), 155-168. doi:10.1007/s10633-014-9433-2

Smith, R., Zabaleta, A., Kume, T., Savinova, O., Kidson, S., Martin, J., . . . John, S. (2000). Haploinsufficiency of the transcription factors FOXC1 and FOXC2 results in aberrant ocular development. *Hum Mol Genet., 9*(7), 1021-1032.

Smith, R., Zabaleta, A., Savinova, O., & John, S. (2001). The mouse anterior chamber angle and trabecular meshwork develop without cell death. *BMC Dev Biol., 1*(3).

Tham, Y. C., Li, X., Wong, T. Y., Quigley, H. A., Aung, T., & Cheng, C. Y. (2014). Global prevalence of glaucoma and projections of glaucoma burden through 2040: a systematic review and meta-analysis. *Ophthalmology, 121*(11), 2081-2090. doi:10.1016/j.ophtha.2014.05.013

Tumer, Z., & Bach-Holm, D. (2009). Axenfeld-Rieger syndrome and spectrum of PITX2 and FOXC1 mutations. *Eur J Hum Genet, 17*(12), 1527-1539. doi:10.1038/ejhg.2009.93

Tümer, Z., & Bach-Holm, D. (2009). Axenfeld–Rieger syndrome and spectrum of PITX2 and FOXC1 mutations. *European Journal of Human Genetics, 17*(12), 1527–1539.

Waring, G. O., 3rd, Bourne, W. M., Edelhauser, H. F., & Kenyon, K. R. (1982). The corneal endothelium. Normal and pathologic structure and function. *Ophthalmology, 89*(6), 531-590.

Weinreb, R. N., Aung, T., & Medeiros, F. A. (2014). The pathophysiology and treatment of glaucoma: a review. *JAMA, 311*(18), 1901-1911. doi:10.1001/jama.2014.3192

West-Mays, J. A., Zhang, J., Nottoli, T., Hagopian-Donaldson, S., Libby, D., Strissel, K. J., & Williams, T. (1999). AP-2alpha transcription factor is required for early morphogenesis of the lens vesicle. *Developmental Biology, 206*(1), 46–62.

Wright, C., Tawfik, M. A., Waisbourd, M., & Katz, L. J. (2016). Primary angle-closure glaucoma: an update. *Acta Ophthalmol, 94*(3), 217-225. doi:10.1111/aos.12784

4.   Chapter 4: Conditional Deletion of AP-2β from the Iridocorneal Angle Region Preserves Unconventional Outflow

I helped design the experiments, completed all experiments, data analyses and manuscript writing. Dr. Aftab Taiyab was involved in research design, assisting with experiments and data analysis, and manuscript writing, while Japnit Dham assisted with experiments. Dr. Judith West-Mays was involved in research design, providing reagents and writing the manuscript. Dr. Teresa Borrás was involved in experimental design, providing the *Mgp*-Cre.KI mice and manuscript writing, while Dr. Trevor Williams was involved in research design, providing the *Tfap2b^{lox/lox}* mice and writing the manuscript. The results for Chapter 3 were extracted from a manuscript in preparation, the details for which are given below:

Monica Akula[1*] Aftab Taiyab[1*], Japnit Dham[1], Paula Deschamps[1], Heather Sheardown[2], Trevor Williams[3], Teresa Borras[4], & Judith A. West-Mays[1]

1. McMaster University, Health Sciences Centre

2. McMaster University, Department of Chemical Engineering

3. University of Colorado, Craniofacial Biology

4. University of North Carolina School of Medicine, Department of Ophthalmology

*First co-authors

Abstract

Abnormalities in the trabecular meshwork and Schlemm's canal leading to a disruption in aqueous humor outflow via the conventional pathway can increase IOP, resulting in glaucoma, with AP-2β being critical in development of structures in this outflow pathway. AP-2β deletion from NCCs results in a central to peripheral iridocorneal adhesion that also blocks the unconventional outflow pathway in the AP-2β NCC KO mice. However, upon deletion of AP-2β specifically from the developing trabecular meshwork region (TMR) using the *Mgp*-Cre.KI mouse line (AP-2β TMR KO), the resulting mice displayed only a peripheral iridocorneal adhesion known as PAS. As a result, this study aimed to investigate whether the unconventional pathway may be functional in TMR KO mice. Results showed that while both TMR KO and NCC KO IOP was significantly higher than that of controls, there was no difference in IOP between TMR KO and NCC KO mice. Additionally, IOP reduced in response to treatment with latanoprost, a prostaglandin analog that increases outflow through the unconventional pathway, in TMR KO mice, whereas NCC KO IOP remained elevated compared with controls. Thus, AP-2β TMR KO mice may serve as a model for testing IOP-lowering drugs targeting the unconventional outflow pathway.

4.1. Introduction

There are two major routes of aqueous humour outflow, which include the conventional outflow pathway and the unconventional pathway (Johnson et al., 2017). Conventional outflow occurs through the trabecular meshwork and Schlemm's canal into the aqueous veins. The improper development of the trabecular meshwork in the AP-2β TMR KO mice is likely impeding

conventional outflow, resulting in the high IOP observed. On the other hand, unconventional outflow passes through the ciliary muscle and exits the eye through the sclera and choroid (Johnson et al., 2017). Since histological analyses revealed that the iridocorneal angle is partially open in the TMR KO mice, the 3rd aim of this thesis was to determine whether the unconventional outflow pathway is functional in AP-2β TMR KO mice. First, the partial open angle phenotype observed in H&E-stained sections of TMR KO eyes was confirmed using *in vivo* imaging of the anterior segment. Due to the angle closure phenotype being less severe in the TMR KO compared to the AP-2β NCC KO mice, IOP differences were also analyzed between the two different types of mutants. Subsequently, unconventional outflow pathway function was tested by treating TMR KO mouse eyes and those of their control littermates topically with latanoprost, a prostaglandin analog. AP-2β NCC KO mouse eyes were also treated with latanoprost to serve as a negative control for the unconventional outflow pathway.

4.2. Methods

4.2.1. Animal Husbandry

All procedures were conducted in accordance with the ARVO Statement for the Use of Animals in Ophthalmic and Vision Research. AP-2β TMR KO and AP-2β NCC KO mice were used to examine the unconventional outflow pathway. In both of these mouse models, the *Tfap2b* gene was deleted using either a Cre transgene under control of the *Mgp* gene (Borrás et al., 2015) or the *Wnt1* gene ($H2az2^{Tg(Wnt1-cre)11Rth}$ Tg(Wnt1-GAL4)11Rth/J, Jackson Lab, Bar Harbor, ME). Male *Mgp*-Cre.KI$^{+/-}$; *Tfap2b*$^{+/-}$ mice or male *Wnt1Cre*$^{+/-}$; *Tfap2b*$^{+/-}$ mice were bred with female *Tfap2b*$^{lox/lox}$ mice to generate *Mgp*-Cre.KI$^{+/-}$; *Tfap2b*$^{-/lox}$ mice (AP-2β TMR KOs) and *Wnt1Cre*$^{+/-}$; *Tfap2b*$^{-/lox}$ mice (AP-2β NCC KOs), respectively, as well as age-matched control

littermates. All genotyping was carried out using standard PCR protocols (Martino et al., 2016), and C57BL/6J was used as the background strain for all genetic crosses (Charles River, Wilmington, MA).

4.2.2. Optical Coherence Tomography (OCT)

For all *in vivo* experiments, mice were deeply anesthetized with 2.5% avertin and eye drops (Alcon, Mississauga, CA) were applied to prevent the cornea from drying. For live imaging of the eye, the cornea was positioned 1-2 cm from the Phoenix Micron IV anterior segment imaging system with an OCT attachment (Phoenix Research Labs, Pleasanton, CA).

4.2.3. IOP

Eye drops (Alcon, Mississauga, CA) were applied to the corneas of anesthetized mice to prevent them from drying, and a minimum of 6 IOP values were acquired from each eye using a rebound tonometer (TonoLab, Vantaa, Finland), with each value being an average of 6 measurements (Martino et al., 2016).

4.2.4. Latanoprost Treatment

In order to test whether the unconventional pathway may be functional in the AP-2β TMR KO, the eyes of anesthetized control, TMR KO and NCC KO mice were all treated topically with 0.005% latanoprost (Pfizer, New York, NY), a prostaglandin analog. Prostaglandins are a class of compounds that increase unconventional outflow by relaxing the ciliary muscle and by reducing the amount of extracellular matrix between the ciliary muscle fibres, both of which serve to

increase the space between the fibres (Winkler & Fautsch, 2014). IOP was acquired immediately before treatment, as well as 20 minutes, 1 hour and 24 hours post-treatment.

4.2.5. Statistical Analysis

Differences in IOP between control, AP-2β TMR KO and AP-2β NCC KO animals were analyzed using a one-way ANOVA on GraphPad Prism, while differences in IOP between controls and both types of mutants were analyzed before latanoprost treatment and at various time points after treatment using a two-way repeated measures ANOVA, and if significance was found, Tukey's post hoc test was carried out.

4.3. Results

In vivo imaging of 2-3 month-old control mice showed a completely open iridocorneal angle (Fig. 4.1A), while AP-2β TMR KO mice displayed a partially open iridocorneal angle (Fig. 4.1B). On the other hand, as shown previously (Martino et al., 2016), the AP-2β NCC KO iridocorneal angle was completely closed, with the iris fully adhered to the cornea (Fig. 4.1C). To test whether variation in severity of the angle closure phenotype is leading to a difference in IOP between TMR KOs and NCC KOs, IOP was compared between the two types of mutants. Although the IOP of both types of mutants was significantly higher than control mice (Fig. 4.2; n=6 eyes per genotype; $p<0.0001$ for both types of mutants when compared with controls), no significant difference was found between the IOP of TMR KO and NCC KO mice. Since the TMR KOs possessed a partially open iridocorneal angle, the functionality of the unconventional outflow pathway was tested by treating 2-3 month-old AP-2β TMR KOs with latanoprost, a prostaglandin analogue that increases outflow through the unconventional pathway (Aihara et al., 2002). For

comparison, the same assay was performed either in control mice or AP-2β NCC KO mice – the latter having a complete peripheral to central iridial adhesion to the cornea (Martino et al., 2016). 20 minutes after latanoprost treatment of the AP-2β TMR KO, there was a significant reduction in IOP (n=6 eyes) when compared to its baseline value (Fig. 4.3). By 60 minutes post-treatment, IOP in the TMR KO increased back to its baseline level (p<0.0001), and this continued to be the case at 24 hours post-treatment (p<0.0001). On the other hand, the AP-2β NCC KO mice retained a high IOP even after latanoprost treatment compared to controls (n=6 eyes; p<0.0001 at all time points), demonstrating that the completely closed angle phenotype has prevented functionality of both the conventional and unconventional pathways. These findings indicate that the two AP-2β mutant models have different effects on disrupting the conventional and unconventional outflow pathways in that IOP in TMR KO can be reduced by latanoprost acting through the latter pathway, whereas this treatment has no benefit in the NCC KO model.
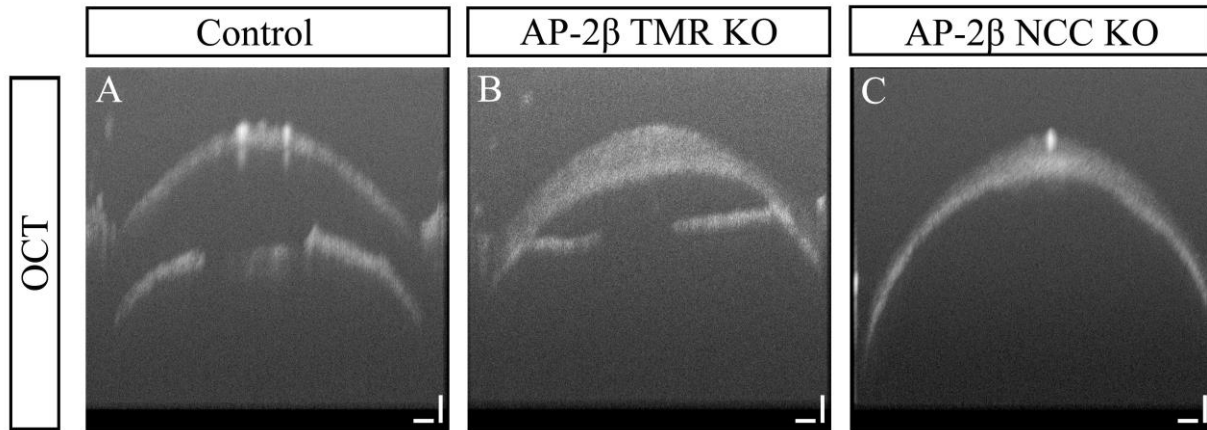
Fig. 4.1. Optical coherence tomography (OCT) images of 2-3 month-old control, AP-2β TMR KO and AP-2β NCC KO eyes. A) OCT images show a fully open iridocorneal angle in control mice. B) The AP-2β TMR KO angle is partially open, displaying a phenotype reminiscent of

peripheral anterior synechia (PAS). C) On the other hand, the AP-2β NCC KO angle is completely closed when compared to both control and AP-2β TMR KO mice. Scale bars 250 μm.
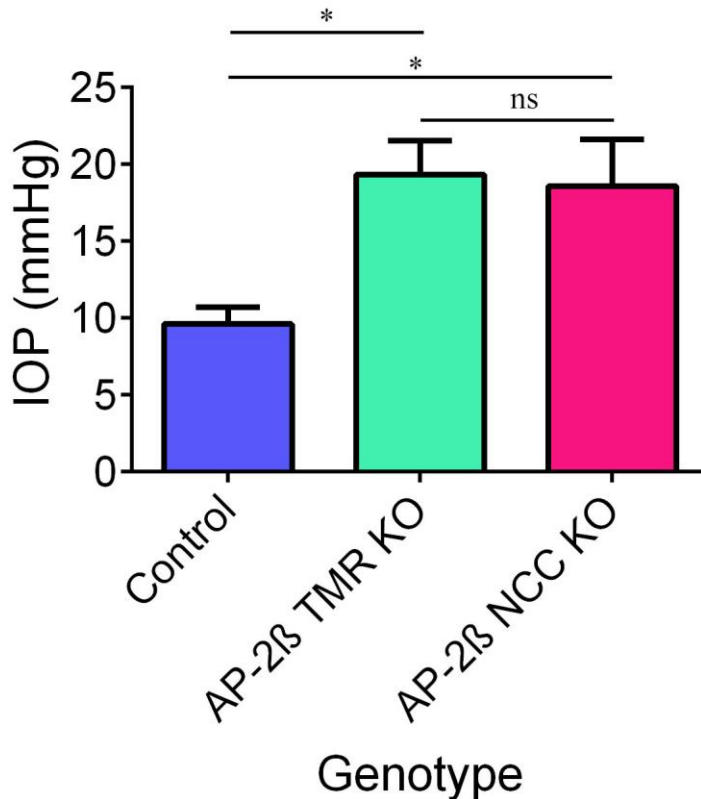
Fig. 4.2. IOP in 2-3 month-old AP-2β TMR KO and AP-2β NCC KO eyes when compared with control eyes. AP-2β TMR KO (n=6 eyes; p<0.0001; all error bars signify standard deviation) and AP-2β NCC KO (n=6 eyes; p<0.0001) mice both display significantly elevated IOP when compared with control mice, but there is no significant difference in IOP between the TMR KO and the NCC KO.
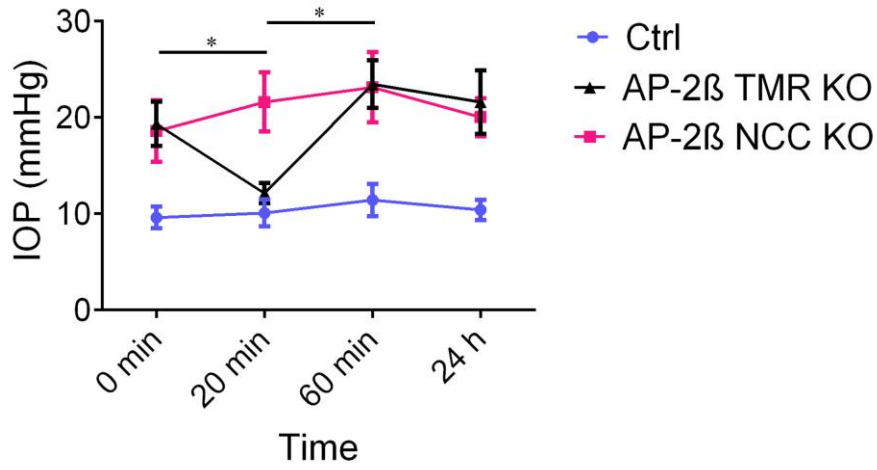
Fig. 4.3. IOP in response to treatment with the prostaglandin analog, latanoprost, in 2-3 month-old AP-2β TMR KO and AP-2β NCC KO mice over time. A) IOP in the AP-2β TMR KO is significantly lower at 20 minutes after latanoprost treatment (n=6 eyes; p<0.0001; all error bars represent standard deviation) when compared to its own baseline IOP. By 60 minutes post-treatment, TMR KO IOP increases significantly compared to the IOP at 20 minutes (p<0.0001). On the other hand, AP-2β NCC KO mice display high IOP both before and after latanoprost treatment (n=6 eyes; p<0.0001 for all time points analyzed compared with controls).

4.4. Discussion

In vivo imaging of the anterior segments of control, AP-2β TMR KO and AP-2β NCC KO mice showed that TMR KO mice had a partially open iridocorneal angle, which corroborates the results from H&E-stained AP-2β TMR KO eye sections (Chapter 3). In comparison, as previously shown (Martino et al., 2016), the AP-2β NCC KO mice displayed complete angle closure. However, despite the angle closure phenotype being less severe in the TMR KO when compared

with the NCC KO, the IOP of TMR KO mice was not significantly different from the IOP of NCC KO mice and was significantly higher than control IOP. The increased IOP in TMR KOs when compared with control mice is likely resulting from improper development of conventional outflow structures (Chapter 3) that is impeding aqueous outflow. On the other hand, the lack of a statistically significant difference between the two different types of KOs could possibly be because the less severe angle closure phenotype in the TMR KO is affecting ciliary body development to a lesser extent when compared to the completely closed angle of the NCC KO, resulting in greater retention of ciliary body function in the TMR KO. Consequently, although the TMR KO may be experiencing greater aqueous outflow, it may also be experiencing greater aqueous humour production compared with the NCC KO, leading to similar IOP values in both types of mutants. Thus, measuring the aqueous humor production in both mutant models would be an interesting avenue to explore in future studies.

Although conventional outflow is blocked in the AP-2β TMR KO mice, as demonstrated by the increased IOP, the unconventional outflow pathway appeared to be functional in these mutants, since the IOP of TMR KO mice was reduced 20 minutes after treatment with latanoprost when contrasted with its baseline IOP value. In comparison, in the AP-2β NCC KO mice used as a negative control, the peripheral to central iridocorneal adhesion prevents outflow through both the conventional and unconventional pathways. As a result, the NCC KO did not exhibit a decrease in IOP following latanoprost treatment. In addition, although the unconventional pathway is functional in the TMR KO, this model displayed similar IOP levels as the NCC KO model (Martino et al., 2016), possibly because unconventional outflow is largely pressure independent (Johnson et al., 2017). In addition, previous studies showed an IOP reduction in wild type mice upon latanoprost treatment (Aihara et al., 2002; Dutca et al., 2018), which was not found to be the

case in control mice in the current study. One possible reason could be that the control mice used in this study were not wild type mice and were age-matched littermates of mutant mice, with these control mice containing at least one transgene. Thus possible differences in genetic background between wild type mice and the control mice used in the current study could be accounting for differences in responsiveness to latanoprost.

In human studies of glaucoma, latanoprost has been shown to lead to a much more sustained reduction in IOP that lasted 6 to 10 hours (Alm, 2014; Garcia-Sanchez et al., 2004; Parrish et al., 2003; Toris et al., 1999), as opposed to the reduction lasting less than 60 minutes in the current study. Despite both mice and humans having a similar aqueous humour turnover rate of 2.5% of the anterior chamber volume per minute (Aihara et al., 2003; Toris et al., 1999), the lack of a sustained effect of latanoprost in mice could be because of the greater percentage of unconventional outflow in mice compared with humans (Johnson et al., 2017). Since conventional outflow is dysfunctional in mouse and human eyes with glaucoma, and since the unconventional pathway accounts for a greater percentage of outflow in mice, latanoprost may be getting cleared from the TMR KO mouse anterior chamber at a more rapid rate compared with the glaucomatous human anterior chamber. Nevertheless, the similar level of effectiveness of latanoprost at reducing IOP in both the TMR KO and humans (Aihara et al., 2002; Parrish et al., 2003) adds to the usefulness of the TMR KO as a mouse model for glaucoma in which the unconventional pathway continues to function, while the NCC KO mouse could be a useful model for studying absence of function of both outflow pathways.

As a potential model of primary angle closure glaucoma, we also propose that the AP-2β TMR KO mouse can be employed to investigate the effects and physiological mechanisms of IOP lowering drugs. Future studies could also look into examining the specific localization of aqueous

humour within the unconventional outflow pathway in AP-2β TMR KO mice. For instance, dextran can be intracamerally injected, and the eyes acquired and sectioned at various time points after injection to examine the time course and specific localization of aqueous outflow through the unconventional pathway (Bernd et al., 2004; Lindsey & Weinreb, 2002) in the TMR KO when compared to control mice.

References

Aihara, M., Lindsey, J. D., & Weinreb, R. N. (2002). Reduction of intraocular pressure in mouse eyes treated with latanoprost. *Invest Ophthalmol Vis Sci, 43*(1), 146-150.

Aihara, M., Lindsey, J. D., & Weinreb, R. N. (2003). Aqueous humor dynamics in mice. *Invest Ophthalmol Vis Sci, 44*(12), 5168-5173. doi:10.1167/iovs.03-0504

Alm, A. (2014). Latanoprost in the treatment of glaucoma. *Clin Ophthalmol, 8*, 1967-1985. doi:10.2147/OPTH.S59162

Bernd, A. S., Aihara, M., Lindsey, J. D., & Weinreb, R. N. (2004). Influence of molecular weight on intracameral dextran movement to the posterior segment of the mouse eye. *Invest Ophthalmol Vis Sci, 45*(2), 480-484. doi:10.1167/iovs.03-0462

Borrás, T., Smith, M., & Buie, L. (2015). A Novel Mgp-Cre Knock-In Mouse Reveals an Anticalcification/Antistiffness Candidate Gene in the Trabecular Meshwork and Peripapillary Scleral Region. *IOVS, 56*(4), 2203–2214.

Dutca, L. M., Rudd, D., Robles, V., Galor, A., Garvin, M. K., & Anderson, M. G. (2018). Effects of sustained daily latanoprost application on anterior chamber anatomy and physiology in mice. *Sci Rep, 8*(1), 13088. doi:10.1038/s41598-018-31280-1

Garcia-Sanchez, J., Rouland, J. F., Spiegel, D., Pajic, B., Cunliffe, I., Traverso, C., & Landry, J. (2004). A comparison of the fixed combination of latanoprost and timolol with the unfixed combination of brimonidine and timolol in patients with elevated intraocular pressure. A six month, evaluator masked, multicentre study in Europe. *Br J Ophthalmol, 88*(7), 877-883. doi:10.1136/bjo.2003.029330

Johnson, M., McLaren, J. W., & Overby, D. R. (2017). Unconventional aqueous humor outflow: A review. *Exp Eye Res, 158*, 94-111. doi:10.1016/j.exer.2016.01.017

Lindsey, J. D., & Weinreb, R. N. (2002). Identification of the mouse uveoscleral outflow pathway using fluorescent dextran. *Invest Ophthalmol Vis Sci, 43*(7), 2201-2205.

Martino, V. B., Sabljic, T., Deschamps, P., Green, R. M., Akula, M., Peacock, E., . . . West-Mays, J. A. (2016). Conditional deletion of AP-2β in the cranial neural crest results in anterior segment dysgenesis and early-onset glaucoma. *Disease Models & Mechanisms, 9*(8), 849–861.

Parrish, R. K., Palmberg, P., Sheu, W. P., & Group, X. L. T. S. (2003). A comparison of latanoprost, bimatoprost, and travoprost in patients with elevated intraocular pressure: a 12-week, randomized, masked-evaluator multicenter study. *Am J Ophthalmol, 135*(5), 688-703. doi:10.1016/s0002-9394(03)00098-9

Toris, C. B., Yablonski, M. E., Wang, Y. L., & Camras, C. B. (1999). Aqueous humor dynamics in the aging human eye. *Am J Ophthalmol, 127*(4), 407-412. doi:10.1016/s0002-9394(98)00436-x

Winkler, N. S., & Fautsch, M. P. (2014). Effects of prostaglandin analogues on aqueous humor outflow pathways. *J Ocul Pharmacol Ther, 30*(2-3), 102-109. doi:10.1089/jop.2013.0179

5.   Chapter 5: General Discussion

AP-2β Plays Important Roles in Development of Anterior Segment Structures Required for

IOP Homeostasis

The study of the molecular mechanisms of ASD is a key area of research that requires further investigation in order to both understand the etiology of congenital glaucoma, but also to help develop novel treatments for this condition. Congenital glaucoma resulting from ASD typically occurs due to increased IOP that can mechanically damage RGCs, thereby causing vision loss (Gould & John, 2002). IOP results from the balance between aqueous humour secretion by the ciliary body (Civan & Macknight, 2004), and aqueous humour outflow through the conventional pathway consisting of the trabecular meshwork and Schlemm's canal (Tamm, 2009), as well as the unconventional pathway including the ciliary muscle (Johnson et al., 2017). Several transcription factors have been shown to play a role in development of anterior segment structures (Chen, 2016; Liu & Johnson, 2010; Pressman et al., 2000; Smith et al., 2000), where conditional deletion of transcription factor AP-2β from NCCs has previously been shown to result in anterior segment defects including a peripheral to central iridocorneal adhesion, coupled with increased IOP and glaucomatous features of the retina (Martino et al., 2016).

The current study aims to investigate the role of AP-2β transcription factor in development of aqueous humour outflow structures important for IOP balance. To do so, the AP-2β NCC KO was used, with data from initial experiments suggesting that AP-2β plays a direct role in trabecular meshwork development and differentiation, whereas AP-2β appeared to be playing an indirect role in Schlemm's canal development (Chapter 2). However, numerous corneal defects have been reported in NCC KOs (Martino et al., 2016), wherein the peripheral to central iridocorneal

adhesion could have also caused the trabecular meshwork defects. Consequently, the AP-2β TMR KO mouse model was generated using *Mgp*-Cre.KI that is more specifically localized to the iridocorneal angle (Borrás et al., 2015), with results showing a similar absence of formation of a trabecular meshwork region (Chapter 3), suggesting that transcription factor AP-2β is required for development of conventional outflow pathway structures. However, the Schlemm's canal of the TMR KO was hypoplastic, as opposed to the complete absence observed in the NCC KO, further supporting an indirect role for AP-2β in development of this structure. In addition, TMR KOs did not display a peripheral to central iridocorneal adhesion, since corneal endothelial cells were present, which led to retention of function of the unconventional outflow pathway in the TMR KO (Chapter 4). The results of this study also demonstrate that increased IOP in TMR KOs is correlated with glaucomatous changes, such as the loss of RGCs, and reduced retinal thickness and function (Chapter 3), making AP-2β a potential gene that requires further investigation in humans with glaucoma.

The Cell-Autonomous Role of AP-2β in Differentiation and Morphogenesis of the Trabecular Meshwork

AP-2β, an important protein in the AP-2 family of transcription factors, is implicated in anterior segment development (Barzago et al., 2017; Chen, 2016; Chen et al., 2016; Martino et al., 2016; West-Mays et al., 1999). However, previous studies have not looked into whether AP-2β plays a role in development of conventional aqueous outflow pathway structures derived from the POM. Upon initial observations of the lack of a morphologically distinct trabecular meshwork region and a reduction in tdTomato expression in the iridocorneal angle using fate mapping experiments in AP-2β NCC KO mice, immunohistochemistry was performed for trabecular

meshwork markers, αSMA and myocilin (Chapter 2). The reduction in expression of these proteins in the NCC KO suggested that AP-2β is likely playing a direct role in trabecular meshwork development. However, since the Wnt1Cre used to generate the NCC KO was expressed in multiple NCC derivatives including the cornea, *Mgp*-Cre.KI that was previously shown to be specifically localized to the iridocorneal angle region in adult mice (Borrás et al., 2015) was used to generate AP-2β TMR KOs to more specifically target the developing POM cell population giving rise to the trabecular meshwork (Chapter 3). These mice also displayed a reduction in expression of trabecular meshwork markers, adding evidence to the hypothesis that AP-2β plays a cell-autonomous role in trabecular meshwork cell differentiation. Moreover, previous studies showed that *Tfap2b* plays a direct role in corneal endothelial cell differentiation (Chen et al., 2016; Hara et al., 2018; Martino et al., 2016), and similar to the corneal endothelium, trabecular meshwork cells are an endothelial-like cell type derived from NCCs. In addition, AP-2α–AP-2β heterodimers are involved in NCC specification at the neural plate border (Rothstein & Simoes-Costa, 2020). The observations from the current study add to these previous studies demonstrating that AP-2β may be playing a cell-autonomous role in differentiation of cranial neural crest derivatives.

Although *Mgp*-Cre.KI expression is more specific to the developing TMR when compared with Wnt1Cre, anterior segment defects in tissues other than aqueous outflow pathway structures still resulted from conditional AP-2β deletion using *Mgp*-Cre.KI (Chapter 3). Consequently, future studies could confirm that AP-2β plays a cell-autonomous role in trabecular meshwork development using a trabecular meshwork-specific temporal Cre mouse line, such as the Myoc-CreER(T2) (Liu et al., 2011), or by creating a temporal *Mgp*-Cre.KI mouse, in order to delete AP-2β from trabecular meshwork cells during the time period of differentiation of this tissue type

between P4 and P10 (Cvekl & Tamm, 2004). Upon deletion of AP-2β, eyes could be histologically examined for gross morphological defects. If POM cells appear to be present at the iridocorneal angle, immunohistochemistry can be performed for markers of trabecular meshwork cell differentiation, including the more broadly expressed marker, myocilin, in addition to the more specific markers, CHI3L1 staining the juxtacanalicular region, as well as FABP4 staining the uveal and corneoscleral beam areas (van Zyl et al., 2020). These experiments could help determine whether all trabecular meshwork sub-types are differentiating appropriately.

AP-2β acts in concert with several other genes as part of a network at specific time points to effect transcriptional changes required for anterior segment development. In addition to *Tfap2b*, other genes, such as *Pitx2*, *Foxc1* and *Foxc2*, as well as *Lmx1b* (Chen, 2016; Liu & Johnson, 2010; Smith et al., 2000), mutations in which lead to a similarly aberrant trabecular meshwork region as AP-2β KO mouse models, also play important roles in development of the trabecular meshwork. In order to determine the requirement of AP-2β in the gene network regulating development and differentiation of conventional aqueous outflow structures, RNA-sequencing of iridocorneal angle tissue containing the trabecular meshwork could be carried out at early postnatal stages in trabecular meshwork-specific temporal KO mice with AP-2β ablated between P4 and P10. This would determine the differential gene expression levels in the conventional outflow pathway upon AP-2β deletion during time periods of differentiation of these tissues. The regulatory role of AP-2β during trabecular meshwork specification, differentiation and morphogenesis can also be studied. For instance, chromatin immunoprecipitation sequencing (ChIP-sequencing) can be performed on wild type iridocorneal angle tissue to determine the gene regulatory sequences to which AP-2β binds during trabecular meshwork differentiation and to determine the function of

the genes regulated by AP-2β, while tissue from trabecular meshwork-specific temporal AP-2β

KOs can be used as a control.

The Non-Cell-Autonomous Role of AP-2β in Development of the Schlemm's Canal

Although AP-2β is not being deleted from the paraxial mesoderm cell population of the POM

in the AP-2β NCC KO, the mesoderm-derived Schlemm's canal was found to be absent in these

animals (Chapter 2). Moreover, upon targeted conditional deletion of AP-2β from the developing

POM cell population giving rise to the future trabecular meshwork and Schlemm's canal, the

resulting AP-2β TMR KO mutants had a hypoplastic Schlemm's canal (Chapter 3). The presence

of a hypoplastic Schlemm's canal in the AP-2β TMR KO indicates that AP-2β is likely playing an

indirect role in development of this structure. This is because the less severe angle closure

phenotype in TMR KOs led to a less severe Schlemm's canal phenotype compared to the absence

of formation of this structure in the NCC KO, which was likely an indirect effect of the peripheral

to central iridocorneal adhesion in the NCC KO. One proposed explanation for the indirect role

for AP-2β in Schlemm's canal development is based on previous studies showing that IOP-induced

expression of transcription factors, such as Prox1, is important for development of this structure

(Choi et al., 2017). Absence of the trabecular meshwork in the NCC KO and TMR KO could

possibly be preventing pressure-induced expression of these genes, which needs to be further

investigated.

The Requirement of AP-2β for IOP Homeostasis

Through its role in development of anterior segment structures (Barzago et al., 2017; Chen

et al., 2016; Hara et al., 2018; Martino et al., 2016), AP-2β is important for function of the

conventional and unconventional outflow pathways, and thus, is required for the maintenance of IOP homeostasis. Since AP-2β plays a role in trabecular meshwork and Schlemm's canal development (Chapters 2 & 3), AP-2β is required for conventional outflow of aqueous humour. On the other hand, the role of AP-2β in function of the unconventional pathway stems from its role in development of the anterior segment. This is because the peripheral to central adhesion of the iris to the cornea in AP-2β NCC KOs (Martino et al., 2016) blocks the unconventional pathway, preventing aqueous humour from being able to flow into the spaces of the ciliary muscle. On the other hand, in the AP-2β TMR KO with PAS, the iridocorneal angle is partially open, resulting in fewer corneal defects in this model compared to the NCC KO, allowing aqueous fluid to flow into the spaces between ciliary muscle fibres. Consequently, when IOP was tested in response to treatment with latanoprost, the TMR KO displayed a reduction in IOP 20 minutes after treatment compared to its baseline IOP (Chapter 4), demonstrating functionality of the unconventional outflow pathway. However, the IOP of the NCC KO serving as a negative control did not change at 20 minutes, remaining significantly elevated compared with control mice. Additionally, although the unconventional pathway was functional in TMR KOs, IOP was not significantly different from that of the NCC KO, since the unconventional pathway is pressure-independent and thus, unresponsive to increased IOP. This is the first time that latanoprost has been tested and compared in two different conditional AP-2β KO mouse models, one with and one without unconventional outflow.

Future studies can measure aqueous humour localization within the unconventional pathway in the TMR KOs using dextran (Bernd et al., 2004; Lindsey & Weinreb, 2002; Weinreb & Lindsey, 2002). Upon intracameral injection of dextran, the eye can be extracted and frozen sections can be examined for localization of aqueous humour within the unconventional outflow pathway at

various time points after injection. Future directions also include investigating the effect of different types of prostaglandin analogs (Winkler & Fautsch, 2014) and other types of drugs that target the unconventional pathway like muscarinic agonists (Johnson et al., 2017) on the IOP of TMR KO mice, as well as exploring various mechanisms of unconventional outflow for each drug type. Additional next steps include elucidating the molecular mechanisms of extracellular matrix remodelling occurring between ciliary muscle fibres during unconventional outflow (Winkler & Fautsch, 2014). This data can then be used to test drugs that target specific mechanistic pathways through which extracellular matrix remodelling occurs. For instance, it has been shown that MMP expression increases upon latanoprost treatment in ciliary muscle cells, leading to the breakdown of extracellular matrix components (Winkler & Fautsch, 2014). Consequently, MMP agonists could be tested in TMR KO eyes to determine whether they would reduce IOP.

Despite the less severe angle closure phenotype in the TMR KO when compared with the NCC KO, IOP was not significantly different between the two models, possibly due to greater retention of ciliary body function in the TMR KO as a result of the angle being partially open. In order to determine whether differences in aqueous humour production between the NCC KO and TMR KO are leading to similar IOP values in both models, aqueous humour production can be measured and compared with control littermates. Fluorescein can be topically added to mouse corneas and the anterior segment can be imaged using a camera equipped with a fluorescence filter at various time points after adding the compound, and the aqueous humour production rate can be calculated by measuring the fluorescence decay in the acquired images over time (Avila et al., 2003; Toris et al., 2016). Based on the results of the current study, the NCC KO mouse can be used as a model to study glaucoma pathophysiology in the absence of both outflow pathways, whereas the TMR KO can be used to study glaucoma pathology in the absence of the conventional

outflow pathway. Furthermore, the NCC KO model can be used to test the effect of IOP-lowering drugs that work through the ciliary body while the TMR KO can be used to test drugs that target the ciliary body and the unconventional outflow pathway (Winkler & Fautsch, 2014).

High IOP in AP-2β TMR KOs is Associated with Glaucomatous Changes

Previous studies in which AP-2β was conditionally deleted from NCCs showed glaucomatous changes in the retina, including reduced retinal thickness and a reduction in the number of RGCs, in addition to a loss of RGC axons and increased microglial activity (Martino et al., 2016). Data from the current study suggests that conditional AP-2β deletion from Mgp-expressing cells leads to increased IOP that then likely results in glaucomatous changes, such as a reduced number of RGCs. While the AP-2β NCC KO central cornea was adhered to the lens (Martino et al., 2016), precluding functional analysis of the retina, the AP-2β TMR KO had an intact corneal endothelium, preventing formation of such an adhesion, allowing for measurement of functional responses of the retina to flashes of light in a full field scotopic ERG, which showed a reduction in retinal function in the TMR KOs (Chapter 3) in comparison to controls.

Further glaucomatous changes in the retina can be studied in the TMR KO, including glial reactivity (Martino et al., 2016) and vascular changes (Gericke et al., 2019). In addition, in order to specifically test RGC function, a pattern ERG can be used (Lu et al., 2020), which can help determine whether the reduction in function of inner retinal neurons observed in the current study is due to a reduction in RGC function. Furthermore, the possibility that loss of other cell types from the thinning inner nuclear layer in the TMR KO could be contributing to the reduction in b-wave amplitude can be tested by immunostaining for markers of cells found in this layer, such as amacrine cells and bipolar cells. Both the AP-2β NCC KO and the AP-2β TMR KO add to

previously established models of glaucoma, such as the optic nerve crush model, the DBA/2J model and the microbead injection model (Johnson & Tomarev, 2010), as well as transgenic mouse models of glaucoma (Chen, 2016; Liu & Johnson, 2010; Mao et al., 2011; Smith et al., 2000), with the added benefit that the NCC KO and TMR KO are acute models that develop increased IOP in a short time span. Both types of KOs can serve as models of primary angle closure glaucoma that can be used to test the effect of neuroprotective drugs (Pardue & Allen, 2018) and RGC rescue experiments (Lu et al., 2020). Moreover, the TMR KO can be used to perform assessments of retinal function.

AP-2β in ASD and Human Glaucoma

AP-2β is involved in development of various anterior segment structures, including not only the trabecular meshwork and the Schlemm's canal, but also the cornea and ciliary body (Chapters 2 & 3). AP-2β has previously been shown to be required for corneal endothelial cell differentiation, in addition to angiogenic privilege in the cornea (Chen et al., 2016; Hara et al., 2018; Martino et al., 2016). Results from the current study showed that upon more specific deletion of AP-2β from the developing iridocorneal angle region, TMR KOs displayed fewer corneal defects than the NCC KO (Chapter 3), suggesting that the corneal defects observed in NCC KOs likely occurred because of a direct role for AP-2β in corneal development. In addition to playing a role in corneal development, AP-2β may also be playing a role in ciliary body development, since there were fewer ciliary folds in both the NCC KO (Chapter 2) and the TMR KO (Chapter 3) when compared with the control ciliary body. Iridocorneal adhesions in both models may be preventing the developing optic cup rim from forming ciliary processes, resulting in a reduction in ciliary body folding. On the other hand, it is also possible that AP-2β expression in the NCC-derived ciliary

stroma may be important for formation of this structure required for aqueous humour secretion, and future directions include separating out these two possibilities in both KO mouse models. Based on the results of the current study demonstrating the role of AP-2β in anterior segment development in mice, the potential role of *TFAP2B* in human ASD can be investigated further, particularly with respect to human trabecular meshwork, Schlemm's canal, ciliary body and corneal development. For example, since mutations in the *TFAP2B* gene are associated with Char syndrome (Zhao et al., 2001), GWAS studies can also be performed on a large sample of human Char syndrome patients to test whether there may be an association between *TFAP2B* and anterior ocular defects in these patients. It would also be interesting to examine ASD and Char syndrome patients to look for an association between this gene and glaucoma.

Conclusions

This study demonstrates a cell-autonomous role for AP-2β in development of the trabecular meshwork and a non-cell-autonomous role in development of the Schlemm's canal, both being conventional aqueous outflow structures, while AP-2β appears to be playing an indirect role in function of the unconventional pathway, all of which provides evidence for the requirement of AP-2β in IOP balance. The AP-2β NCC KO displayed numerous anterior segment defects, including an abnormally developing trabecular meshwork region. However, since Wnt1Cre is broadly expressed in multiple neural crest derivatives, including the cornea, further studies were carried out on the AP-2β TMR KO created using the more specific *Mgp*-Cre.KI to determine the role of AP-2β in trabecular meshwork development independent of its role in corneal development. Results from the TMR KO mice support the postulation that AP-2β plays a cell-autonomous role in trabecular meshwork development and differentiation. On the other hand, AP-2β likely plays an

indirect role in development of the Schlemm's canal. Furthermore, although AP-2β was shown to be directly required for function of the conventional pathway, AP-2β was shown to only be indirectly required for unconventional pathway function through its role in development of the cornea, abnormalities in which cause a central to peripheral iridocorneal adhesion that blocks this outflow pathway in the NCC KO. Since AP-2β NCC KO and AP-2β TMR KO mice exhibit both elevated IOP and a loss of RGCs, they may serve as models of primary angle closure glaucoma. Moreover, the NCC KO and TMR KOs are valuable additions to previous models of glaucoma (Chen, 2016; Johnson & Tomarev, 2010; Liu & Johnson, 2010; Mao et al., 2011; Smith et al., 2000), since they are acute models that consistently develop increased IOP over a shorter time span in comparison to other models, such as the DBA/2J model (Johnson & Tomarev, 2010). One advantage of using the TMR KO mouse over the NCC KO mouse is that AP-2β is being deleted more specifically from the iridocorneal angle region giving rise to the trabecular meshwork. This allows for the study of the cell-autonomous role of AP-2β in development of trabecular meshwork tissue. Another advantage is the ability to use the TMR KO to test IOP-lowering drugs that target unconventional outflow, in addition to being able to examine retinal function. Both the AP-2β TMR KO and the AP-2β NCC KO can also be used for developing molecular therapeutic strategies for human glaucoma, in addition to testing the effect of RGC rescue strategies and neuroprotective drugs.

References

Abu-Hassan, D. W., Acott, T. S., & Kelley, M. J. (2014). The Trabecular Meshwork: A Basic Review of Form and Function. *J Ocul Biol, 2*(1). doi:10.13188/2334-2838.1000017

Acott, T. S., & Kelley, M. J. (2008). Extracellular matrix in the trabecular meshwork. *Exp Eye Res., 86*(4), 543-561.

Aihara, M., Lindsey, J. D., & Weinreb, R. N. (2003). Aqueous humor dynamics in mice. *Invest Ophthalmol Vis Sci, 44*(12), 5168-5173. doi:10.1167/iovs.03-0504

Akula, M., Park, J. W., & West-Mays, J. A. (2019). Relationship between neural crest cell specification and rare ocular diseases. *J Neurosci Res, 97*(1), 7-15. doi:10.1002/jnr.24245

Allison, K., Patel, D., & Alabi, O. (2020). Epidemiology of Glaucoma: The Past, Present, and Predictions for the Future. *Cureus, 12*(11), e11686. doi:10.7759/cureus.11686

Avila, M. Y., Mitchell, C. H., Stone, R. A., & Civan, M. M. (2003). Noninvasive assessment of aqueous humor turnover in the mouse eye. *Invest Ophthalmol Vis Sci, 44*(2), 722-727. doi:10.1167/iovs.02-0386

Bamforth, S. D., Braganca, J., Eloranta, J. J., Murdoch, J. N., Marques, F. I., Kranc, K. R., . . . Bhattacharya, S. (2001). Cardiac malformations, adrenal agenesis, neural crest defects and exencephaly in mice lacking Cited2, a new Tfap2 co-activator. *Nat Genet, 29*(4), 469-474. doi:10.1038/ng768

Barrallo-Gimeno, A., Holzschuh, J., Driever, W., & Knapik, E. W. (2004). Neural crest survival and differentiation in zebrafish depends on mont blanc/tfap2a gene function. *Development, 131*(7), 1463-1477. doi:10.1242/dev.01033

Barzago, M. M., Kurosaki, M., Fratelli, M., Bolis, M., Giudice, C., Nordio, L., . . . Garattini, E. (2017). Generation of a new mouse model of glaucoma characterized by reduced expression of the AP-2β and AP-2δ proteins. *Sci Rep., 7*, 11140.

Bassett, E., Korol, A., Deschamps, P., Buettner, R., Wallace, V., Williams, T., & West-Mays, J. (2012). Overlapping expression patterns and redundant roles for AP-2 transcription factors in the developing mammalian retina. *Dev Dyn., 241*(4), 814-829.

Bassett, E., Pontoriero, G., Feng, W., Marquardt, T., Fini, M., Williams, T., & West-Mays, J. (2007). Conditional deletion of activating protein 2alpha (AP-2alpha) in the developing retina demonstrates non-cell-autonomous roles for AP-2alpha in optic cup development. *Mol Cell Biol., 27*(21), 7497-7510.

Bassett, E., Williams, T., Zacharias, A., Gage, P., Fuhrmann, S., & West-Mays, J. (2010). AP-2alpha knockout mice exhibit optic cup patterning defects and failure of optic stalk morphogenesis. *Hum Mol Genet., 19*(9), 1791-1804.

Beebe, D. C., & Coats, J. M. (2000). The lens organizes the anterior segment: specification of neural crest cell differentiation in the avian eye. *Dev Biol, 220*(2), 424-431. doi:10.1006/dbio.2000.9638

Bernd, A. S., Aihara, M., Lindsey, J. D., & Weinreb, R. N. (2004). Influence of molecular weight on intracameral dextran movement to the posterior segment of the mouse eye. *Invest Ophthalmol Vis Sci, 45*(2), 480-484. doi:10.1167/iovs.03-0462

Borrás, T., Smith, M., & Buie, L. (2015). A Novel Mgp-Cre Knock-In Mouse Reveals an Anticalcification/Antistiffness Candidate Gene in the Trabecular Meshwork and Peripapillary Scleral Region. *IOVS, 56*(4), 2203–2214.

Braganca, J., Eloranta, J. J., Bamforth, S. D., Ibbitt, J. C., Hurst, H. C., & Bhattacharya, S. (2003). Physical and functional interactions among AP-2 transcription factors, p300/CREB-binding protein, and CITED2. *J Biol Chem, 278*(18), 16021-16029. doi:10.1074/jbc.M208144200

Braganca, J., Swingler, T., Marques, F. I., Jones, T., Eloranta, J. J., Hurst, H. C., . . . Bhattacharya, S. (2002). Human CREB-binding protein/p300-interacting transactivator with ED-rich tail (CITED) 4, a new member of the CITED family, functions as a co-activator for transcription factor AP-2. *J Biol Chem, 277*(10), 8559-8565. doi:10.1074/jbc.M110850200

Carreon, T., van der Merwe, E., Fellman, R. L., Johnstone, M., & Bhattacharya, S. K. (2017). Aqueous outflow - A continuum from trabecular meshwork to episcleral veins. *Prog Retin Eye Res, 57*, 108-133. doi:10.1016/j.preteyeres.2016.12.004

Chen, H., Howald, W. N., & Juchau, M. R. (2000). Biosynthesis of all-trans-retinoic acid from all-trans-retinol: catalysis of all-trans-retinol oxidation by human P-450 cytochromes. *Drug Metab Dispos, 28*(3), 315-322.

Chen, L., & Gage, P. J. (2016). Heterozygous Pitx2 Null Mice Accurately Recapitulate the Ocular Features of Axenfeld-Rieger Syndrome and Congenital Glaucoma. *IOVS, 57*, 5023-5030.

Chen, L., Martino, M., Dombkowski, A., Williams, T., West-Mays, J., & Gage, P. J. (2016). AP-2β is a downstream effector of PITX2 required to specify endothelium and establish angiogenic privilege during corneal development. *Invest Ophthalmol Vis Sci., 57*(3), 1072–1081.

Choi, D., Park, E., Jung, E., Seong, Y. J., Hong, M., Lee, S., . . . Hong, Y. K. (2017). ORAI1 Activates Proliferation of Lymphatic Endothelial Cells in Response to Laminar Flow

Through Kruppel-Like Factors 2 and 4. *Circ Res, 120*(9), 1426-1439. doi:10.1161/CIRCRESAHA.116.309548

Choudhary, R., Palm-Leis, A., Scott, R. C., 3rd, Guleria, R. S., Rachut, E., Baker, K. M., & Pan, J. (2008). All-trans retinoic acid prevents development of cardiac remodeling in aortic banded rats by inhibiting the renin-angiotensin system. *Am J Physiol Heart Circ Physiol, 294*(2), H633-644. doi:10.1152/ajpheart.01301.2007

Chow, R. L., & Lang, R. A. (2001). Early eye development in vertebrates. *Annu Rev Cell Dev Biol, 17*, 255-296. doi:10.1146/annurev.cellbio.17.1.255

Civan, M., & Macknight, A. (2004). The Ins and Outs of Aqueous Humour Secretion *Exp Eye Res., 78*(3), 625-631.

Crawford, K., & Kaufman, P. L. (1987). Pilocarpine antagonizes prostaglandin F2 alpha-induced ocular hypotension in monkeys. Evidence for enhancement of Uveoscleral outflow by prostaglandin F2 alpha. *Arch Ophthalmol, 105*(8), 1112-1116. doi:10.1001/archopht.1987.01060080114039

Cvekl, A., & Tamm, E. (2004). Anterior eye development and ocular mesenchyme: new insights from mouse models and human diseases. *Bioessays, 26*(4), 374-386.

Dwivedi, D. J., Pontoriero, G. F., Ashery-Padan, R., Sullivan, S., Williams, T., & West-Mays, J. A. (2005). Targeted deletion of AP-2alpha leads to disruption in corneal epithelial cell integrity and defects in the corneal stroma. *Invest Ophthalmol Vis Sci, 46*(10), 3623-3630. doi:10.1167/iovs.05-0028

Eckert, D., Buhl, S., Weber, S., Jäger, R., & Schorle, H. (2005). The AP-2 family of transcription factors. *Genome Biology, 6*(13), 246.

Gage, P., Rhoades, W., Prucka, S., & Hjalt, T. (2005). Fate maps of neural crest and mesoderm in the mammalian eye. *Invest Ophthalmol Vis Sci., 46*(11), 4200-4208.

Gericke, A., Mann, C., Zadeh, J. K., Musayeva, A., Wolff, I., Wang, M., . . . Prokosch, V. (2019). Elevated Intraocular Pressure Causes Abnormal Reactivity of Mouse Retinal Arterioles. *Oxid Med Cell Longev, 2019*, 9736047. doi:10.1155/2019/9736047

Gestri, G., Osborne, R. J., Wyatt, A. W., Gerrelli, D., Gribble, S., Stewart, H., . . . Ragge, N. K. (2009). Reduced TFAP2A function causes variable optic fissure closure and retinal defects and sensitizes eye development to mutations in other morphogenetic regulators. *Hum Genet, 126*(6), 791-803. doi:10.1007/s00439-009-0730-x

Goel, M., Picciani, R. G., Lee, R. K., & Bhattacharya, S. K. (2010). Aqueous humor dynamics: a review. *Open Ophthalmol J, 4*, 52-59. doi:10.2174/1874364101004010052

Gould, D., Smith, R., & John, S. (2004). Anterior segment development relevant to glaucoma. *Int J Dev Biol., 48*(8-9), 1015-1029.

Gould, D. B., & John, S. W. (2002). Anterior segment dysgenesis and the developmental glaucomas are complex traits. *Hum Mol Genet., 11*(10), 1185-1193.

Gupta, M. P., Herzlich, A. A., Sauer, T., & Chan, C. C. (2016). Retinal Anatomy and Pathology. *Dev Ophthalmol, 55*, 7-17. doi:10.1159/000431128

Hara, S., Kawasaki, S., Yoshihara, M., Winegarner, A., Busch, C., Tsujikawa, M., & Nishida, K. (2019). Transcription factor TFAP2B up-regulates human corneal endothelial cell-specific genes during corneal development and maintenance. *J Biol Chem, 294*(7), 2460-2469. doi:10.1074/jbc.RA118.005527

Hara, S., Kawasaki, S., Yoshihara, M., Winegarner, A., Caleb, B., Tsujikawa, M., & Nishida, K. (2018). Transcription factor TFAP2B up-regulates human corneal endothelial cell–specific

genes during corneal development and maintenance. *Journal of Biol. Chem., 294*, 2460–2469.

Hesse, K., Vaupel, K., Kurt, S., Buettner, R., Kirfel, J., & Moser, M. (2011). AP-2delta is a crucial transcriptional regulator of the posterior midbrain. *PLoS One, 6*(8), e23483. doi:10.1371/journal.pone.0023483

Hicks, E. A., Zaveri, M., Deschamps, P. A., Noseworthy, M. D., Ball, A., Williams, T., & West-Mays, J. A. (2018). Conditional Deletion of AP-2alpha and AP-2beta in the Developing Murine Retina Leads to Altered Amacrine Cell Mosaics and Disrupted Visual Function. *Invest Ophthalmol Vis Sci, 59*(6), 2229-2239. doi:10.1167/iovs.17-23283

Hilger-Eversheim, K., Moser, M., Schorle, H., & Buettner, R. (2000). Regulatory roles of AP-2 transcription factors in vertebrate development, apoptosis and cell-cycle control. *Gene, 260*(1-2), 1-12. doi:10.1016/s0378-1119(00)00454-6

Jain, S., Glubrecht, D. D., Germain, D. R., Moser, M., & Godbout, R. (2018). AP-2epsilon Expression in Developing Retina: Contributing to the Molecular Diversity of Amacrine Cells. *Sci Rep, 8*(1), 3386. doi:10.1038/s41598-018-21822-y

Johnson, M., McLaren, J. W., & Overby, D. R. (2017). Unconventional aqueous humor outflow: A review. *Exp Eye Res, 158*, 94-111. doi:10.1016/j.exer.2016.01.017

Johnson, T. V., & Tomarev, S. I. (2010). Rodent models of glaucoma. *Brain Res Bull, 81*(2-3), 349-358. doi:10.1016/j.brainresbull.2009.04.004

Kerr, C., Zaveri, M., Robinson, M., Williams, T., & West-Mays, J. (2014). AP-2α is required after lens vesicle formation to maintain lens integrity. *Developmental Dynamics, 243*(10), 1298–1309.

Kizhatil, K., Ryan, M., Marchant, J. K., Henrich, S., & John, S. W. M. (2014). Schlemm's Canal Is a Unique Vessel with a Combination of Blood Vascular and Lymphatic Phenotypes that Forms by a Novel Developmental Process. *PLOS Biology, 12*(7), e1001912.

Knight, R. D., Javidan, Y., Nelson, S., Zhang, T., & Schilling, T. (2004). Skeletal and pigment cell defects in the lockjaw mutant reveal multiple roles for zebrafish tfap2a in neural crest development. *Dev Dyn, 229*(1), 87-98. doi:10.1002/dvdy.10494

Ko, M., & Tan, J. (2013). Contractile markers distinguish structures of the mouse aqueous drainage tract. *Mol Vis., 19*, 2561–2570.

Lee, J. Y., Kim, Y. Y., & Jung, H. R. (2006). Distribution and characteristics of peripheral anterior synechiae in primary angle-closure glaucoma. *Korean J Ophthalmol, 20*(2), 104-108. doi:10.3341/kjo.2006.20.2.104

Li, X., Monckton, E. A., & Godbout, R. (2014). Ectopic expression of transcription factor AP-2delta in developing retina: effect on PSA-NCAM and axon routing. *J Neurochem, 129*(1), 72-84. doi:10.1111/jnc.12521

Libby, R. T., Smith, R. S., Savinova, O. V., Zabaleta, A., Martin, J. E., Gonzalez, F. J., & John, S. W. (2003). Modification of ocular defects in mouse developmental glaucoma models by tyrosinase. *Science, 299*(5612), 1578-1581. doi:10.1126/science.1080095

Lin, J. M., Taroc, E. Z. M., Frias, J. A., Prasad, A., Catizone, A. N., Sammons, M. A., & Forni, P. E. (2018). The transcription factor Tfap2e/AP-2epsilon plays a pivotal role in maintaining the identity of basal vomeronasal sensory neurons. *Dev Biol, 441*(1), 67-82. doi:10.1016/j.ydbio.2018.06.007

Lindsey, J. D., & Weinreb, R. N. (2002). Identification of the mouse uveoscleral outflow pathway using fluorescent dextran. *Invest Ophthalmol Vis Sci, 43*(7), 2201-2205.

Liu, P., Fu, X., & Johnson, R. L. (2011). Efficient in vivo doxycycline and cre recombinase-mediated inducible transgene activation in the murine trabecular meshwork. *Invest Ophthalmol Vis Sci, 52*(2), 969-974. doi:10.1167/iovs.09-5052

Liu, P., & Johnson, R. (2010). Lmx1b is required for murine trabecular meshwork formation and for maintenance of corneal transparency. *Dev Dyn., 239*(8), 2161-2171.

Lu, Y., Brommer, B., Tian, X., Krishnan, A., Meer, M., Wang, C., . . . Sinclair, D. A. (2020). Reprogramming to recover youthful epigenetic information and restore vision. *Nature, 588*(7836), 124-129. doi:10.1038/s41586-020-2975-4

Luscher, B., Mitchell, P. J., Williams, T., & Tjian, R. (1989). Regulation of transcription factor AP-2 by the morphogen retinoic acid and by second messengers. *Genes Dev, 3*(10), 1507-1517. doi:10.1101/gad.3.10.1507

Lutjen-Drecoll, E., & Tamm, E. (1988). Morphological study of the anterior segment of cynomolgus monkey eyes following treatment with prostaglandin F2 alpha. *Exp Eye Res, 47*(5), 761-769. doi:10.1016/0014-4835(88)90043-7

Mao, M., Hedberg-Buenz, A., Koehn, D., John, S. W., & Anderson, M. G. (2011). Anterior segment dysgenesis and early-onset glaucoma in nee mice with mutation of Sh3pxd2b. *Invest Ophthalmol Vis Sci, 52*(5), 2679-2688. doi:10.1167/iovs.10-5993

Martino, V. B., Sabljic, T., Deschamps, P., Green, R. M., Akula, M., Peacock, E., . . . West-Mays, J. A. (2016). Conditional deletion of AP-2β in the cranial neural crest results in anterior segment dysgenesis and early-onset glaucoma. *Disease Models & Mechanisms, 9*(8), 849–861.

Matt, N., Dupe, V., Garnier, J. M., Dennefeld, C., Chambon, P., Mark, M., & Ghyselinck, N. B. (2005). Retinoic acid-dependent eye morphogenesis is orchestrated by neural crest cells. *Development, 132*(21), 4789-4800. doi:10.1242/dev.02031

Moser, M., Pscherer, A., Roth, C., Becker, J., Mucher, G., Zerres, K., . . . Fassler, R. (1997a). Enhanced apoptotic cell death of renal epithelial cells in mice lacking transcription factor AP-2beta. *Genes Dev, 11*(15), 1938-1948. doi:10.1101/gad.11.15.1938

Moser, M., Ruschoff, J., & Buettner, R. (1997b). Comparative analysis of AP-2 alpha and AP-2 beta gene expression during murine embryogenesis. *Dev Dyn, 208*(1), 115-124. doi:10.1002/(SICI)1097-0177(199701)208:1<115::AID-AJA11>3.0.CO;2-5

Napier, H., & Kidson, S. (2005). Proliferation and cell shape changes during ciliary body morphogenesis in the mouse. *Dev Dyn., 233*(1), 213-223.

Nottoli, T., Hagopian-Donaldson, S., Zhang, J., Perkins, A., & Williams, T. (1998). AP-2-null cells disrupt morphogenesis of the eye, face, and limbs in chimeric mice. *Proc Natl Acad Sci U S A, 95*(23), 13714-13719. doi:10.1073/pnas.95.23.13714

Overby, D., Bertrand, J., Schicht, M., Paulsen, F., Stamer, W., & Lütjen-Drecoll, E. (2014). The structure of the trabecular meshwork, its connections to the ciliary muscle, and the effect of pilocarpine on outflow facility in mice. *Invest Ophthalmol Vis Sci., 55*(6), 3727-3736.

Pardue, M. T., & Allen, R. S. (2018). Neuroprotective strategies for retinal disease. *Prog Retin Eye Res, 65*, 50-76. doi:10.1016/j.preteyeres.2018.02.002

Peces-Pena, M. D., de la Cuadra-Blanco, C., Vicente, A., & Merida-Velasco, J. R. (2013). Development of the ciliary body: morphological changes in the distal portion of the optic cup in the human. *Cells Tissues Organs, 198*(2), 149-159. doi:10.1159/000353648

Pontoriero, G., Deschamps, P., Ashery-Padan, R., Wong, R., Yang, Y., Zavadil, J., . . . West-Mays, J. (2008). Cell autonomous roles for AP-2alpha in lens vesicle separation and maintenance of the lens epithelial cell phenotype. *Dev Dyn., 237*(3), 602-617.

Pressman, C. L., Chen, H., & Johnson, R. L. (2000). LMX1B, a LIM homeodomain class transcription factor, is necessary for normal development of multiple tissues in the anterior segment of the murine eye. *Genesis, 26*(1), 15-25.

Romero, P., Sanhueza, F., Lopez, P., Reyes, L., & Herrera, L. (2011). c.194 A>C (Q65P) mutation in the LMX1B gene in patients with nail-patella syndrome associated with glaucoma. *Mol Vis, 17*, 1929-1939.

Rothstein, M., & Simoes-Costa, M. (2020). Heterodimerization of TFAP2 pioneer factors drives epigenomic remodeling during neural crest specification. *Genome Res, 30*(1), 35-48. doi:10.1101/gr.249680.119

Seo, S., Chen, L., Liu, W., Zhao, D., Schultz, K. M., Sasman, A., . . . Kume, T. (2017). Foxc1 and Foxc2 in the Neural Crest Are Required for Ocular Anterior Segment Development. *Invest Ophthalmol Vis Sci, 58*(3), 1368-1377. doi:10.1167/iovs.16-21217

Smith, R., Zabaleta, A., Kume, T., Savinova, O., Kidson, S., Martin, J., . . . John, S. (2000). Haploinsufficiency of the transcription factors FOXC1 and FOXC2 results in aberrant ocular development. *Hum Mol Genet., 9*(7), 1021-1032.

Smith, R., Zabaleta, A., Savinova, O., & John, S. (2001). The mouse anterior chamber angle and trabecular meshwork develop without cell death. *BMC Dev Biol., 1*(3).

Stamer, W. D., & Clark, A. F. (2017). The many faces of the trabecular meshwork cell. *Exp Eye Res, 158*, 112-123. doi:10.1016/j.exer.2016.07.009

Swamynathan, S. K. (2013). Ocular surface development and gene expression. *J Ophthalmol, 2013*, 103947. doi:10.1155/2013/103947

Tamm, E. R. (2009). The trabecular meshwork outflow pathways: structural and functional aspects. *Exp Eye Res, 88*(4), 648-655. doi:10.1016/j.exer.2009.02.007

Tian, B., Gabelt, B. T., Geiger, B., & Kaufman, P. L. (2009). The role of the actomyosin system in regulating trabecular fluid outflow. *Exp Eye Res, 88*(4), 713-717. doi:10.1016/j.exer.2008.08.008

Toris, C. B., Fan, S., Johnson, T. V., Camras, L. J., Hays, C. L., Liu, H., & Ishimoto, B. M. (2016). Aqueous Flow Measured by Fluorophotometry in the Mouse. *Invest Ophthalmol Vis Sci, 57*(8), 3844-3852. doi:10.1167/iovs.14-15144

Tumer, Z., & Bach-Holm, D. (2009). Axenfeld-Rieger syndrome and spectrum of PITX2 and FOXC1 mutations. *Eur J Hum Genet, 17*(12), 1527-1539. doi:10.1038/ejhg.2009.93

Ueda, J., Wentz-Hunter, K., & Yue, B. Y. (2002). Distribution of myocilin and extracellular matrix components in the juxtacanalicular tissue of human eyes. *Invest Ophthalmol Vis Sci, 43*(4), 1068-1076.

Ueda, J., & Yue, B. Y. (2003). Distribution of myocilin and extracellular matrix components in the corneoscleral meshwork of human eyes. *Invest Ophthalmol Vis Sci, 44*(11), 4772-4779. doi:10.1167/iovs.02-1002

Van Otterloo, E., Li, H., Jones, K. L., & Williams, T. (2018). AP-2α and AP-2β cooperatively orchestrate homeobox gene expression during branchial arch patterning. *Development, 145*. doi:doi: 10.1242/dev.157438

van Zyl, T., Yan, W., McAdams, A., Peng, Y. R., Shekhar, K., Regev, A., . . . Sanes, J. R. (2020). Cell atlas of aqueous humor outflow pathways in eyes of humans and four model species

provides insight into glaucoma pathogenesis. *Proc Natl Acad Sci U S A, 117*(19), 10339-10349. doi:10.1073/pnas.2001250117

Volkmann, B. A., Zinkevich, N. S., Mustonen, A., Schilter, K. F., Bosenko, D. V., Reis, L. M., . . . Semina, E. V. (2011). Potential novel mechanism for Axenfeld-Rieger syndrome: deletion of a distant region containing regulatory elements of PITX2. *Invest Ophthalmol Vis Sci, 52*(3), 1450-1459. doi:10.1167/iovs.10-6060

Walker, H., Akula, M., & West-Mays, J. A. (2020). Corneal development: Role of the periocular mesenchyme and bi-directional signaling. *Exp Eye Res, 201*, 108231. doi:10.1016/j.exer.2020.108231

Weinreb, R. N., & Lindsey, J. D. (2002). Metalloproteinase gene transcription in human ciliary muscle cells with latanoprost. *Invest Ophthalmol Vis Sci, 43*(3), 716-722.

Werling, U., & Schorle, H. (2002). Transcription factor gene AP-2 gamma essential for early murine development. *Mol Cell Biol, 22*(9), 3149-3156. doi:10.1128/mcb.22.9.3149-3156.2002

West-Mays, J. A., Zhang, J., Nottoli, T., Hagopian-Donaldson, S., Libby, D., Strissel, K. J., & Williams, T. (1999). AP-2alpha transcription factor is required for early morphogenesis of the lens vesicle. *Developmental Biology, 206*(1), 46–62.

Williams, A. L., & Bohnsack, B. L. (2015). Neural crest derivatives in ocular development: discerning the eye of the storm. *Birth Defects Res C Embryo Today, 105*(2), 87-95. doi:10.1002/bdrc.21095

Williams, T., & Tjian, R. (1991a). Analysis of the DNA-binding and activation properties of the human transcription factor AP-2. *Genes Dev, 5*(4), 670-682. doi:10.1101/gad.5.4.670

Williams, T., & Tjian, R. (1991b). Characterization of a dimerization motif in AP-2 and its function in heterologous DNA-binding proteins. *Science, 251*(4997), 1067-1071. doi:10.1126/science.1998122

Winkler, N. S., & Fautsch, M. P. (2014). Effects of prostaglandin analogues on aqueous humor outflow pathways. *J Ocul Pharmacol Ther, 30*(2-3), 102-109. doi:10.1089/jop.2013.0179

Wright, C., Tawfik, M. A., Waisbourd, M., & Katz, L. J. (2016). Primary angle-closure glaucoma: an update. *Acta Ophthalmol, 94*(3), 217-225. doi:10.1111/aos.12784

Zhao, F., Weismann, C. G., Satoda, M., Pierpont, M. E., Sweeney, E., Thompson, E. M., & Gelb, B. D. (2001). Novel TFAP2B mutations that cause Char syndrome provide a genotype-phenotype correlation. *Am J Hum Genet, 69*(4), 695-703. doi:10.1086/323410

Zhou, J., & Kochhar, D. M. (2004). Cellular anomalies underlying retinoid-induced phocomelia. *Reprod Toxicol, 19*(1), 103-110. doi:10.1016/j.reprotox.2004.06.012